8629694

Gelman, Alexander David

ON SOME ISSUES OF CODE DIVISION MULTIPLE ACCESS COMMUNICATION

City University of New York PH.D. 1986

University Microfilms International 300 N. Zeeb Road, Ann Arbor, MI 48106

ON SOME ISSUES OF CODE DIVISION MULTIPLE ACCESS COMMUNICATION

by

Alexander D. Gelman

A dissertation submitted to the Graduate Faculty in Engineering in partial fulfillment of the requirements for the degree of Doctor of Philosophy, The City University of New York.

1986

This manuscript has been read and accepted for the Graduate Faculty in Engineering in satisfaction of the dissertation requirement for the degree of Doctor of Philosophy.

6/12/86
date

Professor D. L. Schilling
Chairman of Examining Committee

6/12/86
date

Dean P. Karmel
Executive Officer

Professor L. Bergstein

Professor T. Saadawi

Professor N. Scheinberg

Professor J. Barba

Supervisory Committee

The City University of New York

Abstract

ON SOME ISSUES OF CODE DIVISION MULTIPLE ACCESS COMMUNICATION

by

Alexander D. Gelman

Adviser: Professor Donald L. Schilling

A solution to Asynchronous Multiple User Real Time Communications is proposed. That is to employ Spread Spectrum Signaling technique and Code Division Multiplexing of multiple user signals into a Fiber Optic medium.

Direct Sequence, Time-Hopped, Color-Hopped and Hybrid (Time/Color-Hopped) signaling schemes are analyzed and the probability of error is determined as a function of employed codes' parameters and the channel traffic.

The assumptions for channel models are Poisson arrivals of multiple user signals and hard limiting of the composite channel signal.

It is shown that Probability of Error of 10^{-5} can be achieved at 22 % channel load for systems with Passive Pause Signaling and at 10 % for systems with Active Pause Signaling.

As the number of active users increases the channels demonstrate graceful performance degradation in terms of the probability of error.

A presense of optimal code sizes has been demonstrated for all signaling schemes and it has been shown that this optimum is a function of the channel load.

It has been determined that in a hybrid, Time/Color-Hopped system Trade off is possible of the Electronic Bandwidth expansion for Optical and vice-versa.

Synchronization Algorithms for Time-Hopped Code Division Multiple Access Systems are proposed and expressions for False Acquisition Probability and Average False Tracking Time are derived.

Two typical applications of the proposed signaling techniques to Rate-Invariant Signals Multiplexing and to Local Area Networking are described.

To my wife Galina and daughters Fanya and Freida who have put up with my research for years.

To my mistress — Communications Theory.

To the City College of New York that became my second Alma Mater.

To my mentor, Professor Donald Schilling, for guidance in this research and for help in my scientific career.

CONTENTS

LIST OF FIGURES

1. CODE DIVISION MULTIPLE ACCESS COMMUNICATION IN GUIDED AND UNGUIDED MEDIA

1.1 INTRODUCTION

Multiple access communications is characterized by the population of users exceeding the number of communication channels. The users share a common medium and access it in a spontaneous fashion. A typical example of such an environment is a Local Area Network (LAN). Over the last few years networking technology achieved noticeable progress in creating a multiplicity of networks for a variety of applications. Among the most known networking products are ETHERNET, APOLLO DOMAIN, WANGNET, FASNET, etc. Creation of these networks was preceded by intensive research of channelization and networking algorithms performed by international multi-disciplinary army of enginners and scientists.

The most important characteristics of a multiple access communication channel, (Fig.1.1), are the number of users, their accessing capability and the system throughput. In other words to characterize the system two basic questions have to be answered:

1. What is each user's chance to gain access to the common medium when he has a message to transmit?

2. What is each user's chance to have his message, if transmitted, successfully received by the destination receiver?

The evolution of multiple access techniques progressed from the simple ALOHA protocol to sophisticated contention algorithms such as carrier sensing, collision detection, token passing techniques and combinations thereof. The major factors that limit applications of these techniques to voice, video and graphics communications are the necessity to packetize the signal and delays in the packet delivery due to collisions and retransmissions.

All existing LAN products were developed for data communications. That is the reason why they employ contention resolution techniques designed for error-less packet delivery on the expense of time. In the mean time voice and video signals, even if packetized, do not tolerate delays in delivery. No delays can be tolerated for inter-media operation and control as well. On the other hand voice and video signals as well as some other media often possess enough redundancy to tolerate bit error rates of 10^{-5} while delays can destroy the signal.

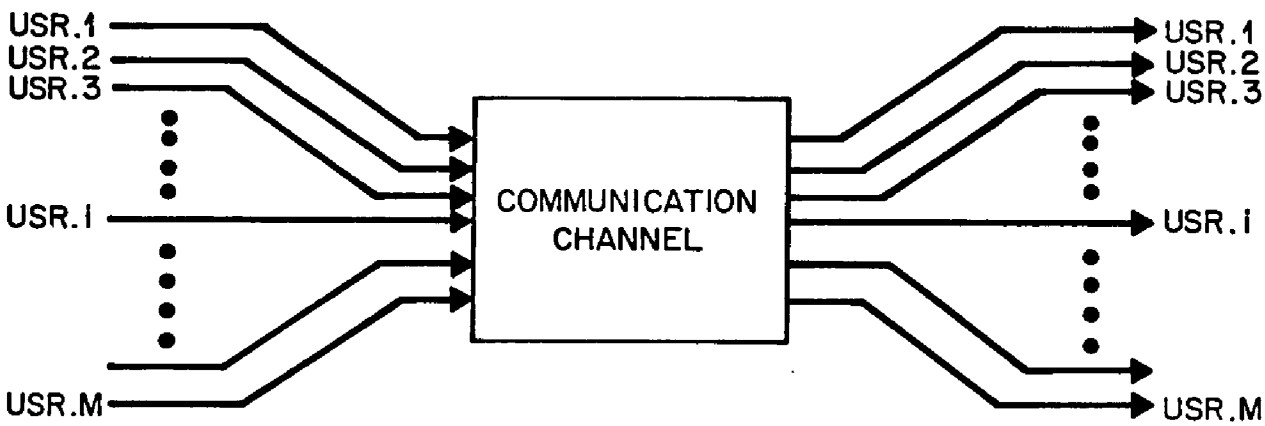

Fig.1.1 Multiple Access Channel

1.2 MOTIVATION FOR THE RESEARCH

1.2.1 To Spread Or Not To Spread

That is the question.

One of the solutions to real time communications needs is using non-orthogonal signaling for multiplexing the multiple user signals into a single channel. Applications of Spread Spectrum Techniques to Radio communications is first of all motivated by the necessity to sustain electronic counter measures and to insure some reasonably low probability of intercept [1]. Using this technique for Code Division Multiplexing of multiple signals is also known and researched to some degree for HF channels. In [12] a SSMA Telephone system is analyzed, in [33] an integrated voice/data network is described. Less researched is non-orthogonal multiplexing and multiple accessing of guided media.

1.2.2 Back To Aloha

Recently CDMA applications to Local Area Networks attracts more and more researchers due to potential of creating an asynchronous network with no routing overhead and no definite failures upon collisions but rather graceful performance degradation as the number of active users increases.

In other words Aloha-like protocols can be designed to guarantee access when needed but with a significant advantage of not having to retransmit every time a collision is detected. Also CDMA allows to set up virtual circuit links in point-to-point or point-to-multi-point modes to conduct a nonbursty communication session. This feature is important for full motion video communication, per example.

Adaptation of the Spread Spectrum Techniques for Multiple Access on the coaxial cable was first described in [13].

One of the first publications on fiber optic Code Division Multiplexing techniques were [5] and [24]. Later Code Division Multiplexing using Gold Sequences was proposed in [6]. These papers represented first attempts to study non-orthogonal signals multiplexing in Fiber Optics. They do not yet contain enough information to understand the phenomena of the multiple user interference in CDMA Fiber Optic systems and evaluate their performance.

1.2.3 Statement Of The Problem

In this work we propose a new type of a multiple access channel suitable for real time communications. This channel takes advantage of inherent multiple access capability of the spread spectrum signaling as well as of the high bandwidth and stability offered by the fiber optic medium.

We propose and analyze three different signaling techniques and evaluate systems performance by means of the probability of error. We also propose synchronization strategy and analyze it's performance. As an application of the channel we propose a new type of a Local Area Network suitable for real time communications and capable of supporting multiple users, multiple media and multiple information rates.

The phenomena of the multiple user interference in the fiber optic multiple access channel is quite different from the one in other media due to limitation of positive only signaling. This results in non-gaussian statistics of the system noise and does not allow to use well known and researched detection strategies. The main assumption that we make for the system analysis is Poisson distribution of the multiple user signal arrival times. We investigate the statistics of the multiple user noise which is a result of an OR operation on a finite set of coinciding pulse trains. We find the average rate and pulse durations of the noise pulses as well as their distributions. These parameters allow us to track the signal and noise statistical properties through the detection and synchronization processes and finally determine the system probability of error and analyze the performance of the proposed acquisition and tracking schemes. The approach which is used for the analysis was first proposed in [50] and was later used in [22], [41], [60] and other publications on Random Access Discrete Address (RADA) communications.

1.3 ON SOME PROPERTIES OF PN AND RELATED SEQUENCES

In this section we will review some useful properties of Pseudo-Noise and related sequences and describe their applications to Code Division Multiple Access communications.

The two main requirements to any set of Pseudo-Random signals are:

1. distinguishability of any signal from time-shifted version of itself
2. distinguishability of any signal from any other signal in the set.

First property is useful in the acquisition mode of a communication session when the receiver is trying to acquire synchronism with the transmitter by determining the exact phase-shift of the pseudo-random code which is used for the information transport.

The second property is useful for multiple access communication when every station is assigned a pseudo-random sequence according to some rules.

The types of pseudo-random sequences that we will review are the Maximal Length sequences (m-sequences), Gold sequences, and Pseudo Random Interval Sequences.

Binary Maximal Length sequences

The studies of m-sequences started back in 1950's by Gilbert, Golomb, Welch and Zierler [2]. Most of known today results of the correlation properties of m-sequences are given in [45].

The Binary Maximal Length sequences are generated using shift-registers (Fig.1.2). It is conventional to specify the configuration of the shift-register by a corresponding polynomial:

$$h(x) = h_0x^n + h_1x^{n-1} + \cdots + h_{n-1}x + h_n \qquad (1.3.1)$$

and it's binary vectors. For example the polynomial:

$$h(x) = x^5 + x^2 + 1 \qquad (1.3.2)$$

can be represented by a binary vector 100101 or 45 in the octal notation.

The period of the sequence generated by the shift register can be at most equal to:

$$L = 2^n - 1 \qquad (1.3.3)$$

where n-is the degree of the polynomial and also the number of cells in the shift-register.

If a sequence has maximal period it is called a maximal length sequence, or m-sequence.

The m-sequences have the following properties:

Property 1. For an m-sequence u and a pair of integers i and j such that $0 \leq i,j < L$ there is a unique integer k, $0 \leq k < L$, and:

$$T^i\, u \oplus T^j\, u = T^k\, u$$

a sequence of period L is an m-sequence if and only if it has property 1 (shift-and-add property).

Property 2. Let wt(u) denote the Hamming weight of the sequence u, i.e. specify the number of ones in the sequence. Then for an m-sequence:

$$wt(u) = 2^{n-1} = \frac{1}{2}(L+1) \tag{1.3.4}$$

What this means is that the difference between the number of ones, n_1 and the number of zeroes, n_0, is equal to one:

$$n_1 - n_0 = 1$$

Property 3. Let $\theta_{uu}(l)$ be a discrete-time auto-correlation function:

$$\theta_{uu}(l) = \sum_{j=1}^{L} \chi(u_j)\,\chi(u_{j+l}) \tag{1.3.5}$$

where

$\chi(u_j)$ — is a bipolar code value derived by the following transformation:

$$\chi(u_j) = (-1)^{u_j} \tag{1.3.6}$$

Then for a m-sequence:

$$\theta_{uu}(l) = \begin{cases} L, & \text{for } l = 0, L, 2L, \ldots \\ -1, & \text{for } l \neq 0, L, 2L, \ldots \end{cases} \tag{1.3.7}$$

So the binary m-sequences have two-valued autocorrelation function.

A continuous-time autocorrelation function can be defined as follows:

$$R_{uu}(\tau) = \int_{0}^{LT_c} \chi[u(t)]\,\chi[u(t+\tau)]\,dt \tag{1.3.8}$$

The autocorrelation function of the m-sequence is depicted in Fig.1.3.

Let's define a discrete-time crosscorrelation function of two m-sequences u and v as:

$$\theta_{uv}(l) = \sum_{j=1}^{L} \chi(u_j)\, \chi(v_{j+l}) \tag{1.3.9}$$

And for continuous-time crosscorrelation function:

$$R_{uv}(\tau) = \int_{0}^{LT_c} \chi[u(t)]\, \chi[v(t+\tau)]\, dt \tag{1.3.10}$$

According to [29] the discrete-time crosscorrelation function of two m-sequences can be written as follows:

$$\theta_{uv}(l) = N - 2\, wt(u \oplus T^l v) \tag{1.3.11}$$

One of the useful properties of the crosscorrelation functions of the m-sequences is the upper bound:

$$|\theta_{uv}(l)| \leq L \tag{1.3.12}$$

The m-sequences do not allow to construct large sets. This fact limits their applications in CDMA systems.

Gold Sequences

A very useful class of pseudo-random sequences that provide an opportunity of creating a significantly large set of sequences with good crosscorrelation properties is the class of Gold sequences.

The set of Gold sequences G(u,v) is defined by:

$$G(u,v) \equiv \left\{ u, v, u \oplus v, u \oplus Tv, u \oplus T^2v, \ldots, u \oplus T^{L-1}v \right\} \quad (1.3.13)$$

Where T^iu denotes sequence u shifted i chips with respect to itself.

The set G(u,v) contains L+2 sequences of period L.

The values of the autocorrelation functions for sequences of G(u,v) are the same as the values of the autocorrelation for sequences u and v.

Following [29] we will consider the crosscorrelation function of two distinct sequences $y,z \epsilon G(u,v)$.

It can be proved that the discrete-time crosscorrelation function:

$$\theta_{y,z}(l) = L - 2wt(y \oplus T^l z) \quad (1.3.14)$$

either equals -1 or:

$$\theta_{y,z}(l) = L - 2wt(u \oplus T^{j-i}v) - \theta_{u,v}(j-i) \quad (1.3.15)$$

When the number n ($L = 2^n - 1$) is odd then the lawer bound on the maximum crosscorrelation is:

$$\theta_{max} \geq t(n) - 2 \quad (1.3.16)$$

Where:

$$t(n) = 1 + 2^{\lfloor (n+2)/2 \rfloor} \tag{1.3.17}$$

For example there are 12 different sets of Gold sequences of period 31. Each set contains 33 sequences and the crosscorrelation functions of these sequences can take one of the three values: 7, -1, -9.

There exist 6 sets of Gold sequences of period 63. Each set consists of 65 sequences with crosscorrelation function values: 15, -1, -17.

For the application of the sequence sets to the multiple user communication an important characteristics is the crosscorrelation of a sequence to the asynchronous sum of the sequences of the set modulated by binary symmetric data sources. This property is important when the study of multiple user interference is being performed of a system with a correlation receiver.

The hystogram of a crosscorrelation function between one of the Gold sequences and the asynchronous sum of other sequences of the Gold sequences set of period 31 is illustrated in Fig.1.6.

As it should be expected due to the central limit theorem the shape of the hystogram implies Gaussian probability density function when the number of sequences is large.

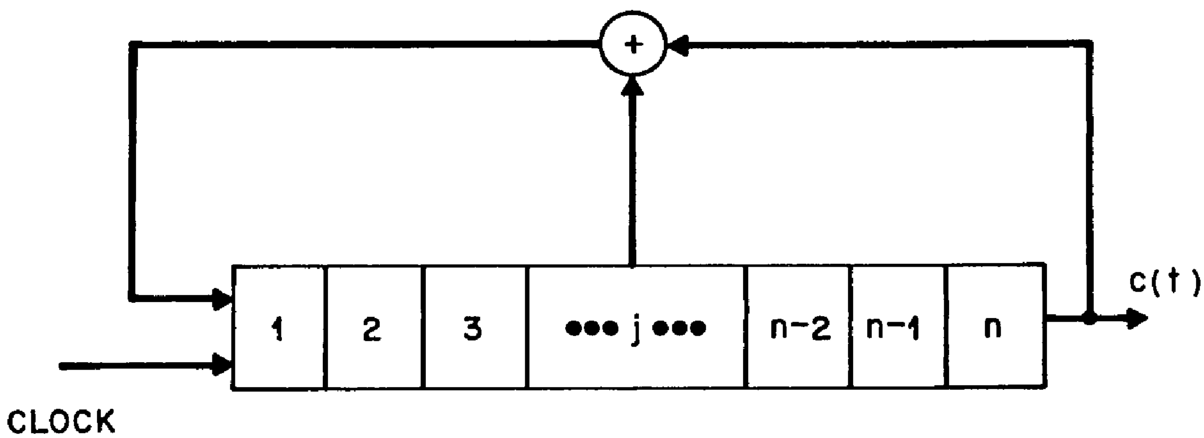

Fig.1.2 PN-Sequence Generator

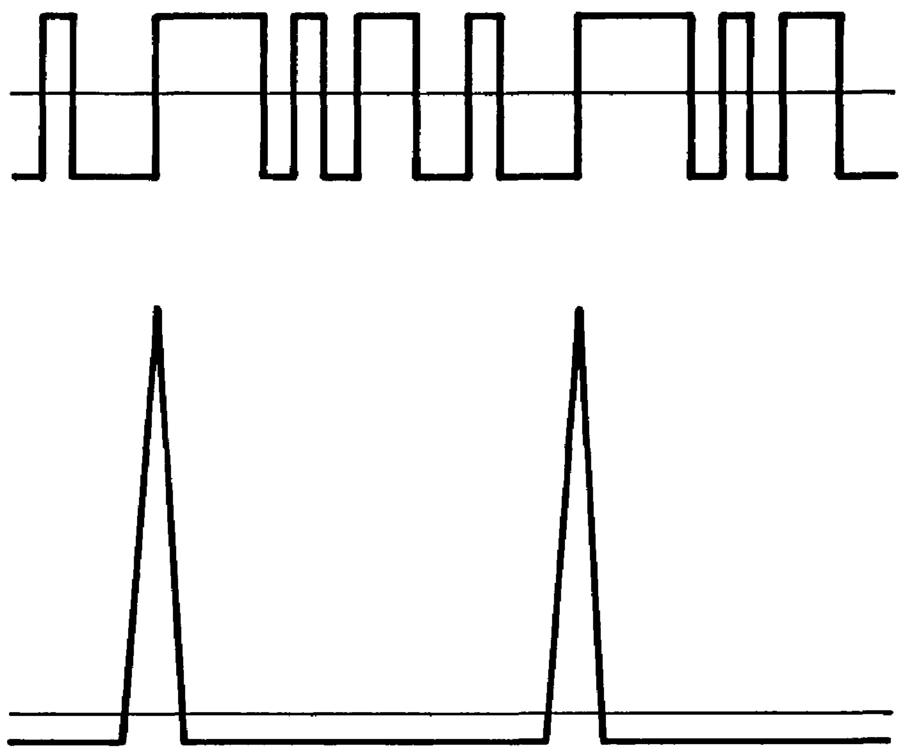

Fig.1.3. Autocorrelation Function of a PN-Sequence

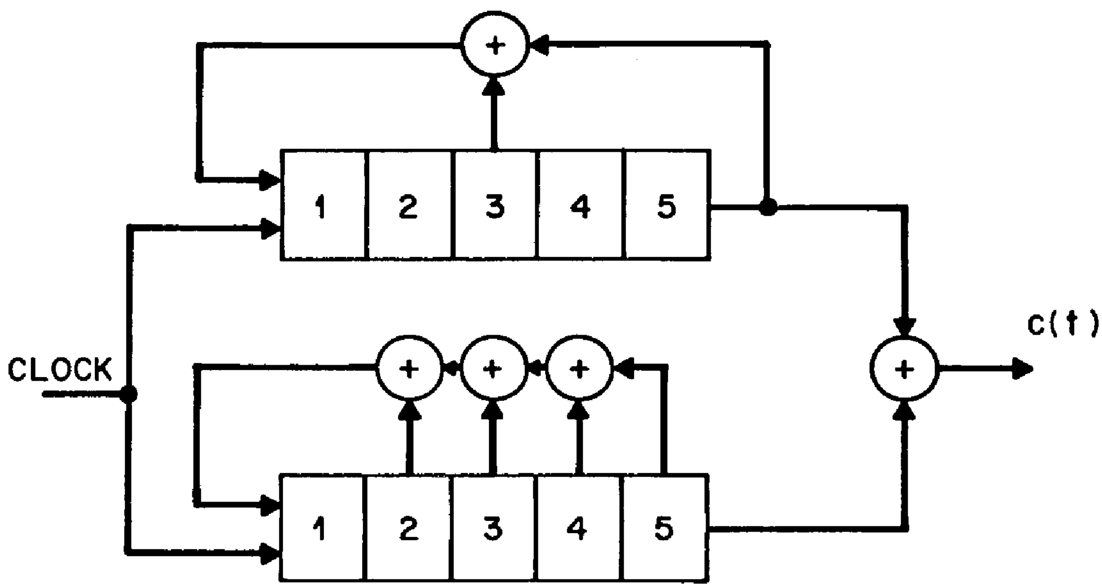

Fig.1.4. Gold Sequence Generator

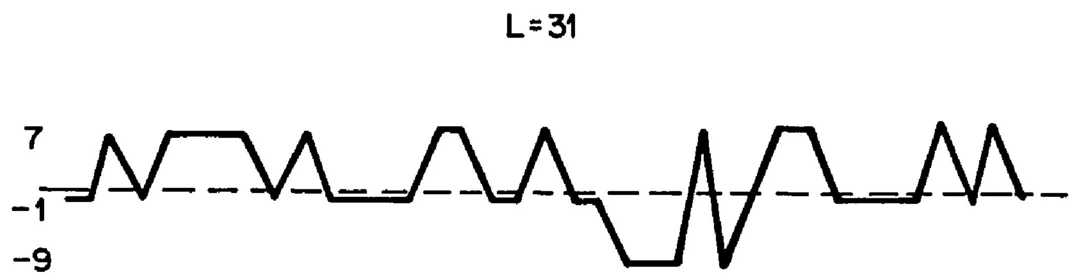

Fig.1.5. Crosscorrelation Function of Gold Sequences

```
mode...............................tracking
transmitter's code.................unipolar gold code
receiver's code....................bipolar gold code
bitrate............................8191 bits/sec.
duration...........................1 sec.
shift register stages..............5
total users........................18
user #1 included?..................no  .
offset of user # 1 wrt user #1.....183 samples
offset of user # 2 wrt user #1.....299 samples
offset of user # 3 wrt user #1.....190 samples
offset of user # 4 wrt user #1.....130 samples
offset of user # 5 wrt user #1.....76 samples
offset of user # 6 wrt user #1.....52 samples
offset of user # 7 wrt user #1.....239 samples
offset of user # 8 wrt user #1.....2 samples
offset of user # 9 wrt user #1.....264 samples
offset of user #10 wrt user #1.....105 samples
offset of user #11 wrt user #1.....71 samples
offset of user #12 wrt user #1.....133 samples
offset of user #13 wrt user #1.....145 samples
offset of user #14 wrt user #1.....72 samples
offset of user #15 wrt user #1.....135 samples
offset of user #16 wrt user #1.....262 samples
offset of user #17 wrt user #1.....142 samples
```

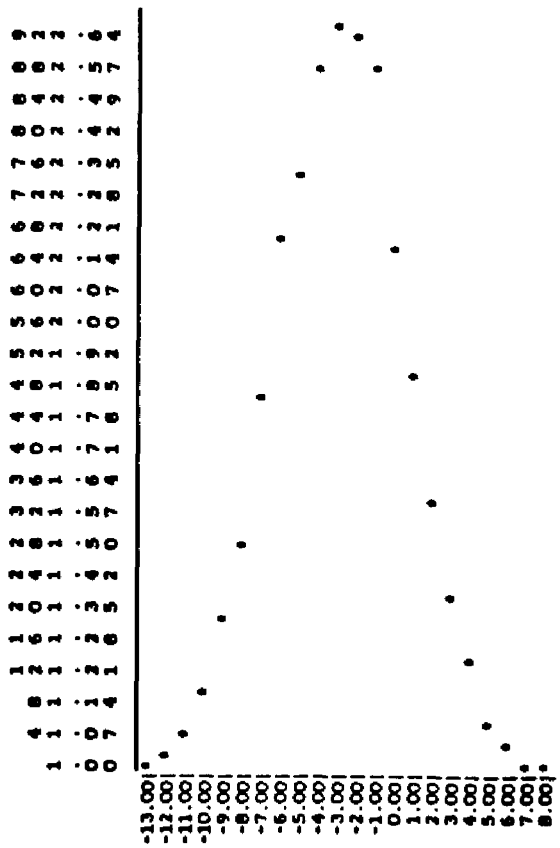

Fig.1.6. Gold Sequence-to-Set Crosscorrelation Distribution

Pseudo Random Interval Sequences

As it will be shown in later chapters for CDMA application in fiber optics it is effective to use sequences with low duty cycles.

One of the methods of generating such sequences is to map the PN sequences into the pseudo random time intervals. We will call this type of code "Pseudo-Random Intervals Sequence", or PRIS.

The simplest way of mapping the PN-code into a PRIS is to produce impulses corresponding to all positive transitions in the PN-code, Fig.1.7. Another way is to generate impulses at the beginning of every positive chip, Fig.1.8. However sequences generated in a arbitrary way might not possess the right properties to be used in Code Division Multiple Access systems. There is a necessity to design PRIS codes with desirable auto and Cross-correlation properties suitable for this application.

One of the methods for creating "Time Mapped" sequences is proposed in [14]. We will modify this method for the purpose of construction of a set of PRIS codes.

A condition that has to be imposed on the sequence set is the upper bound on the crosscorrelation function for any pair of sequences. Then knowing the size of the sequence set one can always estimate the upper bound of the crosscorrelation of any sequence with the asynchronous sum of all other sequences of the set.

In the PRIS code the values of the sequence elements specify the interval between adjacent pulses. The intervals are given in multiple integers of the pulse duration τ_c .

The length of the code is partitioned into frames as it is shown in Fig.1.9.

The condition we impose is that the crosscorrelation function for any two sequences c_i and c_j $(i \neq j)$ of the set is to be bounded:

$$\theta_{ij}(l) \leq 2 \tag{1.3.22}$$

Another constraint is that each frame must contain a pulse.

As it is shown in [14] a Time mapped sequence can be constructed by using the multiplication table of the elements of the Galois field GF(p), where p is a prime number. Upon selecting the prime number the field elements have to be written down in ascending order. Then the absolute positions of the pulses in the frames are computed by multiplying modulo p this row by the field element. The PRIS code elements can be derived from the absolute positions by the following transformation:

$$C_j = p + P_j - P_{j-1} \tag{1.3.23}$$

Where:

C_j – is the j-th element of the PRIS code.

P_j – is the absolute position of the pulse in the j-th frame, $1 < j \leq p-1$.

The first element of the interval sequence is equal to the absolute pulse position value in the frame 0:

$$C_1 = P_1 \tag{1.3.24}$$

We will now show an example of the PRIS set construction by creating a set of 17 codes with 17 pulses per pattern.

The prime number is selected to be: p=17. Then the field elements are:

GF(17): 0, 1, 2, 3, 4, 5, 6, 7, 8, 9,10,11,12,13,14,15,16

By multiplying modulo 17 this row by the field elements we receive sequences whose elements are the absolute pulse positions in the frames:

s_0: 0, 0, 0, 0, 0, 0, 0, 0, 0, 0, 0, 0, 0, 0, 0, 0, 0

s_1: 0, 1, 2, 3, 4, 5, 6, 7, 8, 9,10,11,12,13,14,15,16

s_2: 0, 2, 4, 6, 8,10,12,14,16, 1, 3, 5, 7, 9,11,13,15

s_3: 0, 3, 6, 9,12,15, 1, 4, 7,10,13,16, 2, 5, 8,11,14

s_4: 0, 4, 8,12,16, 3, 7,11,15, 2, 6,10,14, 1, 5, 9,13

s_5: 0, 5,10,15, 3, 8,13, 1, 6,11,16, 4, 9,14, 2, 7,12

s_6: 0, 6,12, 1, 7,13, 2, 8,14, 3, 9,15, 4,10,16, 4,10

s_7: 0, 7,14, 4,11, 1, 8,15, 5,12, 2, 9,16, 5,12, 2, 9

s_8: 0, 8,16, 7,15, 6,14, 5,13, 4,12, 3,11, 2,10, 1, 9

s_9: 0, 9, 1,10, 2,11, 3,12, 4,13, 5,14, 6,15, 7,16, 8

s_{10}: 0,10, 3,13, 6,16, 9, 2,12, 5,15, 8, 1,11, 4,14, 7

s_{11}: 0,11, 5,16,10, 4,15, 9, 3,14, 8, 2,13, 7, 1,12, 6

s_{12}: 0,12, 7, 2,14, 9, 4,16,11, 6, 1,13, 8, 3,15,10, 5

s_{13}: 0,13, 9, 5, 1,14,10, 6, 2,15,11, 7, 3,16,12, 8, 4

s_{14}: 0,14,11, 8, 5, 2,16,13,10, 7, 4, 1,15,12, 9, 6, 3

s_{15}: 0,15,13,11, 9, 7, 5, 3, 1,16,14,12,10, 8, 6, 4, 2

s_{16}: 0,16,15,14,13,12,11,10, 9, 8, 7, 6, 5, 4, 3, 2, 1

(1.3.25)

Then using (1.3.23) we receive the set of PRIS codes:

$c_{0:}$ 0,17,17,17,17,17,17,17,17,17,17,17,17,17,17,17,17

$c_{1:}$ 0,18,18,18,18,18,18,18,18,18,18,18,18,18,18,18,18

$c_{2:}$ 0,19,19,19,19,19,19,19,19,02,19,19,19,19,19,19,19

$c_{3:}$ 0,20,20,20,20,20,03,20,20,20,20,20,03,20,20,20,20

$c_{4:}$ 0,21,21,21,21,04,21,21,21,04,21,21,21,04,21,21,21

$c_{5:}$ 0,22,22,22,05,22,22,05,22,22,22,05,22,22,05,22,22

$c_{6:}$ 0,23,23,06,23,23,06,23,23,06,23,23,06,23,23,06,23

$c_{7:}$ 0,24,24,07,24,07,24,24,07,24,07,24,24,07,24,07,24

$c_{8:}$ 0,25,25,08,25,08,25,08,25,08,25,08,25,08,25,08,25

$c_{9:}$ 0,26,09,26,09,26,09,26,09,26,09,26,09,26,09,26,09

$c_{10:}$ 0,10,10,27,10,27,10,10,27,10,27,10,10,27,10,27,10

$c_{11:}$ 0,11,11,28,11,11,28,11,11,28,11,11,28,11,11,28,11

$c_{12:}$ 0,12,12,12,29,12,12,29,12,12,12,29,12,12,29,12,12

$c_{13:}$ 0,13,13,13,13,30,13,13,13,30,13,13,13,30,13,13,13

$c_{14:}$ 0,14,14,14,14,14,31,14,14,14,14,14,31,14,14,14,14

$c_{15:}$ 0,15,15,15,15,15,15,15,15,32,15,15,15,15,15,15,15

$c_{16:}$ 0,16,16,16,16,16,16,16,16,16,16,16,16,16,16,16,16

(1.3.26)

The above PRIS codes set can be considered quasi-optimal because while the crosscorrelation function for any pair is bounded, the autocorrelation function is not optimal.

Fig.1.9 illustrates some sequences from this set.

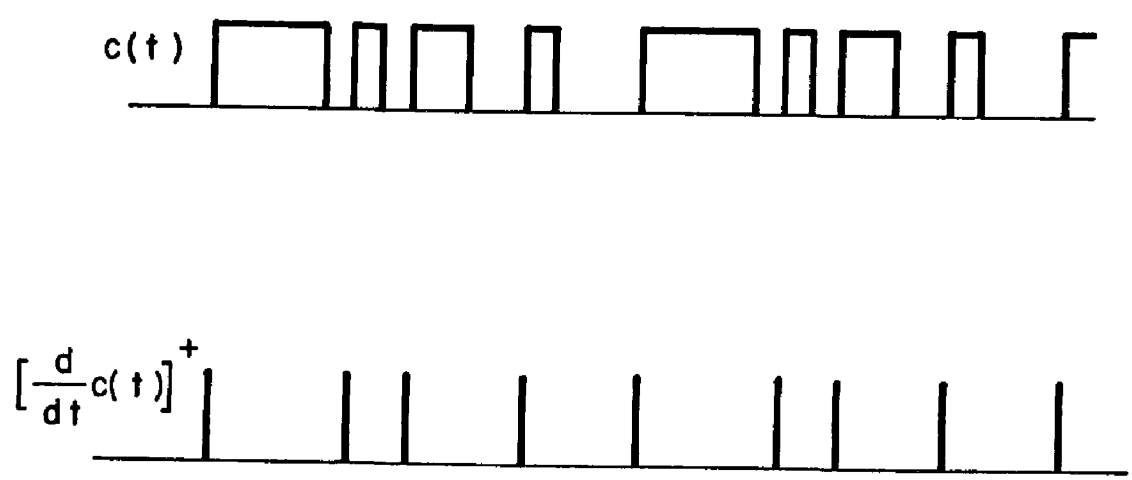

Fig.1.7. PRIS.

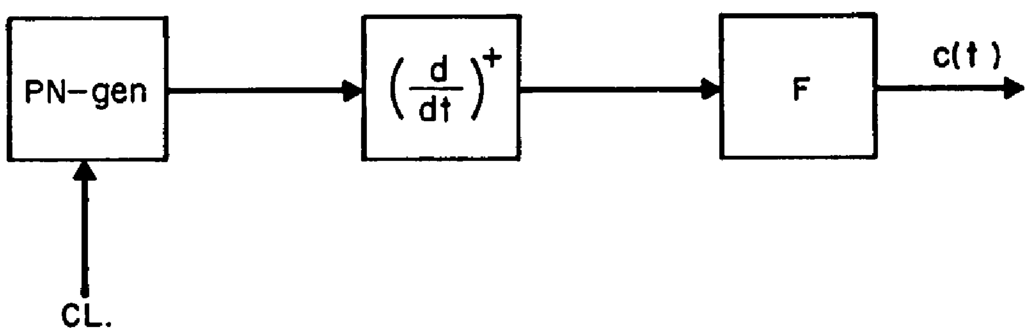

Fig.1.8. Generation of PRISs

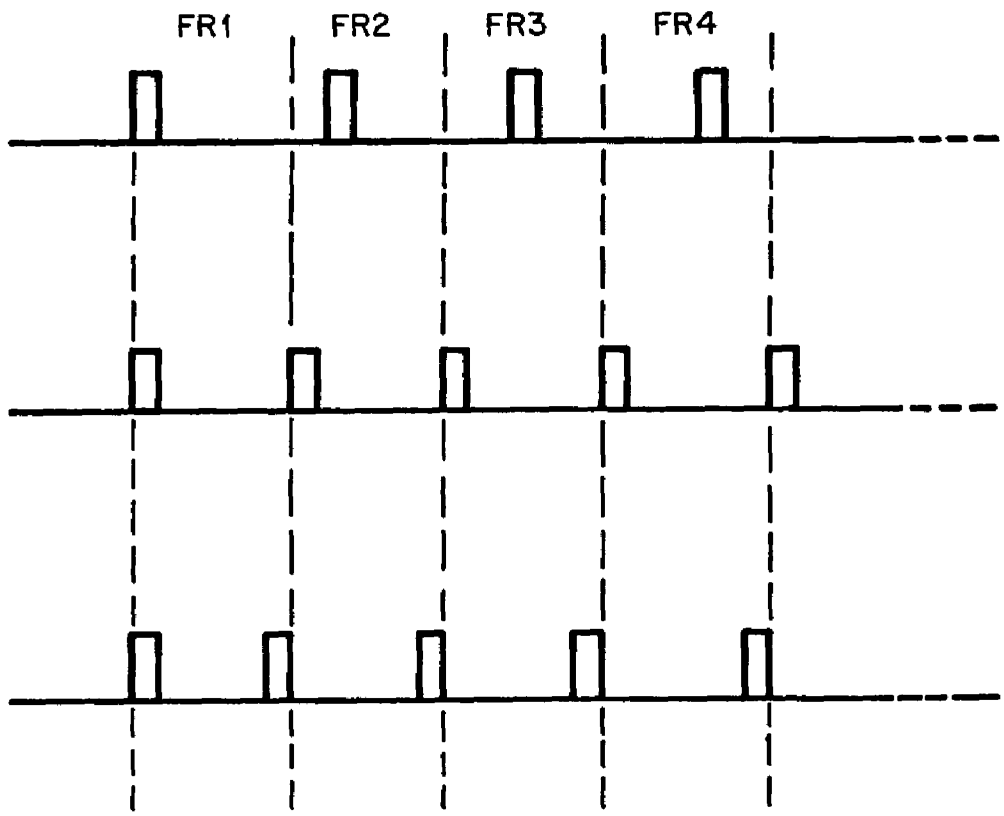

Fig.1.9. Quasi-Optimal PRIS Set

1.4 ASYNCHRONOUS FIBER OPTIC CDMA COMMUNICATION

There are two ways in which the signals can be multiplexed in a optical communications system. One of them is electrical multiplexing (TDM, FDM), another is optical [6]. The latter is preferable because it does not require the conversion of the optical signals to electrical in order to perform the multiplexing function. Optical multiplexer can consist of a unidirectional passive tap. Optical demultiplexing will be wide spread in the future as the optical signal processing devices become practical [10].

We will consider a situation which is suitable for the application in the local area networks. The scheme we have in mind is optical multiplexing and electrical or optical demultiplexing of the multiple user signals.

We will describe few different signaling schemes and state their advantages and disadvantages and compare their performance in terms of the probability of error that can be achieved depending on the system parameters.

Classification of the Fiber Optic CDMA Systems

We propose to follow the following classification of the Fiber Optic CDMA systems.

By the front end the system can be:

- Digital, OR Channel
- Binary Input - Linear Output

By the spreading code used:

- Direct Sequence
- Time-Hopped

- Color-Hopped
- Hybrid: Time/Color Hopped (TλH)

  Color-Hopped/Direct Sequence (λHDS)

By the address assignment scheme:

- Unique Transmitter
- Unique Receiver
- Code Reservation (Code Assignment for Session)

By bandwidth allocation strategy:

- Constant bandwidth
- Dynamically allocatable bandwidth

1.5 CDMA COMMUNICATION USING OOK/OR CHANNEL

1.5.1 OR CHANNEL MODEL

When hard limiting of the channel signal takes place all signals appear at the same level. This situation creates a robust channel which is less succeptable to environment variations and the requirements to the dynamic range of the receiver are less strict. Multiple user signals that build up in the common medium are also hard limited thus their interference can be modeled as an OR operation. That is why we will call this system OR Channel, Fig.1.10.

In this section we will analyze the statistical properties of the multiple user signal in the optical OOK/OR channel.

Let all users emit pulses of light independently from each other. These pulses arrive at random instants of time and if the number of users is sufficiently large (more than ten), we can assume that the arrival times follow Poisson distribution, [50].

The signal resulted from the OR operation on the users' signals we call Multiple User Noise.

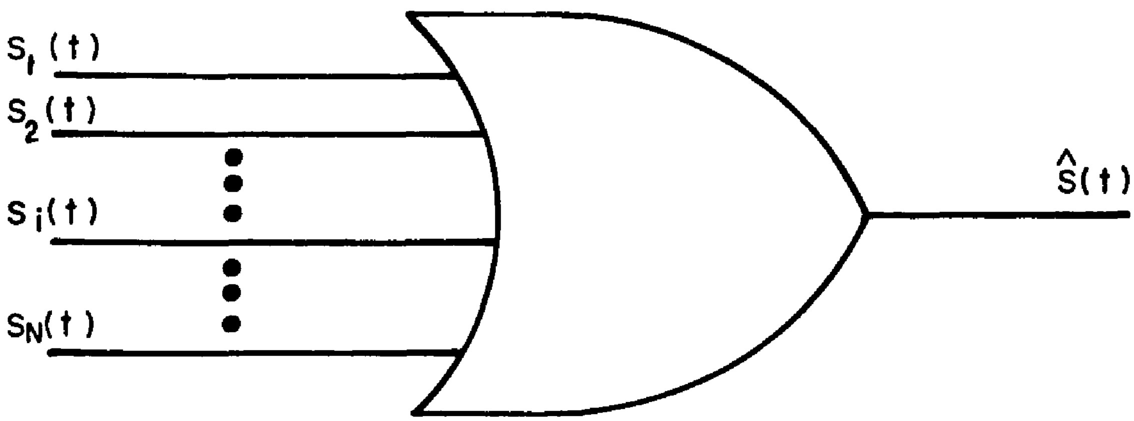

Fig.1.10. OR Channel

1.5.2 Multiple User Noise in OOK/OR Channel

Following [50] we will call the start times of the interfering pulses primary process. The probability to encounter exactly k events of the primary process over the interval t is as follows:

$$P_k(t) = \frac{(\nu\, t)^k}{k!}\, e^{\nu\, t} \tag{1.5.3}$$

The phenomena of the multiple user noise in this system is illustrated in Fig.1.11. The multiple user noise is the composite pulse train which is a result of overlapping of the pulses whose start times constitute the primary process. That is why we will also refer to this interference signal as to a secondary process. In order to analyze the performance of the system, i.e. in order to quantify the effect of interference on each users' signal we have to determine the statistical properties of the multiple user noise.

We will now determine the probability density function of the pulse durations for the secondary process. Every pulse of the secondary process is constructed of k+1 pulses of the primary process, where k=0,1,2,3,... The duration of the secondary pulse is equal to the sum of k intervals between events of the Poisson process t_i , Fig.1.11. plus the duration of the (k+1)-st pulse, which is τ_c :

$$\tau = \sum_{i=1}^{k} \Delta t_i + \tau_c \tag{1.5.4}$$

where:

$$\Delta t_i = t_{i+1} - t_i$$

It is clear from Fig.1.11 that:

$$\begin{aligned} \Delta t_i &< \tau_c \qquad \text{for } 1 \leq i \leq k \\ \Delta t_i &> \tau_c \qquad \text{for } i = k+1 \end{aligned} \tag{1.5.5}$$

The probability for the interval Δt between two Poisson events to take on some value which is less than Δt_i is equal to the probability that at least one Poisson event will occur during the interval Δt_i:

$$p(\Delta t < \Delta t_i) = 1 - e^{-\nu \Delta t_i} \tag{1.5.6}$$

Then the probability density function:

$$g(\Delta t_i) = \frac{d}{d}\Delta t_i \; p(\Delta t < \Delta t_i) = \nu \, e^{-\nu \Delta t_i} \tag{1.5.7}$$

The probability for the secondary process to contain k+1 pulses is equal to the probability of exactly k of the Δt_i intervals to be less than τ_c and the (k+1)-st to be greater than τ_c:

$$P_{k+1} = \left[\int_0^{\tau_c} g(x)\, dx \right]^k \int_{\tau_c}^{\infty} g(y)\, dy \tag{1.5.8}$$

Substituting (1.5.7) and performing the integration we receive:

$$P_{k+1} = \left[1 - e^{-\nu \tau_c} \right]^k e^{-\nu \tau_c} \tag{1.5.9}$$

To find the probability density function for the duration of the multiple user noise pulses given by (1.5.4) we have to perform the convolution of the density functions of all k of the Δt_i intervals and of the (k+1)-st primary pulse. Since it is required for the intervals Δt_i that form the secondary process to be shorter than τ_c their probability density function can be found as follows:

$$g_s(x) = \frac{g(x)}{\int_0^{\tau_c} g(y)\, dy} \tag{1.5.10}$$

Or substituting (1.5.7) into (1.5.10) we receive:

$$g_s(x) = \frac{\nu\, e^{-\nu x}}{1 - e^{-\nu \tau_c}} \tag{1.5.11}$$

where:

$$0 \leq x \leq \tau_c$$

For the probability density function of the (k+1)-st pulse we have:

$$g_{k+1} = \delta(\tau - \tau_c) \tag{1.5.12}$$

since its duration is deterministic.

The characteristic function for the density $g_s(x)$ is:

$$L_{g_s}(x) = \int_0^{\tau_c} g(s)\, e^{-s\xi}\, d\xi \tag{1.5.13}$$

or using (1.5.11) and (1.5.12) we receive:

$$L_{g_r}(s) = \frac{\nu}{s+\nu} \frac{1-e^{-(s+\nu)\tau_c}}{1-e^{-\nu\tau_c}} \tag{1.5.14}$$

and

$$L_{g_{(k+1)}}(s) = e^{-s\tau_c} \tag{1.5.15}$$

The probability density function $f(\tau)$ for the durations of the multiple user noise pulses is the average over all possible values of k:

$$f(\tau) = \sum_{k=0}^{\infty} P_{k+1}\, h_{k+1}(\tau)\, U(\tau - k\tau_c) \tag{1.5.16}$$

where $h_{k+1}(\tau)$ is the probability density function for the secondary pulse that contains exactly k+1 primary pulses.

For arbitrary k we have the characteristic function:

$$L_h(s) = \nu^k \left[\frac{1-e^{-(\nu+s)\tau_c}}{(\nu+s)\,(1-e^{-\nu\tau_c})}\right] e^{-s\tau_c} \tag{1.5.17}$$

Using (1.5.9) and (1.5.17) we receive the characteristic function for the probability density function (1.5.16):

$$L_f(s) = \sum_{k=0}^{\infty} \frac{\nu}{(\nu+s)^k} \left[1-e^{-(\nu+s)\tau_c}\right]^k e^{-(\nu+s)\tau_c} \tag{1.5.18}$$

or:

$$L_f(s) = e^{-(\nu+s)\tau_c} \sum_{k=0}^{\infty} \nu^k \left[\frac{1-e^{-(\nu+s)\tau_C}}{\nu+s}\right]^k \tag{1.5.19}$$

It can be observed that:

$$\frac{1 - e^{-(\nu+s)\tau_c}}{\nu + s} < 1 \qquad (1.5.20)$$

Then the sum in (1.5.19) represents the geometric progression and can be written as follows:

$$\sum_{k=0}^{\infty} \nu^k \left[\frac{1 - e^{-(\nu+s)\tau_c}}{\nu + s}\right]^k = \frac{\nu + s}{s + \nu\, e^{-(\nu+s)\tau_c}} \qquad (1.5.21)$$

then:

$$L_f(s) = \frac{(\nu + s)\, e^{-(\nu+s)\tau_c}}{s + \nu\, e^{-(\nu+s)\tau_c}} \qquad (1.5.22)$$

and the corresponding probability density function:

$$f(\tau) = e^{-\nu\tau_c}\, \delta(\tau-\tau_c) + \nu e^{-\nu\tau_c}\, U(\tau-\tau_c) + \sum_{k=1}^{\infty}(-1)^k \nu^k\, e^{-\nu(k+1)\tau_c} \quad x$$

$$\frac{\left[\tau - (k+1)\tau_c\right]^k}{(k-1)!} \left\{1 + \frac{\nu}{k}\left[\tau - (k+1)\tau_c\right]\right\} U\left[\tau-(k+1)\tau_c\right] \qquad (1.5.23)$$

As it can be seen from (1.5.23) there is some finite probability for the pulses with durations equal to τ_c. One can expect the number of these pulses to decrease as the number of interfering users increases due to increasing probability of pulse overlapping.

The probability to find the interference signal at any time is equal to the probability that during the interval τ_c prior to that instant at least one event of the primary Poisson process occurred:

$$P_x = 1 - e^{-\nu\tau_c} \tag{1.5.24}$$

The average pulse rate can be found as a derivative of this probability:

$$\overline{\mu_x} = \frac{dP_x}{d\tau_c} = \nu\, e^{-\nu\tau_c} \tag{1.5.25}$$

And the average pulse width:

$$\overline{\tau_x} = \frac{P_x}{\overline{\mu_x}} = \frac{1 - e^{-\nu\tau_c}}{\nu e^{-\nu\tau_c}} \tag{1.5.26}$$

We just derived the expression for the probability density function for the pulse durations of the multiple users noise. We also found the average duration, rate and duty cycle of the interfering pulses. The main assumptions to keep in mind when applying these parameters is the Poisson approximation of the process of the arrivals of the pulses from all users and the total randomness of the PRIS codes intervals.

The probability for the pulses of x(t) signal to exceed some value τ can be found as follows:

$$F_{c,x}(\tau) = 1 - \int_0^{\tau} f(\xi)d\xi \tag{1.5.27}$$

This is the complementary integral distribution function. The Laplace transform of this function can be found using the following expansion:

$$L_{F_{c,x}}(s) = \frac{1}{s} - \frac{L_f(s)}{s} \tag{1.5.28}$$

Substituting (1.5.22) into (1.5.28) we receive:

$$L_{F_{c,x}}(s) = \frac{1 - e^{-(s+\nu)\tau_c}}{s + \nu e^{-(s+\nu)\tau_c}} \tag{1.5.29}$$

By taking the inverse transform we receive:

$$F_{c,x}(\tau) = 1 + \sum_{k=1}^{\infty} (-1)^k \, \nu^{k-1} \, e^{-\nu k \tau_c} \, \frac{(\tau - k\tau_c)^{k-1}}{(k-1)!}$$

$$\left[1 + \frac{\nu}{k}\,(\tau - k\tau_c)\right] U(\tau - k\tau_c) \tag{1.5.30}$$

We will use this expression very often when analyzing the CDMA systems performance.

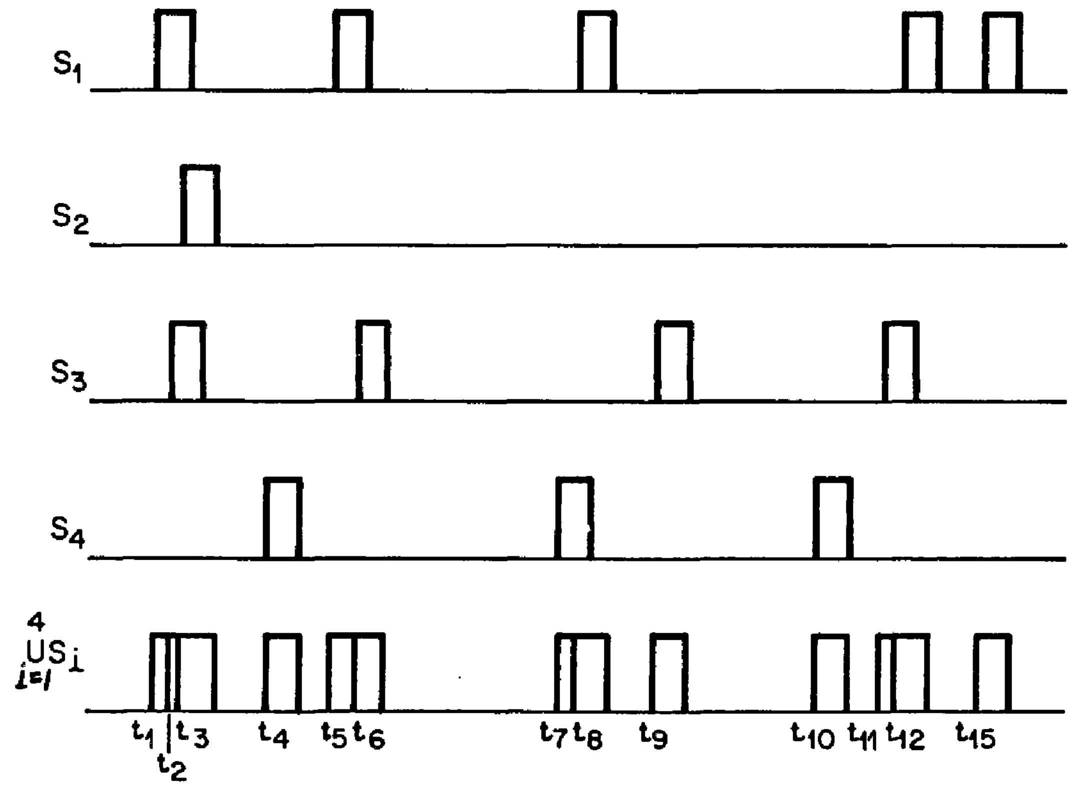

Fig.1.11. OOK/OR Channel: Multiple User Noise

1.6 CDMA COMMUNICATIONS OVER OOK/ADDER CHANNEL

In the Adder Channel the optical signals from multiple sources are added resulting in a multi-level signal as it is shown in Fig.1.12. Multiple user pulses while having Poisson distribution of the arrival times have different distributions of pulse durations on different levels.

Adder channel communications could offer better throughput due to information embedded in the multi-level signal. But in the optical channel it does not seem to be practical because of the high dynamic range of the signal required. It can be used only for systems with few users. In the mean time the mathematical analysis of the multiple user interference in this channel is rather complicated and is not attempted in this research. For a thorough analysis of the Adder channel the non-linearity and limitations of the receiver dynamic range have to be considered as well.

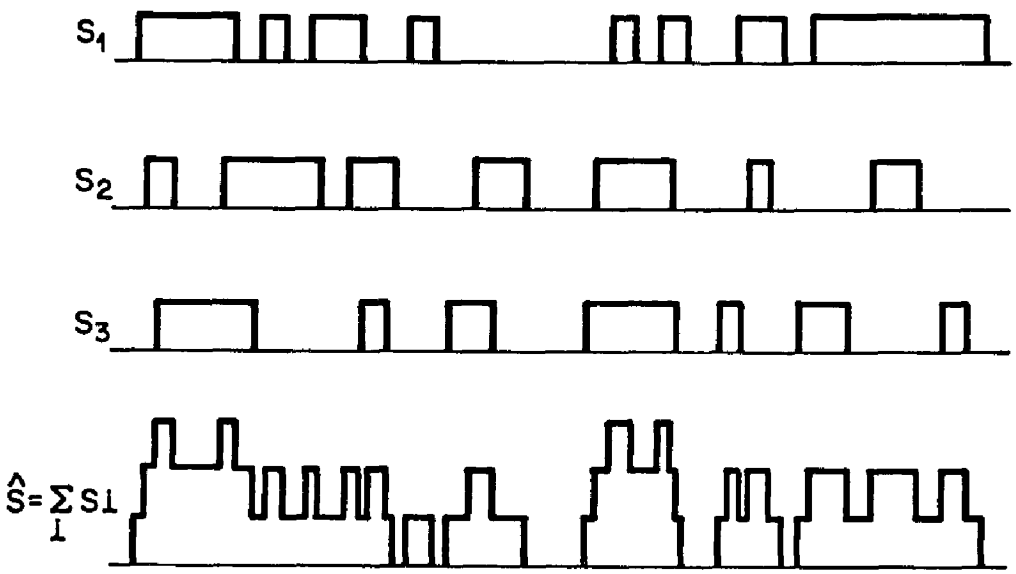

Fig.1.12. Multiple User Noise in OOK/ADDER Channel

1.7 CONCLUSIONS

We presented the motivation for the research which is to create and analyze fiber optic Code Division Multiple Access signaling schemes that will allow construction of a collision resistant Local Area network suitable for real time communication.

Some important properties of pseudo random sequences were described and a simulation study was performed of asynchronous sums of the Gold Sequence sets for the purpose of illustrating the phenomena of the multiple user noise in the Fiber Optic Direct Sequence systems.

A new type of sequences was defined and called Pseudo Random Interval Sequences. Methods of constructing of non-optimal Pseudo Random Interval Sequences out of the PN codes and quasi-optimal sequences out of One-Coincidence sequences were described.

We modeled the CDMA OOK/OR Channel assuming Poisson arrivals of the multiple user signal pulses and determined the statistical properties of the multiple user noise that will be used in subsequent chapters for the analysis of CDMA systems.

2. CDMA DIRECT SEQUENCE COMMUNICATION

2.1 INTRODUCTION

Direct Sequence communications over HF channel is the most popular among all types of spread spectrum signaling due to the advantages it offers, [1]. The main idea behind this technique is as follows. The data is being modulated by a pseudo random sequence of a rate that is higher than the one of the data signal. The receiver generates it's own replica of the pseudo random code and performs detection by crosscorrelating the local replica with the incoming signal and discriminating the crosscorrelation function at a fixed threshold.

In the Intensity Modulated/Direct Detection, (IM/DD), fiber optic systems the properties of the pseudo random sequences that were described in chapter one can not be fully utilized due to the specifics of the positive signaling and therefore the adoption of this technique is not at all straight-forward.

In this research we conduct rather limited analysis of the DS spread spectrum communications. The following sections illustrate some specifics of the fiber optic OR and ADDER channels DS signaling that we propose and show the results of the simulation studies of the OOK/ADDER/DS systems.

2.2 OOK/OR DIRECT SEQUENCE CHANNEL

In the OOK/OR/DS Channel the PN-sequence is modulo two added to the data bit stream. So if the data bit is zero the code is unchanged, and if data bit is one the code is complemented. This process is illustrated in Fig.2.1.

Digital EXOR Receiver

The base-band signal recovery of the signal in the receiver is shown in Fig.2.2. We assume perfect synchronization of the transmitter and the receiver in terms of the timing recovery as well as perfect Synchronization of the transmitter's and receiver's PN-code generators. A local PN-Sequence replica is modulo two added to the received signal thus despreading it and then the Integrate and Dump algorithm is being performed.

Correlator Receiver

The block diagram of a correlator receiver for a OOK/OR/DS channel is shown in Fig.2.3.

The received signal S(t) is correlated with $\overline{c_{r_i}(t)}$, the inverted bipolar replica of the PN-Code and the output is discriminated at zero.

The reference code can be written as follows:

$$c_{r_i}(t) = \sum_{j=1}^{L} (-1)^{C_{ij}} \psi(t - jT_c) \tag{2.2.1}$$

Then the correlation process yields the following correlation function:

$$R_{Sc_{r_i}}(LT_c) = \int_{kLT_c}^{(k+1)LT_c} \sum_{j=1}^{L} [d_{i,k} \oplus C_{ij}\psi(t-jT_c)] [(-1)^{C_{ij}} \psi(t-jT_c)] \, dt \qquad (2.2.2)$$

By interchanging linear operators we receive:

$$R_{Sc_{r_i}}(LT_c) = \sum_{j=1}^{L} \int_{kLT_c}^{(k+1)LT_c} (d_{i,k} \oplus C_{ij}) (-1)^{C_{ij}} \psi(t-jT_c) \, dt \qquad (2.2.3)$$

or:

$$R_{Sc_{r_i}}(LT_c) = \sum_{j=1}^{L} (-1)^{C_{ij}} \int_{(kL+j-1)T_c}^{[(k+1)L+j]T_c} (d_{i,k} \oplus C_{ij}) \psi(t-jT_c) \, dt \qquad (2.2.4)$$

The output of the correlator is being sampled at kLT_c instants and the sampled value

$$D_{i,k} = R_{Sc_{r_i}}(LT_c)$$

is discriminated at a fixed threshold to estimate the data bit.

Since the channel is digital and therefore effectively the hard-limiting of the signal takes place the value of $D_{i,k}$ is bounded:

$$\begin{aligned} D_{i,k_{d_{i,k}=1}} &\leq n_1 \; T_c \\ D_{i,k_{d_{i,k}=0}} &\geq n_0 \; T_c \end{aligned} \qquad (2.2.5)$$

Where:

n_1 - is the number of positive chips in the one-pattern

n_0 - is the number of positive chips in the zero-pattern

If maximal length sequences are used to modulate the data at the transmitter then:

$$n_1 = \frac{L-1}{2}$$

$$n_0 = \frac{L-1}{2} + 1$$

In case when the difference in the number of pulses in the one- and zero-pattern is significantly large the transition probabilities of the channel will depend on this difference. This kind of signaling is not desirable for symmetric sources.

Applications of OOK/OR/DS channel to multiple access communications is very limited due to it's poor performance which is explained by non-optimal signal design. It will become more clear when we analyze the Time-Hopped channel.

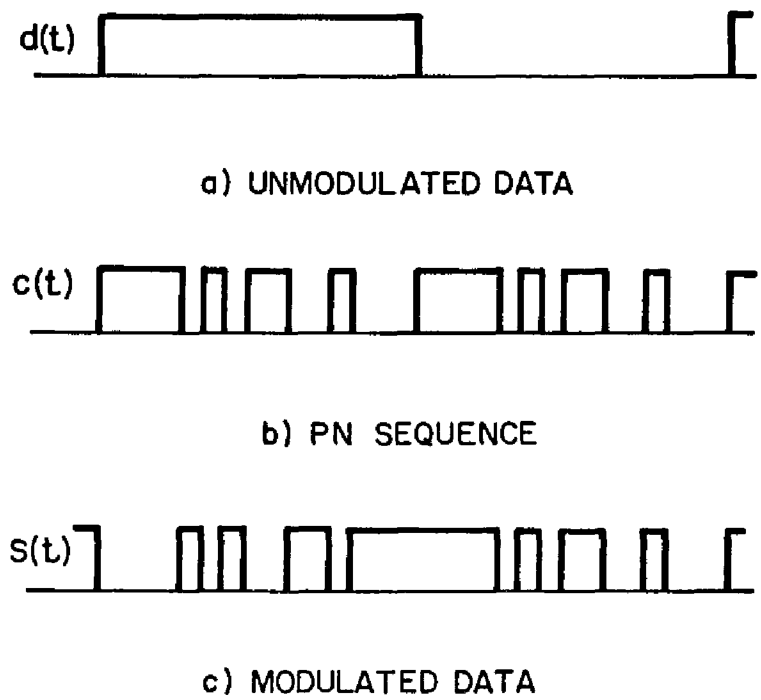

Fig.2.1 Modulation of Data by a PN-Sequence.

Fig.2.2 Base-band Signal Recovery in EXOR Receiver

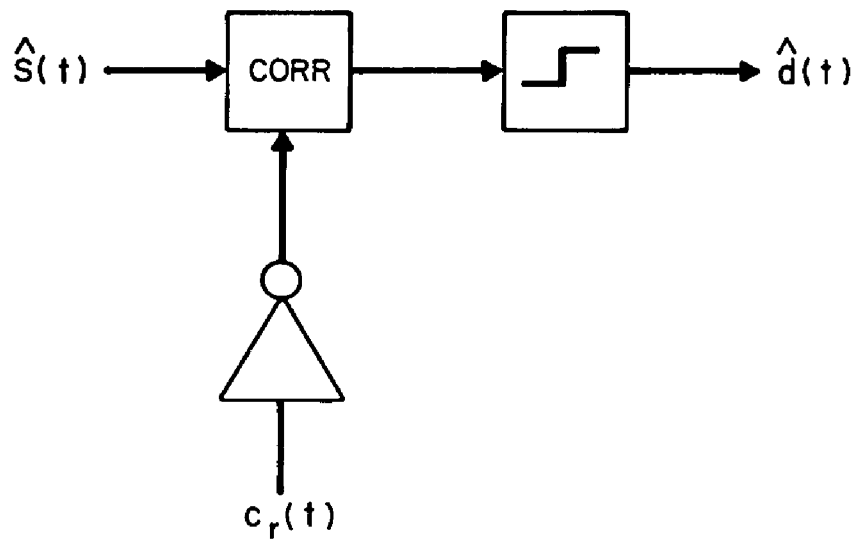

Fig.2.3 Correlator Receiver.

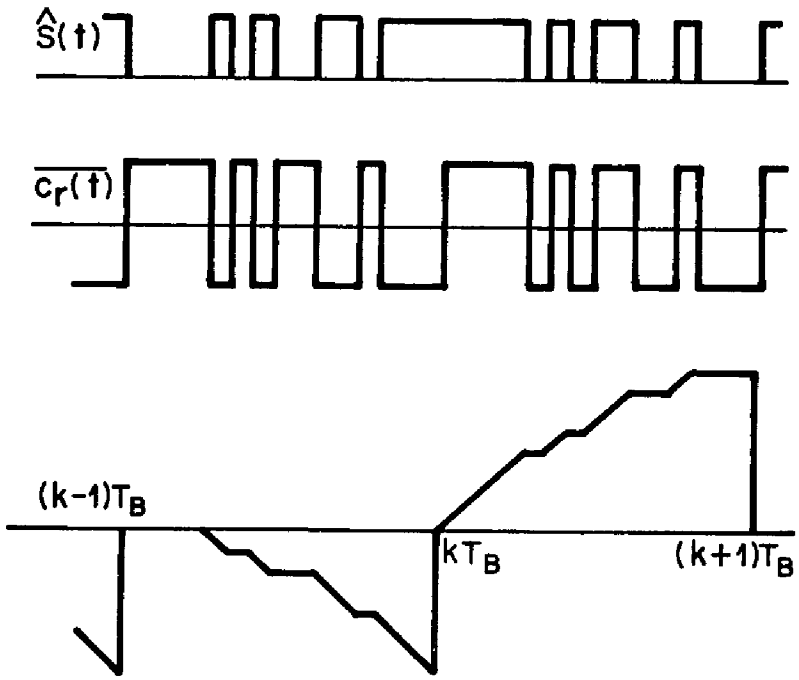

Fig.2.4 Base-band Signal Recovery in Correlator Receiver

2.3 OOK/ADDER/DS CHANNEL

In this section we will show the results of the simulation study of the OOK/ADDER/DS Channel. The study was performed on a time domain simulator. Fig.2.5 illustrates the block-diagram of the simulated system. Multiple users were assigned unipolar Gold codes generated by pairs of shift registers.

A special random numbers generator produced time-offsets for each user. The number of users varied from one to the maximum possible that corresponds to the number of Gold codes in the set.

The receiver was realized as a correlator that crosscorrelated a local bipolar replica of first user's code with the incoming multi-level signal. The bipolar local replica was synchronized to the unipolar code of the first user. The crosscorrelation signal was discriminated at zero and errors were counted.

The results of the study is shown in Fig.2.6. As it can be seen from the figure the system displays 10^{-5} probability of error when the number of users is less than 10 % of the processing gain K_p .

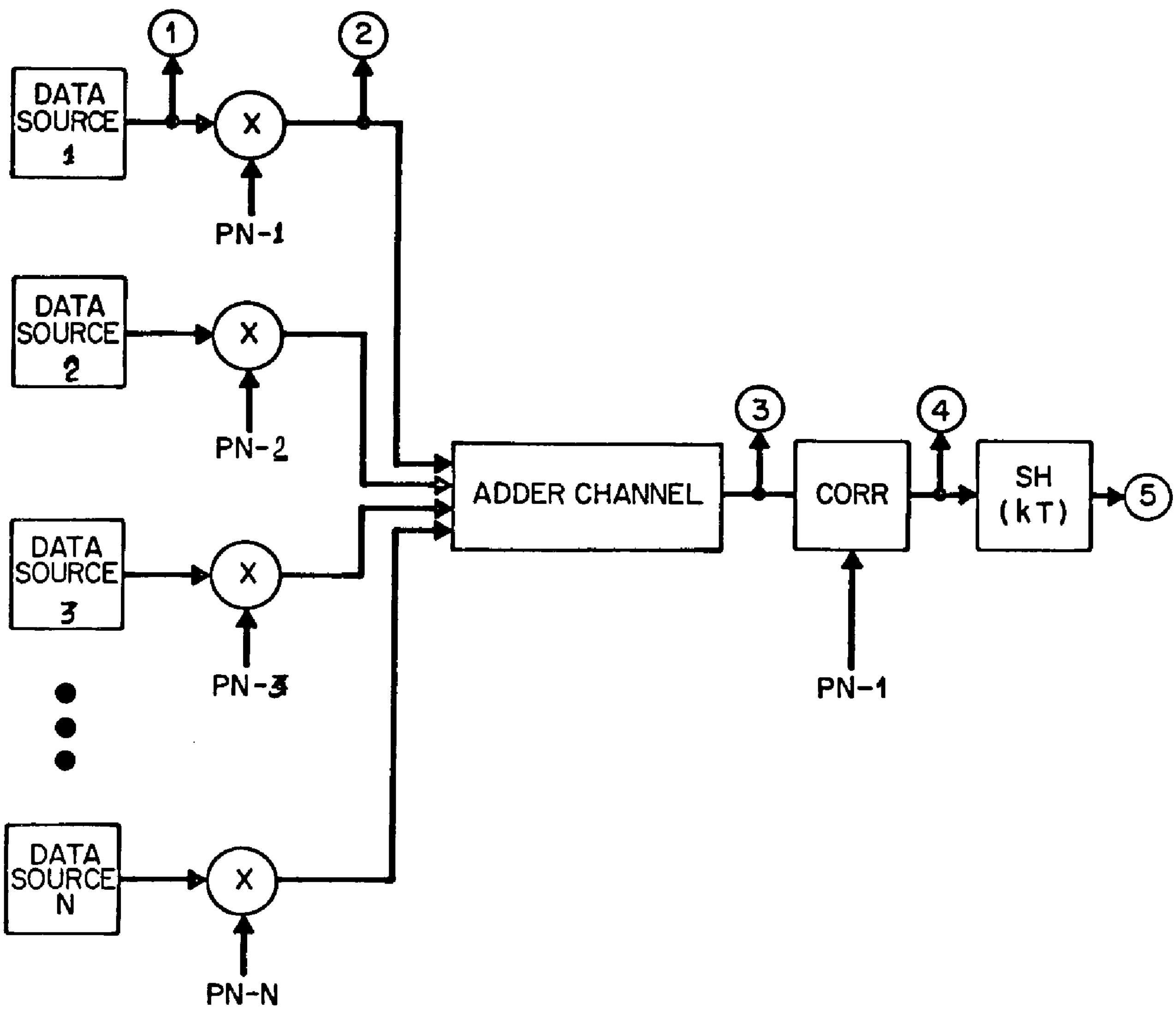

Fig.2.5. OOK/ADDER/DS System Simulation

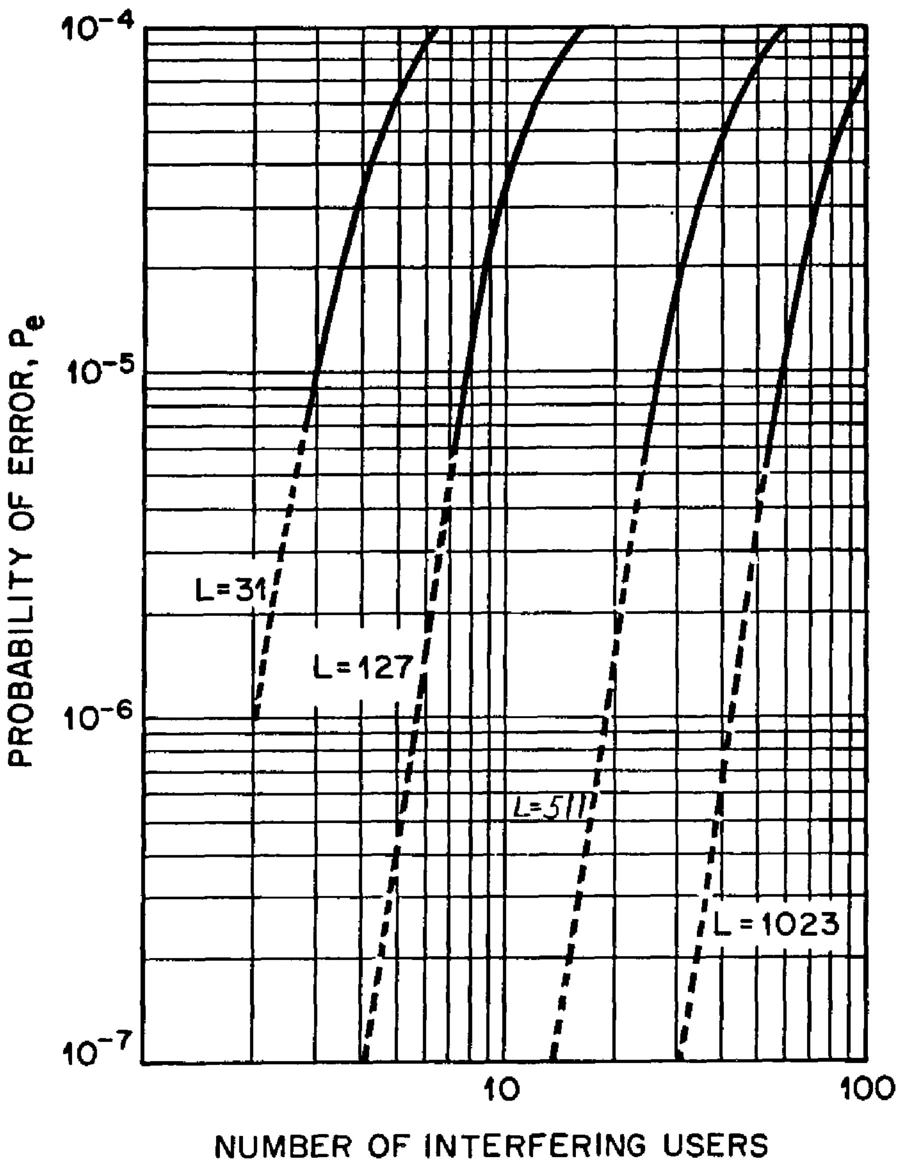

Fig.2.6. OOK/ADDER/DS System: Probability of Error

2.4 CONCLUSIONS

We described the OOK/OR/DS and OOK/ADDER/DS systems and performed the simulation study of the OOK/ADDER/DS channel performance. As it could be expected due to the positive signaling and therefore non-gaussian statistics of the multiple user noise the fiber optic Direct Sequence CDMA channel demonstrates less than 10 % throughput for 10^{-5} probability of error. In addition we have to point out rather high dynamic range of the light power required that limits applications of this technique.

3. TIME-HOPPED CDMA SYSTEM

3.1 INTRODUCTION

An effective way of Code Division Multiplexing in the OOK/OR channel is to use signals with low duty cycles.

The method we propose and analyze in this chapter employs modulation of the data by sequences that have pseudo random intervals between the pulses. It is called Time Hopping (TH). The sequences that are used in this system are called Pseudo Random Intervals Sequences (PRIS). They are described in chapter one.

We will call the Time Hopping process Slow if there is one or less time hops corresponding to one data bit, and we will call Fast Time Hopping the method when data is modulated by a sequence with pseudo random time intervals between the consecutive pulses and with more than one of such pulses (Time Hops) per data bit.

The OOK/OR channel where Time Hopping is used to spread the data we will denote as: OOK/OR/TH Channel.

In this research we address only systems that employ the Fast Hopping method.

The process of modulating the data signal by a PRIS code derived from a PN-Sequence is shown in Fig.3.1. The data signal in this case is modulo two added to the PN code and then the resulting signal is mapped into the time intervals sequence by generating short pulses corresponding to positive transitions in the signal. The synchronization pulses are then may be inserted to serve as timing reference for the receiver.

The process of data recovery is depicted in Fig.3.2. The receiver contains a matched filter which can be an electronic or optical correlator. Fig.3.2 illustrates the operation of an electronic correlator. The reference code W(t) is crosscorrelated with the incoming signal S(t) which is the resultant signal of the optical to electrical conversion process that takes place at the front end of the receiver. The crosscorrelation function is then sampled at kT_d instants and discriminated at a fixed threshold. Another type of a correlator is the one that employs Tapped Delay Lines (TDL) that are matched to the time intervals of the target code. It is called TDL correlator. The diagram of the TDL correlator receiver is shown in Fig.3.3. The Tapped Delay Line itself can be realized in electronic, [50], or in optical domain, [10], which will increase potentials of the system since the parameters of the receiver will be less sensitive to environment variations.

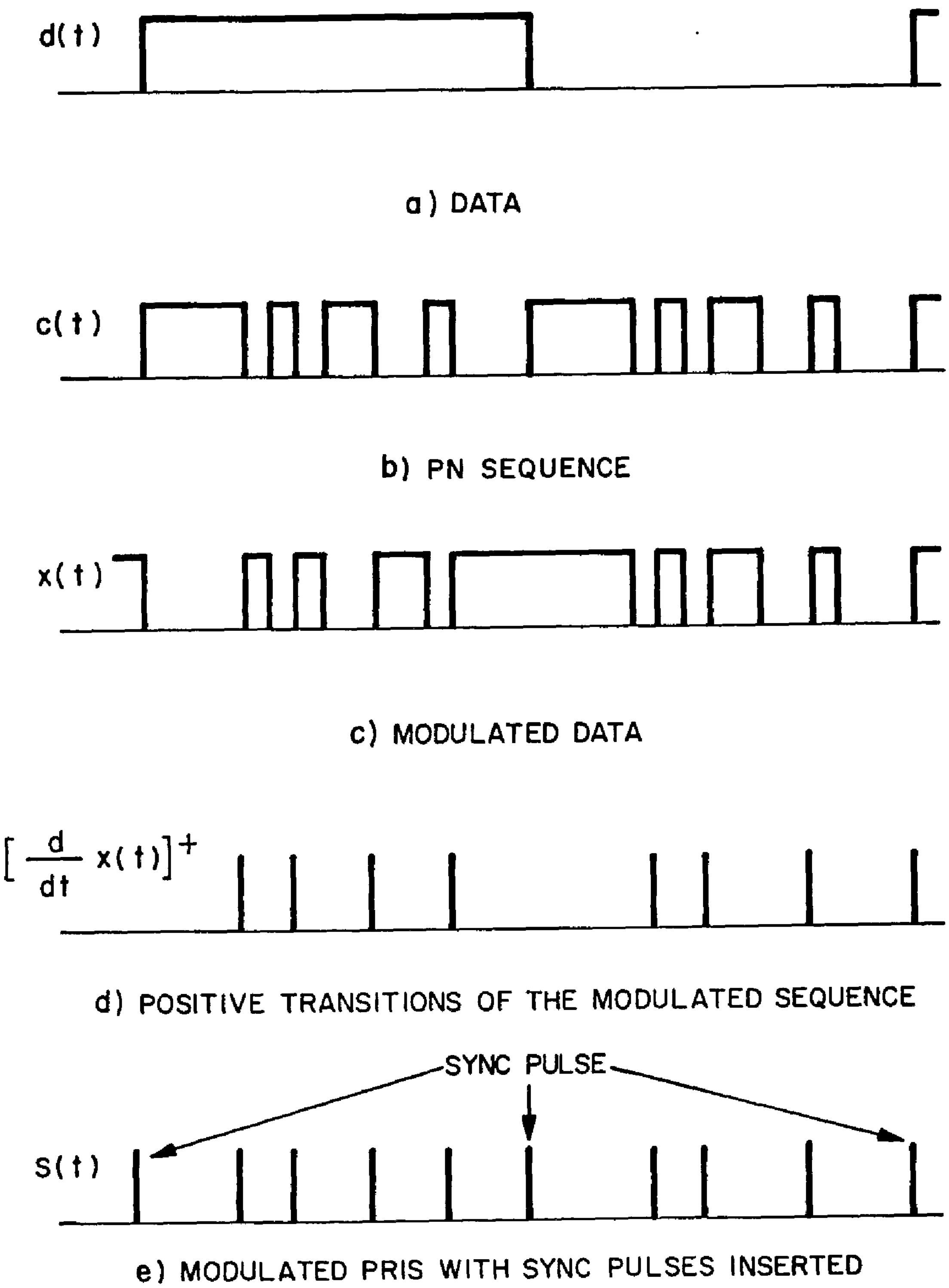

Fig.3.1 OOK/OR/TH Channel: Modulation of Data by PRIS Code

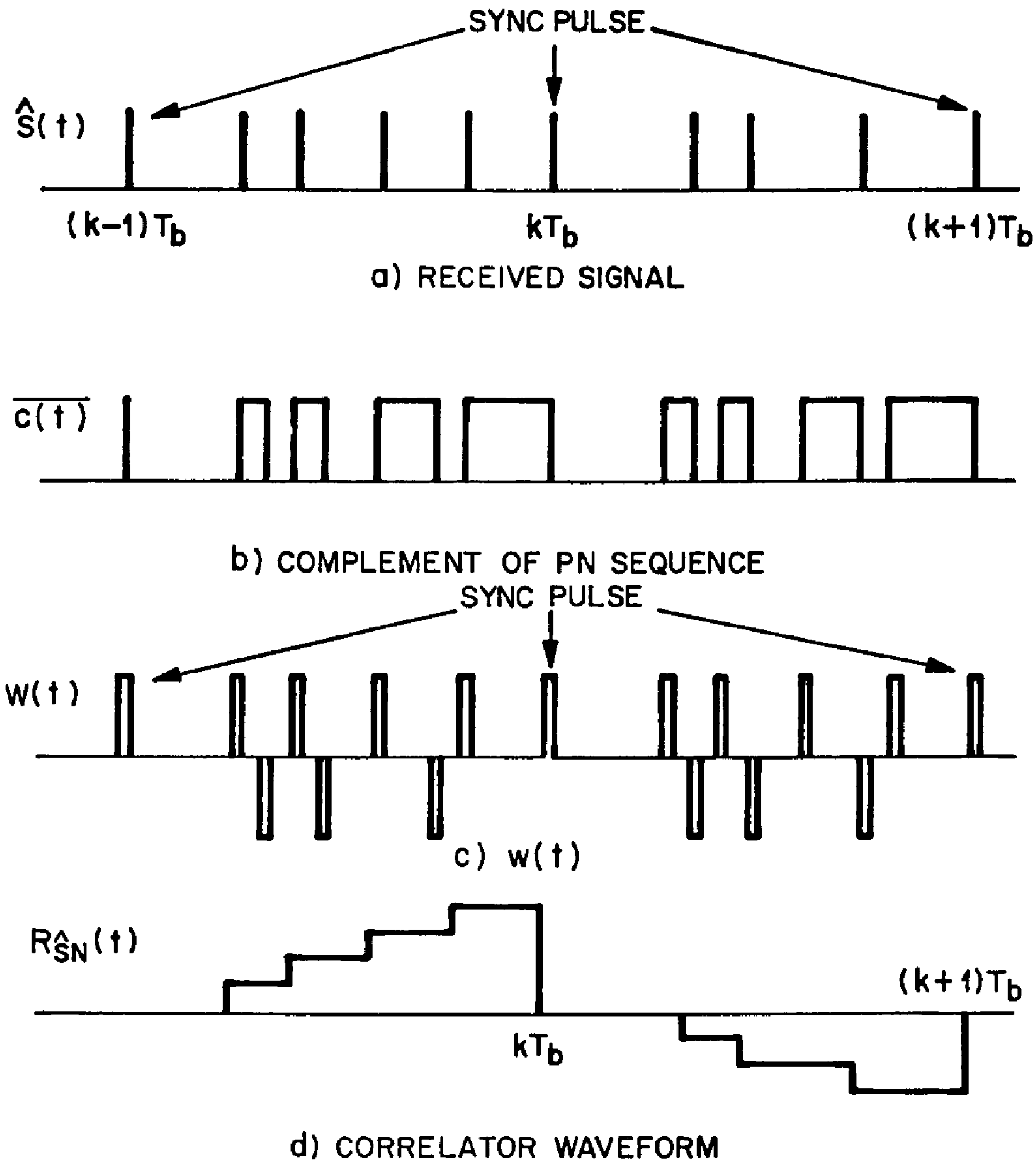

Fig.3.2 OOK/OR/TH Channel: Data Recovery

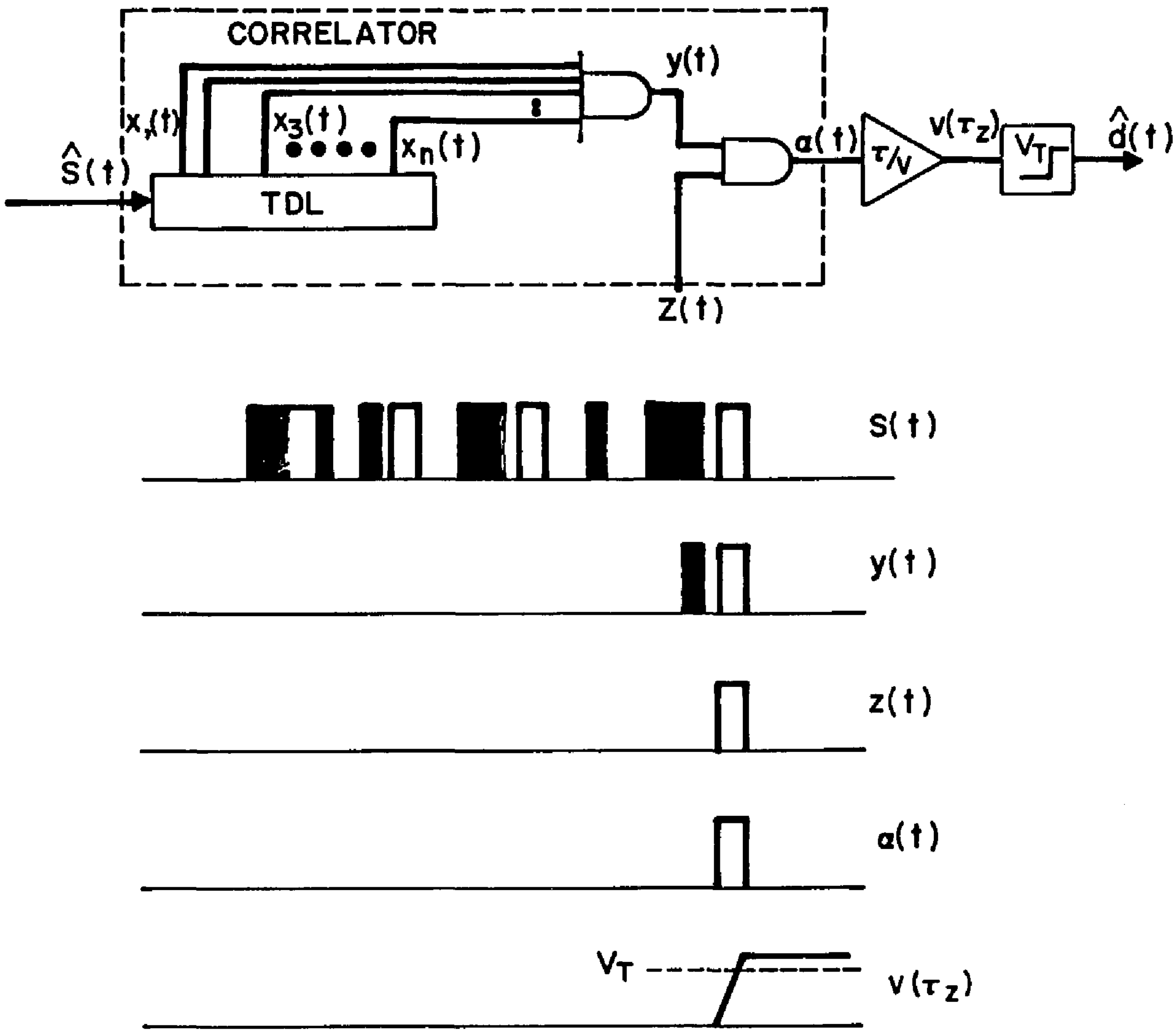

Fig.3.3 OOK/OR/TH System: TDL Correlator Receiver

3.2 MULTIPLE USER INTERFERENCE IN OOK/OR/TH SYSTEM

It is necessary to determine the characteristics of the multiple user noise in the system. One has to realize that the properties of this noise and its effect on each users signal is very much dependent on the signaling scheme employed and the receiver design.

For binary data communications we propose two different signaling schemes. The first scheme to be analyzed is what we call Passive Pause Signaling, (PPS), uses only one PRIS code per user to communicate the data value of one. When the data value is zero no signal is being generated. The second scheme uses two sequences per user as i it is shown in Fig.3.1. One is to represent the data value of one the other is to represent the data value of zero. This concept can be generalized for m-ry signaling where each user is assigned m distinct PRIS codes.

First we analyze the performance of the OOK/OR/TH system that employs passive pause signaling.

Let:

N be the number of interfering users,

n is the number of pulses in the one-pattern (hops per bit),

T_d is the duration of the data bit,

τ_c is the duration of the time hop,

p(0) and p(1) are the probabilities of zero and one in the data stream.

On the average each user contributes ν_i pulses per second to the multiple user noise. This parameter depends on the number of hopes per bit, the probability of one in the data signal and the data bit rate:

$$\nu_i = \frac{n\ p(1)}{T_d} \tag{3.2.1}$$

If the number of interfering users is large (more than ten) it is safe to assume that the start times of the interfering pulses have Poisson distribution with the parameter ν:

$$\nu = N\ \nu_i = \frac{N\ n\ p(1)}{T_d} \tag{3.2.2}$$

This is the worst case value since it is computed assuming infinite data sources. In other words for the sake of this analysis we consider each of the N users and the target transmitter constantly transmitting data.

3.3 PROBABILITY OF ERROR IN THE OOK/OR/TH SYSTEM

We will now analyze performance of the system that employs Tapped Delay Line receiver and the Passive Pause Signaling, (PPS). The diagram of the receiver is shown in Fig.3.3. The receiver acts as a matched filter for the target users signal if the delays DL_j are mirror images of the intervals of the PRIS code assigned to the user.

The signal from the Optical to Electrical, (O/E), converter is routed to the delay lines whose outputs are connected to the n-input AND gate. The output of the AND gate is strobed by the synchronization pulses z(t). After that an Integrate-And-Dump operation is performed. The decision about the transmitted data bit value is done by comparison of the integrator output with a fixed threshold.

If Passive Pause Signaling is employed then the OOK/OR/TH channel can be viewed as Z-channel assuming no pulse jitter in the signal is present. Even though we make this assumption the receiver which is depicted if Fig.3.3 is designed with the notion of some uncertainty in the positions of the pulses in the pattern. The sensitivity of the receiver to the pulse jitter can be reduced by lowering the threshold in the comparator. But one should realize that this will increase the probability of false detection.

The assumption of no jitter in the signal and perfect synchronization between the transmitter and the receiver will lead to no loss of the target user signal when data value of one is transmitted and some false signals detected when the transmitted data value is zero.

To determine the probability of error we have to find the parameters of the multiple user noise signal y(t) at the output of the AND gate, Fig.3.3.

Due to the assumption of completely random codes we can also assume that the pulse trains $x_i(t)$ are statistically identical. Following [50] and [8] for the overlapping pulse train y(t) the complementary integral distribution can be found as follows:

$$F_{c,y}(\tau) = \left[1 - \frac{1}{\overline{\tau}_x} \int_0^{\tau} F_{c,x}(\xi) d\xi \right]^{n-1} F_{c,x}(\tau) \qquad (3.3.1)$$

From (1.5.28) we observe that:

$$F_{c,x}(\tau) = 1, \qquad \text{for } \; 0 \leq \tau \leq \tau_c$$

Then for the same interval of the τ values:

$$F_{c,y}(\tau) = \left(1 - \frac{\tau}{\overline{\tau}_x}\right)^{n-1} \qquad (3.3.2)$$

Substituting (1.5.26) into (3.3.2) we receive for the complementary integral distribution of the pulse durations of the signal y(t):

$$F_{c,y}(\tau) = \left[1 - \frac{\nu\, \tau\, e^{-\nu \tau_c}}{1 - e^{-\nu \tau_c}}\right]^{n-1} \qquad (3.3.3)$$

A necessary part of the detection process is strobing the output of the AND gate by the synchronization signal z(t). The period of the sync pulses is equal to the period of the data T_d . The duration of the sync pulses τ_z is not greater than that of the user signal pulses τ_c to reduce the probability of false detection.

The pulse rate of the signal z(t) is:

$$\mu_z = \frac{1}{T_d} \tag{3.3.4}$$

The rate of the y(t) pulses can be found from the following formula, [8]:

$$\overline{\mu_y} = \prod_{i=1}^{n} \overline{\mu_{x_i}}\,\overline{\tau_{x_i}} \sum_{i=1}^{n} \frac{1}{\overline{\tau_{x_i}}} \tag{3.3.5}$$

Then:

$$\overline{\mu_y} = n\,\overline{\mu_x}\,P_x^{\,n-1} \tag{3.3.6}$$

And the average duration of the y(t) pulses:

$$\overline{\tau_y} = \frac{P_y}{\overline{\mu_y}} = \frac{\prod_{i=1}^{n} \overline{\mu_{x_i}}\,\overline{\tau_{x_i}}}{\prod_{i=1}^{n} \overline{\mu_{x_i}}\,\overline{\tau_{x_i}} \sum_{i=1}^{n} \frac{1}{\overline{\tau_{x_i}}}} \tag{3.3.7}$$

or since the pulse trains are statistically identical:

$$\overline{\tau_y} = \frac{\overline{\tau_x}}{n} \tag{3.3.8}$$

For the strobed signal a(t) we receive using formulas identical to (3.3.5) and (3.3.7):

$$\overline{\mu_a} = \overline{\mu_y}\,\mu_z\,(\overline{\tau_y} + \tau_z)$$

$$\overline{\tau_a} = \frac{\overline{\tau_y}\ \tau_z}{\overline{\tau_y} + \tau_z} \tag{3.3.9}$$

The signal a(t) is integrated:

$$V(t) = \frac{1}{\tau_z} \int_0^t a(\xi)\, d\xi \tag{3.3.10}$$

The output of the integrator is sampled at the instants of time immediately following the z(t) pulse. The decision about the transmitted data value is made based on the comparison of the integrator output $V(\tau_z)$ to a fixed threshold V_T . If $V(\tau_z) \geq V_T$ the decision is in favor of data value of one, otherwise the decision is in favor of zero.

In ideal situation when there is absolutely no jitter in the signal the value of threshold can be made very close to the integrator output when no interference is present. But in reality there will be some loss in the value of the signal at the output of the integrator due to non-perfect tracking as well as other factors. Therefore the value of the threshold has to be selected lower than maximum possible. This in it's turn will increase the probability of false detection.

The pulses a(t) will cause false detection to take place only if their durations fall within the interval:

$$\tau_T \leq \tau \leq \tau_z \tag{3.3.11}$$

The average rate of these pulses will be:

$$\overline{\mu_T} = \overline{\mu_a}\ P_r(\tau \geq \tau_T) \tag{3.3.12}$$

where $P_r(\tau \geq \tau_T) = F_{c,a}(\tau_T)$ is the probability of the a(t) pulses to last longer than τ_T. The complementary distribution $F_{c,a}$ can be found from the following formula, [8], [50]:

$$F_{c,a}(\tau) = \frac{\overline{\tau_a}}{\overline{\tau_z}} F_{c,z}(\tau) \left[1 - \frac{1}{\overline{\tau_y}} \int_0^{\tau} F_{c,y}(\xi)\, d\xi\right] + \frac{\overline{\tau_a}}{\overline{\tau_y}} F_{c,y}(\tau) \left[1 - \frac{1}{\tau_z} \int_0^{\tau} F_{c,z}(\xi)\, d\xi\right] \tag{3.3.13}$$

or substituting (3.3.3) into (3.3.13) we receive:

$$F_{c,a}(\tau) = \frac{1}{\overline{\tau_y} + \tau_z} \left(1 - \frac{\tau}{\overline{\tau_x}}\right)^{n-1} \left(\frac{\overline{\tau_x} - \tau}{n} + \tau_z - \tau\right) \tag{3.3.14}$$

for $\qquad 0 \leq \tau \leq \tau_z$

Then substituting (3.3.14) into (3.3.12) we receive the average rate of the multiple user noise pulses that can potentially cause false detections:

$$\overline{\mu_T} = \overline{\mu_a} \frac{1}{\overline{\tau_y} + \tau_z} \left(1 - \frac{\tau_T}{\overline{\tau_x}}\right)^{n-1} \left(\frac{\overline{\tau_x} - \tau_T}{n} + \tau_z - \tau_T\right) \tag{3.3.15}$$

The errors will occur only when data values of zero are transmitted thus the probability of error will depend on the a priori probability p(0):

$$P_e = \overline{\mu_T}\, T_d\, p(0) \tag{3.3.16}$$

Taking to consideration (3.3.9) we receive:

$$P_e = \overline{\mu_y} \left(1 - \frac{\tau_T}{\overline{\tau_x}}\right)^{n-1} \left(\frac{\overline{\tau_x} - \tau_T}{n} + \tau_z - \tau_T\right) p(0) \tag{3.3.17}$$

Or using (3.3.6) and (1.5.22) we finally receive the probability of error for the OOK/OR/TH system that employs Passive Pause Signaling:

$$P_e = n\, \nu\, e^{-\nu\tau_c}\, p(0) \left(1 - e^{-\nu\tau_c}\right)^{n-1} \left(1 - \frac{\tau_T}{\overline{\tau_x}}\right)^{n-1} \left(\frac{\overline{\tau_x} - \tau_T}{n} + \tau_z - \tau_T\right) \tag{3.3.18}$$

where:

$$\tau_T < \tau_z \le \tau_c$$

$$\nu = \frac{N\, n\, p(1)}{T_d}$$

We can express the average duration of the multiple user noise pulses via the number of interfering users and the parameters of the signal:

$$\overline{\tau_x} = \frac{1 - e^{-\frac{nN\tau_c}{2T_d}}}{\frac{nN}{2T_d}\, e^{-\frac{nN\tau_c}{2T_d}}} \tag{3.3.19}$$

Let us introduce a parameter K_f that we will call Bandwidth Expansion Coefficient:

$$K_f = \frac{T_d}{\tau_c} \tag{3.3.20}$$

Then the expression (3.3.19) becomes:

$$\overline{\tau_x} = \frac{1 - e^{-\frac{nN}{2K_f}}}{\frac{nN}{2T_d} e^{-\frac{nN}{2K_f}}} \tag{3.3.21}$$

And the probability of error:

$$P_e = \frac{1}{2}\left[1 - e^{-\frac{nN}{2K_f}}\left(1 + \frac{nN}{2}\frac{\tau_T}{T_d}\right)\right]^{n-1} \quad x$$

$$\left[1 - e^{-\frac{nN}{2K_f}}\left(1 + \frac{nN}{2}\frac{\tau_T}{T_d} - \frac{n^2N}{2}\frac{\tau_z}{T_d} + \frac{n^2N}{2}\frac{\tau_T}{T_d}\right)\right] \tag{3.3.22}$$

for $$p(1) = p(0) = \frac{1}{2}$$

We will now introduce the Strobing Factor:

$$K_z = \frac{\tau_z}{\tau_c} \tag{3.3.23}$$

It indicates the duration of the synchronization pulse as a fraction of the time-hop duration. And the Thresholding Coefficient:

$$K_T = \frac{V_T}{V_{max}} = \frac{\tau_T}{\tau_z} \tag{3.3.24}$$

This coefficient indicates the value of the threshold as a fraction of the maximum possible integrator output.

Then we can rewrite the expression for the probability of error:

$$P_e = \frac{1}{2}\left[1 - e^{-\frac{nN}{2K_f}}\left(1 + \frac{n}{2}\frac{N}{K_f}K_T K_z\right)\right]^{n-1} \quad x$$

$$\left[1 - e^{-\frac{nN}{2K_f}}\left(1 + \frac{n}{2}\frac{N}{K_f}K_T K_z - \frac{n^2}{2}\frac{N}{K_f}K_z + \frac{n^2}{2}\frac{N}{K_f}K_T K_z\right)\right] \tag{3.3.25}$$

To characterize the system performance it is convenient to introduce a parameter that we will call Channel Load and define as:

$$C_l = \frac{N}{K_f} \tag{3.3.26}$$

Channel load illustrates the channel utilization by indicating the number of interfering users in the CDMA system relative to the number of users that could be packed into a TDMA channel without overhead. The probability of error then becomes:

$$P_e = \frac{1}{2}\left[1 - e^{-\frac{nC_l}{2}}\left(1 + \frac{nK_T K_z}{2}C_l\right)\right]^{n-1} \quad x$$

$$\left[1 - e^{-\frac{nC_l}{2}} \left(1 + \frac{K_T - n + nK_T}{2} \, nK_z C_l\right)\right] \tag{3.3.27}$$

Fig.3.4 illustrates the curves of the probability of error for the OOK/OR/TH channel. As it can be seen from the figure the probability of error monotonically increases with increasing number of interfering users. The Bandwidth Expansion Coefficient $K_f = 127$ yields Bit Error Rate $P_e = 10^{-5}$ when the number of interfering users is approximately 25 and when 8 to 12 hops per bit PRIS code is being used. Fig.3.5 shows identical curves for $K_f = 255$. As the number of hops per bit increases it becomes more unlikely for the multiple user noise pulses to align in a way favorable to the appearance of a false pattern. But on the other hand the contribution of each user's signal to the system noise is greater when the number of hops per bit is large. These two factors cause existence of the optimal number of hops per bit for a given number of interfering users.

Fig.3.6 illustrates the Probability of Error as a function of the channel load and the number of hops per bit in the PRIS codes assigned to the users. These curves are applicable to any value of the Bandwidth Expansion Coefficient K_f .

Fig.3.7 illustrates the presence of the optimal number of hops per bit for a given channel load. The more users are interfering the lower is the optimal value of n. Luckily the range of the optimal values of n is rather small, but the sensitivity of the Bit Error Rate to the variation of n is very much noticeable. The designer might have to know the expected load when selecting the code set for the system. The dependence of the optimal number of hops per bit from the channel load is illustrated in Fig.3.8. For small loads larger codes will make false detection less probable, but for large channel loads the tendency is towards less hops per bit in order to reduce the system noise. Optimal n obviously yields the minimum achievable Probability of Error for all other parameters fixed, such as the duration of the sync pulse and the threshold in the decision making comparator.

Fig.3.9 illustrates the minimum achievable Probability of Error versus the channel load. It can be seen that Probability of Error can be 10^{-5} or better if the channel load does not exceed 21 %.

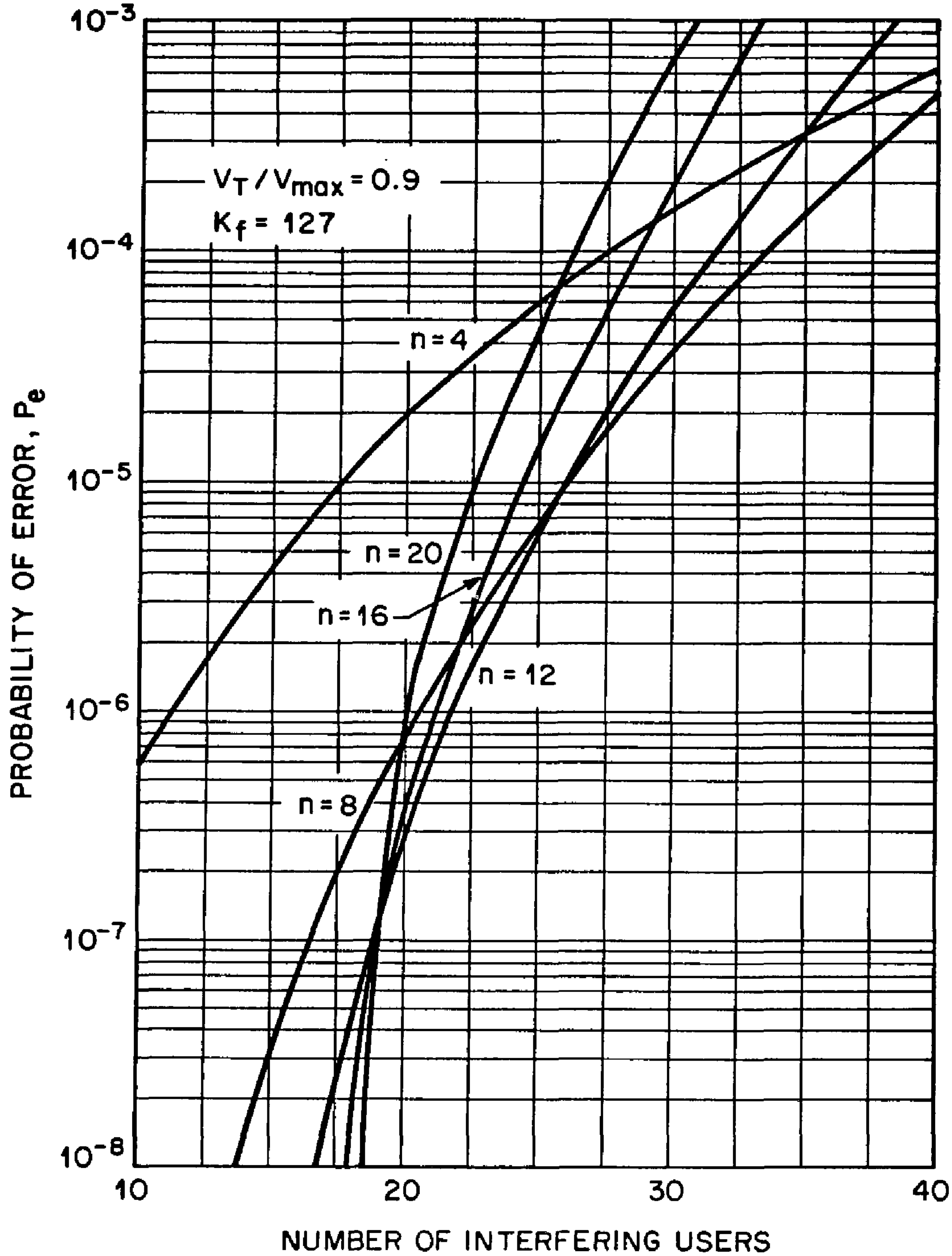

Fig.3.4. OOK/OR/TH Channel with PPS: Probability of Error vs Number of users

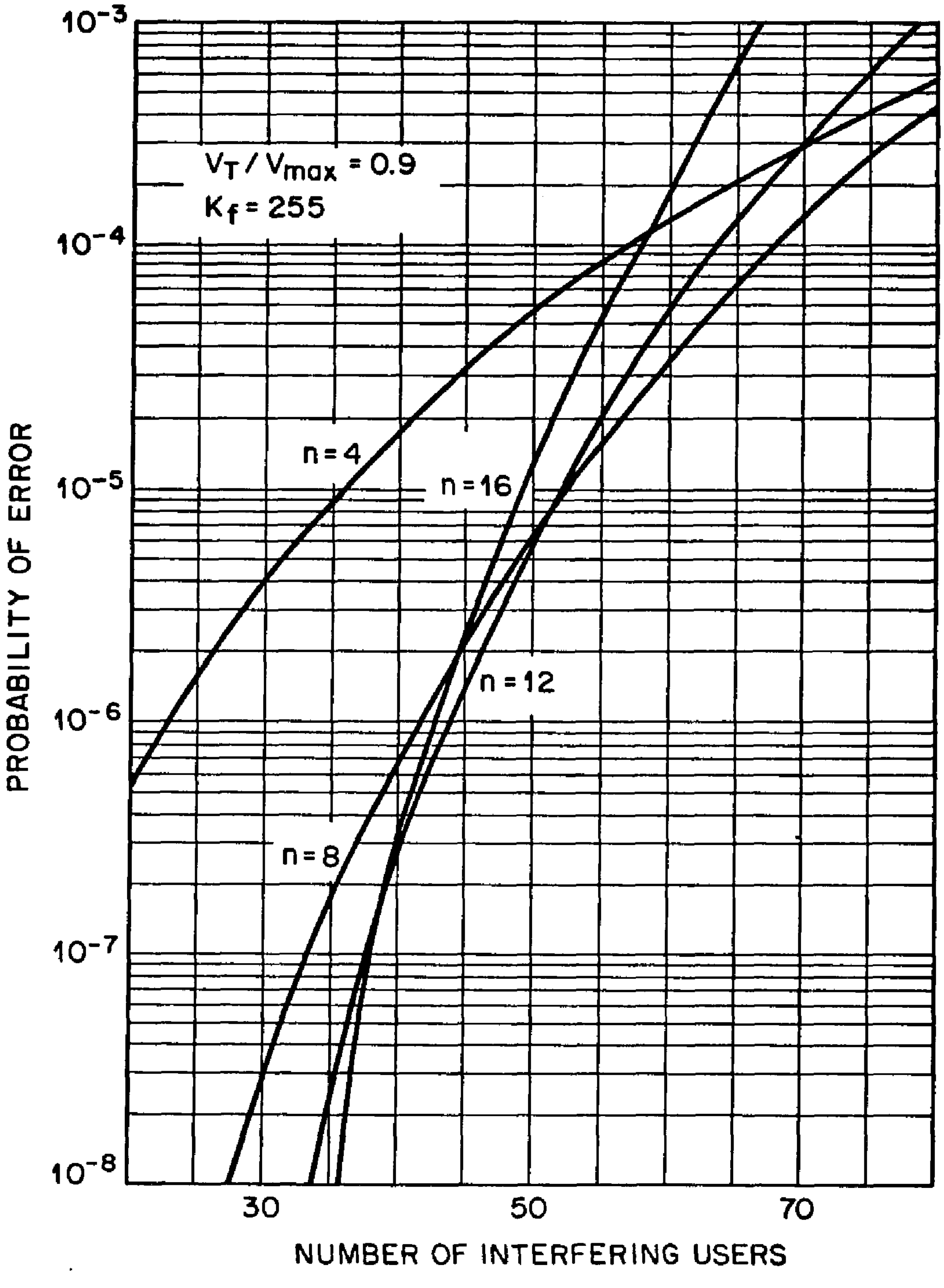

Fig.3.5. OOK/OR/TH Channel with PPS: Probability of Error vs Number of users

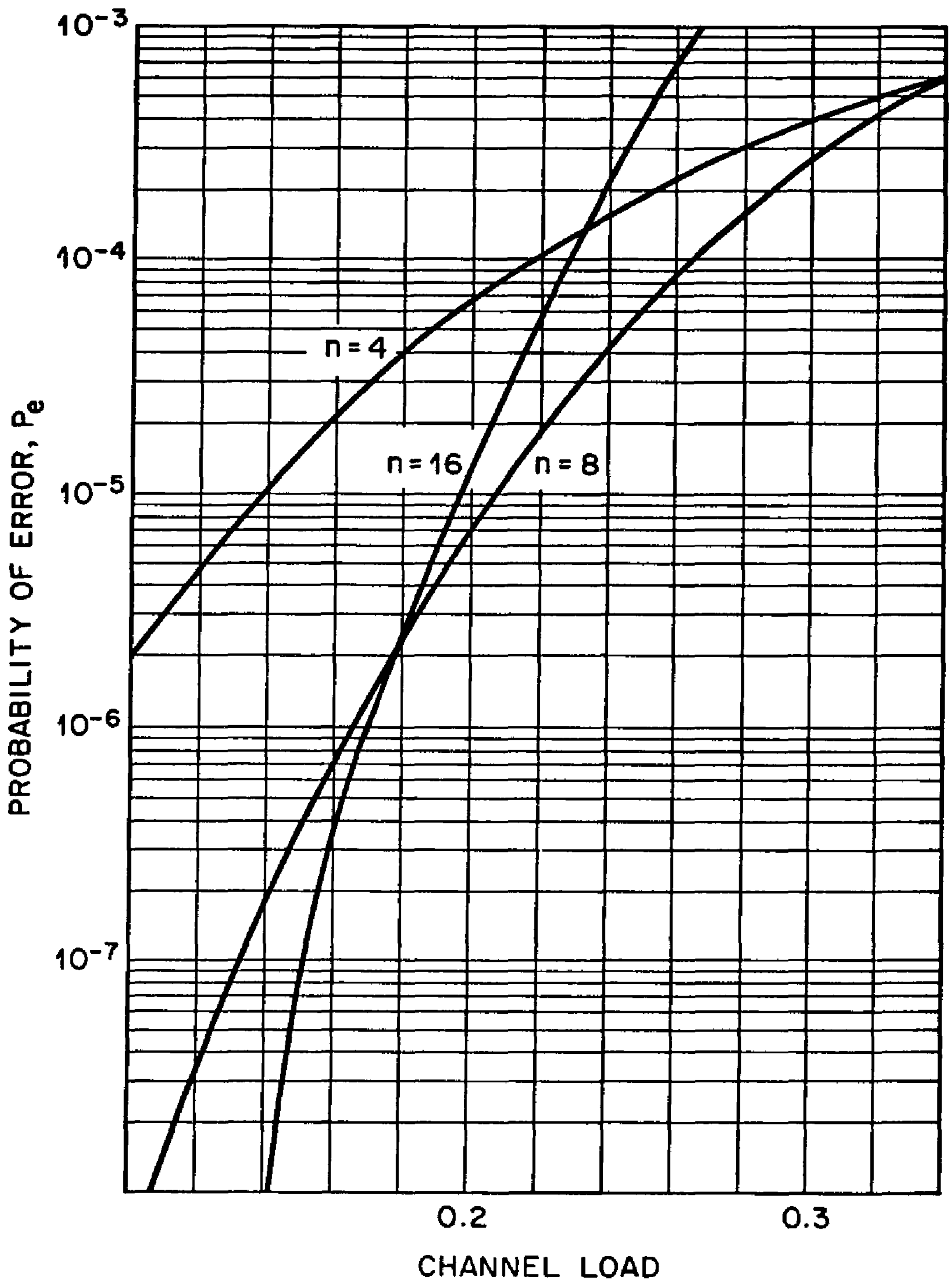

Fig.3.6. OOK/OR/TH Channel with PPS: Probability of Error vs Channel load

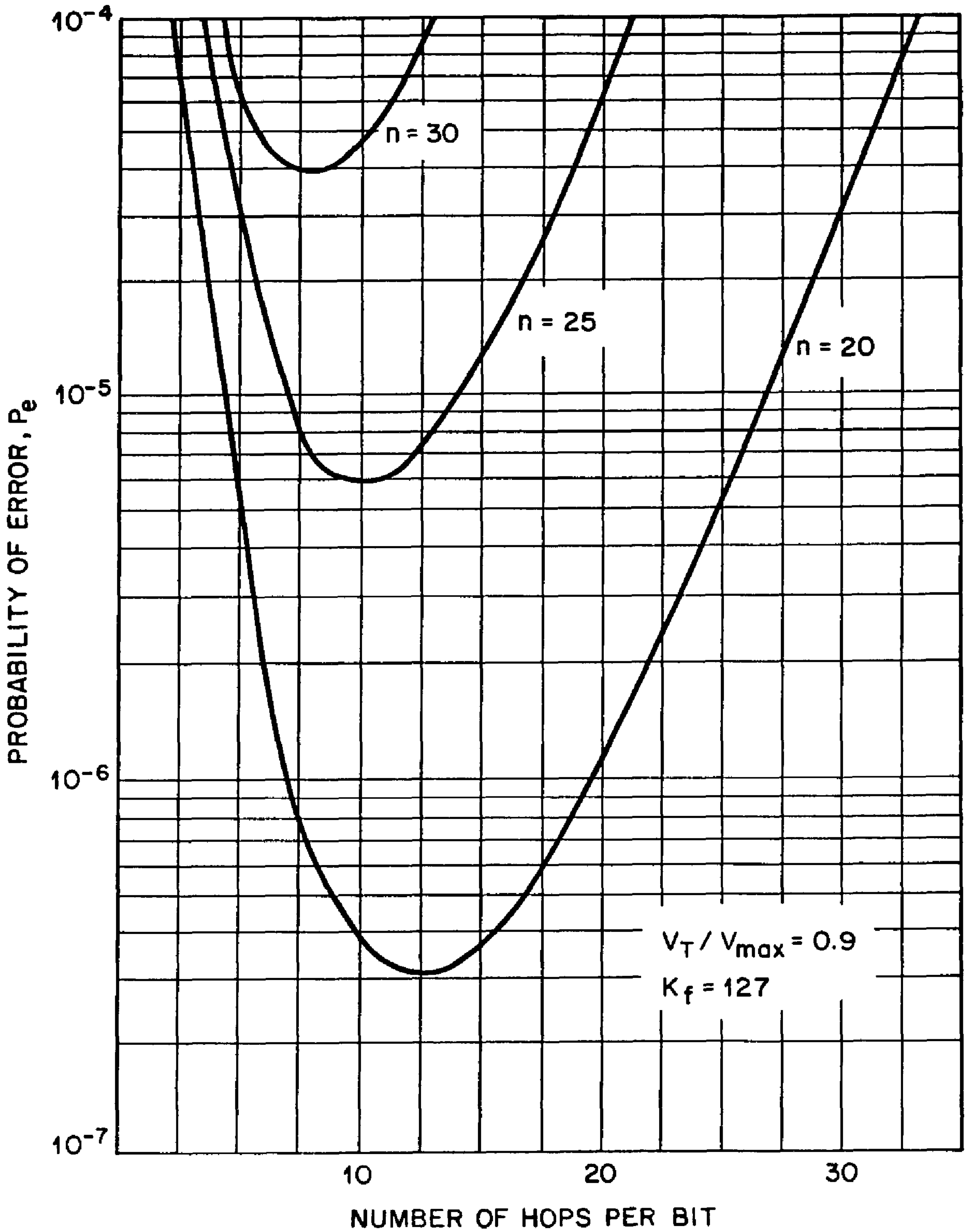

Fig.3.7. OOK/OR/TH Channel with PPS: BER vs number of hops per bit

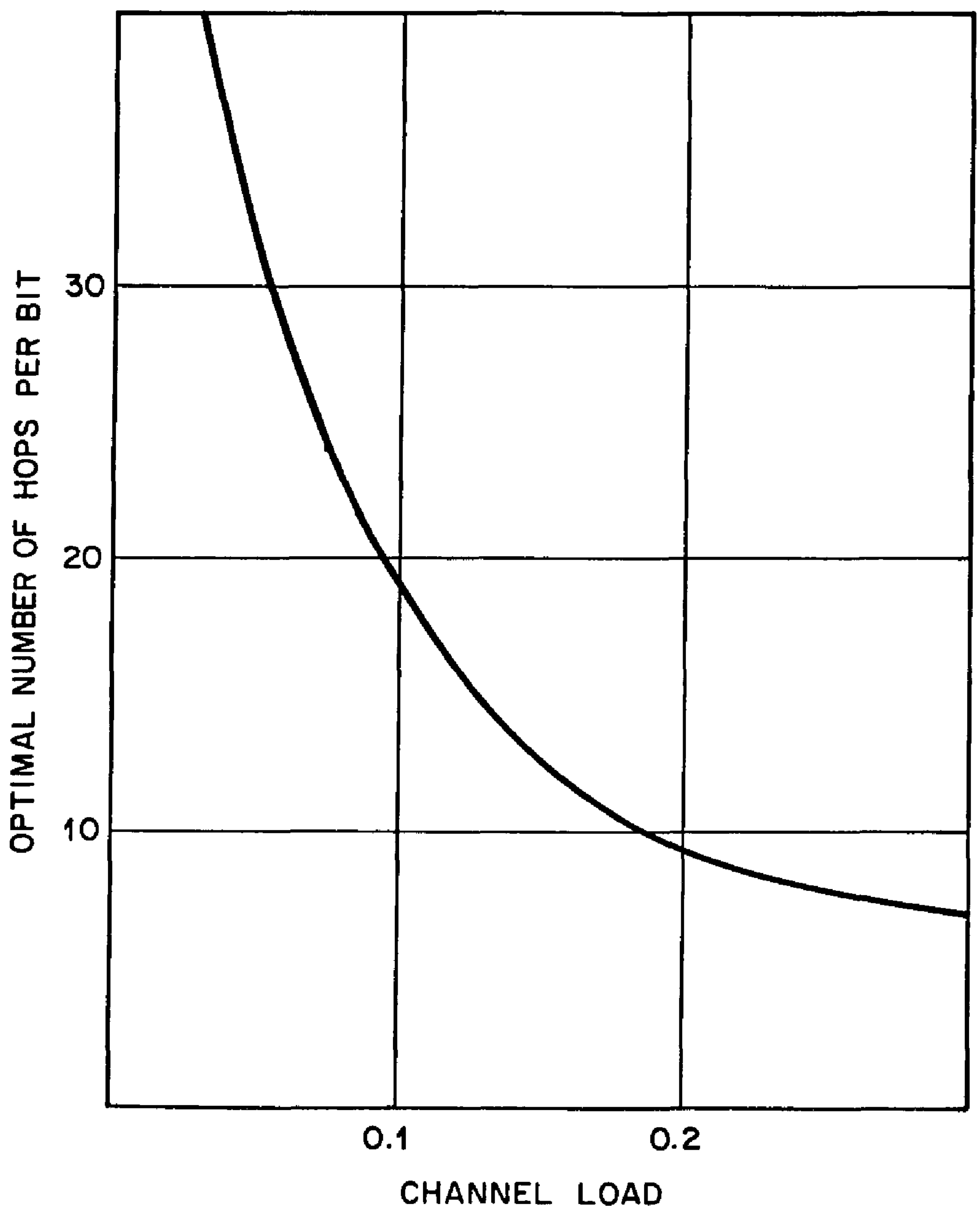

Fig.3.8. OOK/OR/TH Channel with PPS: Optimal number of hops per bit

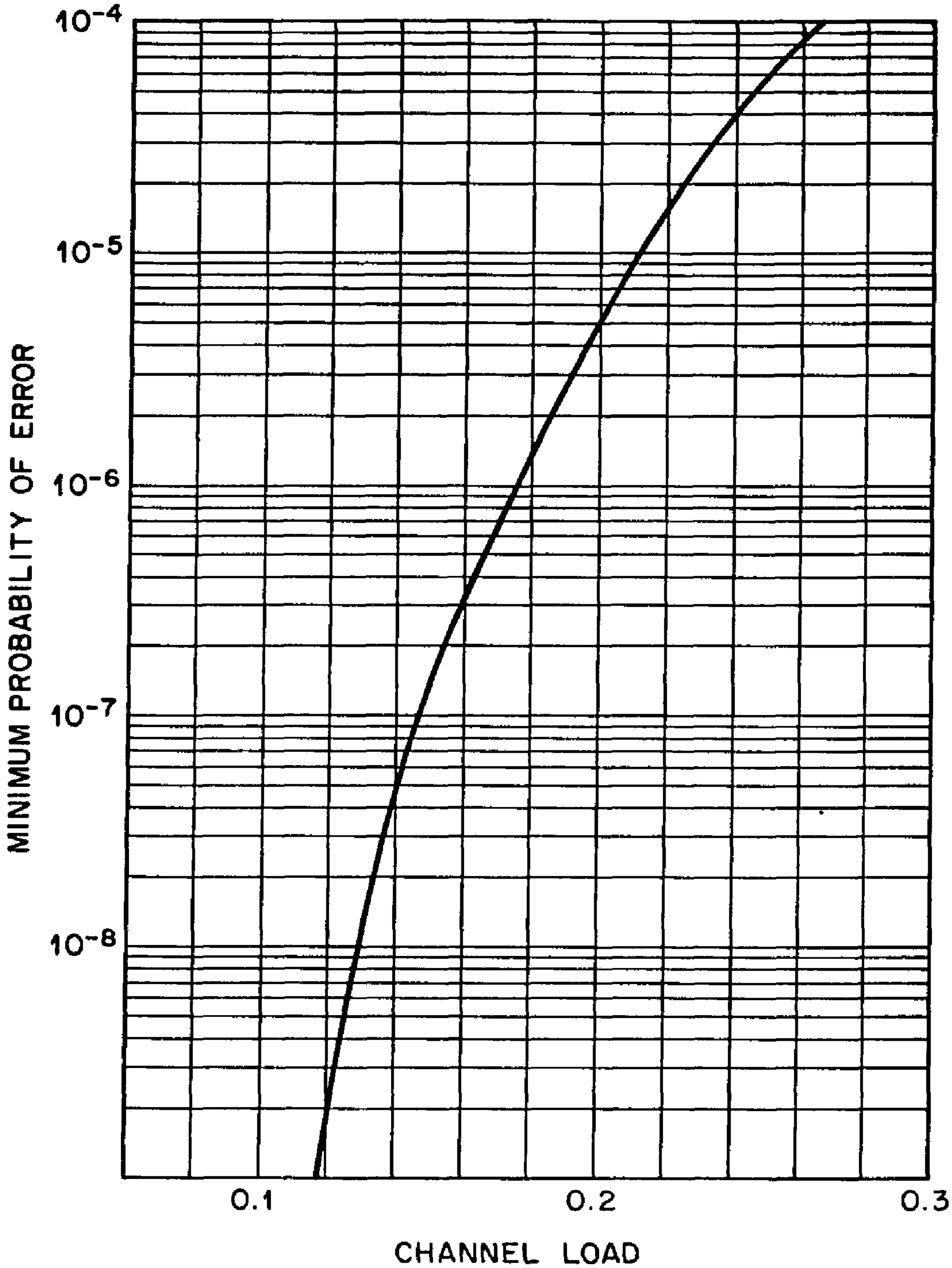

Fig.3.9. OOK/OR/TH Channel with PPS: Minimum Probability of Error

Active Pause signaling

Let us analyze a system that employs now Active Pause Signaling, (APS), scheme. In this system each user is assigned two distinct sequences $c_{i,0}$ and $c_{i,1}$ to represent the binary data values of zero and one correspondently, Fig.3.1.

Let the PRIS code that represents the data value of one, or one-pattern, consist of n_1 pulses (hops per bit) and the code representing the data value of zero have n_0 pulses. Then on the average per unit of time each user contributes to the channel ν_i pulses, where:

$$\nu_i = \frac{n_0\, p(0) + n_1\, p(1)}{T_d}$$

Assuming infinite data sources all N interfering users will contribute to the multiple user noise ν pulses per second, where:

$$\nu = N\, \nu_i$$

The Tapped Delay Line correlator receiver for the system consists of two tapped delay line filters matched to each of the PRIS codes. The synchronization pulse is used to strobe the output of the tapped delay line filter. The strobed signal is then routed to the Integrate-and-Dump circuits. The decision is made by comparing the outputs of the integrators. For the error to occur in the jitter-less system both integrators outputs have to be saturated, i.e. reach maximum possible value. Then the decision will be up to the gaussian component of noise in the receiver.

Using reasoning as for passive signaling system we receive for the multiple user noise at the output of the tapped delay line filter matched to the one-pattern:

$$F_{c,y_1}(\tau) = \left[1 - \frac{\nu\tau e^{-\nu\tau_c}}{1 - e^{-\nu\tau_c}}\right]^{n_1-1} \qquad (3.3.28)$$

And for the filter matched to the zero-pattern:

$$F_{c,y_0}(\tau) = \left[1 - \frac{\nu\tau e^{-\nu\tau_c}}{1 - e^{-\nu\tau_c}}\right]^{n_0-1} \qquad (3.3.29)$$

The average durations of the pulses are:

$$\overline{\tau_{y_1}} = \frac{\overline{\tau_x}}{n_1} \qquad (3.3.30)$$

$$\overline{\tau_{y_0}} = \frac{\overline{\tau_x}}{n_0} \qquad (3.3.37)$$

For the strobed signals we receive using (3.3.9):

$$\overline{\mu_{a_1}} = \overline{\mu_{y_1}}\, \mu_z\, (\overline{\tau_{y_1}} + \tau_z) \qquad (3.3.32)$$

$$\overline{\mu_{a_0}} = \overline{\mu_{y_0}}\, \mu_z\, (\overline{\tau_{y_0}} + \tau_z) \qquad (3.3.33)$$

And the average pulse durations:

$$\overline{\tau_{a_1}} = \frac{\overline{\tau_{y_1}}\tau_z}{\overline{\tau_{y_1}} + \tau_z} \qquad (3.3.34)$$

$$\overline{\tau_{a_0}} = \frac{\overline{\tau_{y_0}}\tau_z}{\overline{\tau_{y_0}} + \tau_z} \qquad (3.3.35)$$

The complementary integral distribution function then becomes:

$$F_{c,a_1}(\tau) = \frac{1}{\overline{\tau_{y_1}} + \tau_z} \left[1 - \frac{\tau}{\overline{\tau_x}}\right]^{n_1-1} \left(\frac{\overline{\tau_x} - \tau}{n_1} + \tau_z - \tau\right) \tag{3.3.36}$$

$$F_{c,a_0}(\tau) = \frac{1}{\overline{\tau_{y_0}} + \tau_z} \left[1 - \frac{\tau}{\overline{\tau_x}}\right]^{n_0-1} \left(\frac{\overline{\tau_x} - \tau}{n_0} + \tau_z - \tau\right) \tag{3.3.37}$$

The probability for these pulses to reach maximum possible duration that will yield in it's turn the maximum possible output of the integrator is as follows:

$$F_{c,a_1}(\tau_z) = \frac{1}{\overline{\tau_{y_1}} + \tau_z} \left(1 - \frac{\tau_z}{\overline{\tau_x}}\right)^{n_1-1} \frac{\overline{\tau_x} - \tau_z}{n_1} \tag{3.3.38}$$

$$F_{c,a_0}(\tau_z) = \frac{1}{\overline{\tau_{y_0}} + \tau_z} \left(1 - \frac{\tau_z}{\overline{\tau_x}}\right)^{n_0-1} \frac{\overline{\tau_x} - \tau_z}{n_0} \tag{3.3.39}$$

The average rate of the pulses that can potentially cause an error is then:

$$\overline{\mu_{e_1}} = \overline{\mu_{a_1}} F_{c,a_1}(\tau_z) \tag{3.3.40}$$

$$\overline{\mu_{e_0}} = \overline{\mu_{a_0}} F_{c,a_0}(\tau_z) \tag{3.3.41}$$

Due to the symmetry of the gaussian noise distribution only half of these pulses can cause errors. Then the probability of error for this system becomes:

$$P_e = p(0)\frac{\overline{\mu_{e_0}}/2}{1/2T_d} + p(1)\frac{\overline{\mu_{e_1}}/2}{1/2T_d} \tag{3.3.42}$$

Or for a symmetric data source:

$$P_e = \frac{\overline{\mu_{e_1}} + \overline{\mu_{e_0}}}{2} T_d \qquad (3.3.43)$$

If both PRIS codes contain the same number of pulses, i.e.:

$$n_1 = n_0 = n$$

And thus:

$$\overline{\mu_{e_1}} = \overline{\mu_{e_0}} = \overline{\mu_e}$$

We receive for the probability of error:

$$P_e = \overline{\mu_e} T_d \qquad (3.3.44)$$

Using (3.3.31), (3.3.29) and (3.3.25) we have:

$$P_e = \overline{\mu_y} \left(1 - \frac{\tau_z}{\overline{\tau_x}} \right)^{n-1} \left(\frac{\overline{\tau_x} - \tau_z}{n} \right) \qquad (3.3.45)$$

Assuming symmetric data sources and using (1.5.24) and (3.3.6) we receive for the probability of error:

$$P_e = \left[1 - e^{-\frac{nN}{K_f}} \left(1 + \frac{nNK_z}{K_f} \right) \right]^n \qquad (3.3.46)$$

And introducing the channel load parameter we receive:

$$P_e = \left[1 - e^{-nC_l}\left(1 + nK_zC_l\right)\right]^n \tag{3.3.47}$$

Fig.3.10 illustrates the probability of error as a function of the channel load for different numbers of hops per bit. The channel throughput is noticeably smaller for the system that employs active pause signaling due to greater contribution of each user to the multiple user noise. The crossings of the curves that correspond to different values of n indicate presence of an optimal number of hops per bit for a fixed channel load. Fig.3.11 illustrates this fact. By comparing graphs on Fig.3.11 with the ones on Fig.3.6 we can conclude that the system with passive pause signaling offers approximately two times greater throughput. The reasoning in favor of active pause signaling is reduction in complexity of the synchronization circuitry and no restrictions have to be imposed on run-length distribution in the data bit stream.

Fig.3.12 shows the optimal number of pulses in the PRIS code versus channel load. As the channel load increases the optimal number of hops per bit goes down. Fig.3.13 illustrates the minimum achievable probability of error as a function of channel load for a system employing the active pause signaling scheme. To insure BER of 10^{-5} or better the channel load has to be kept less than 12 % .

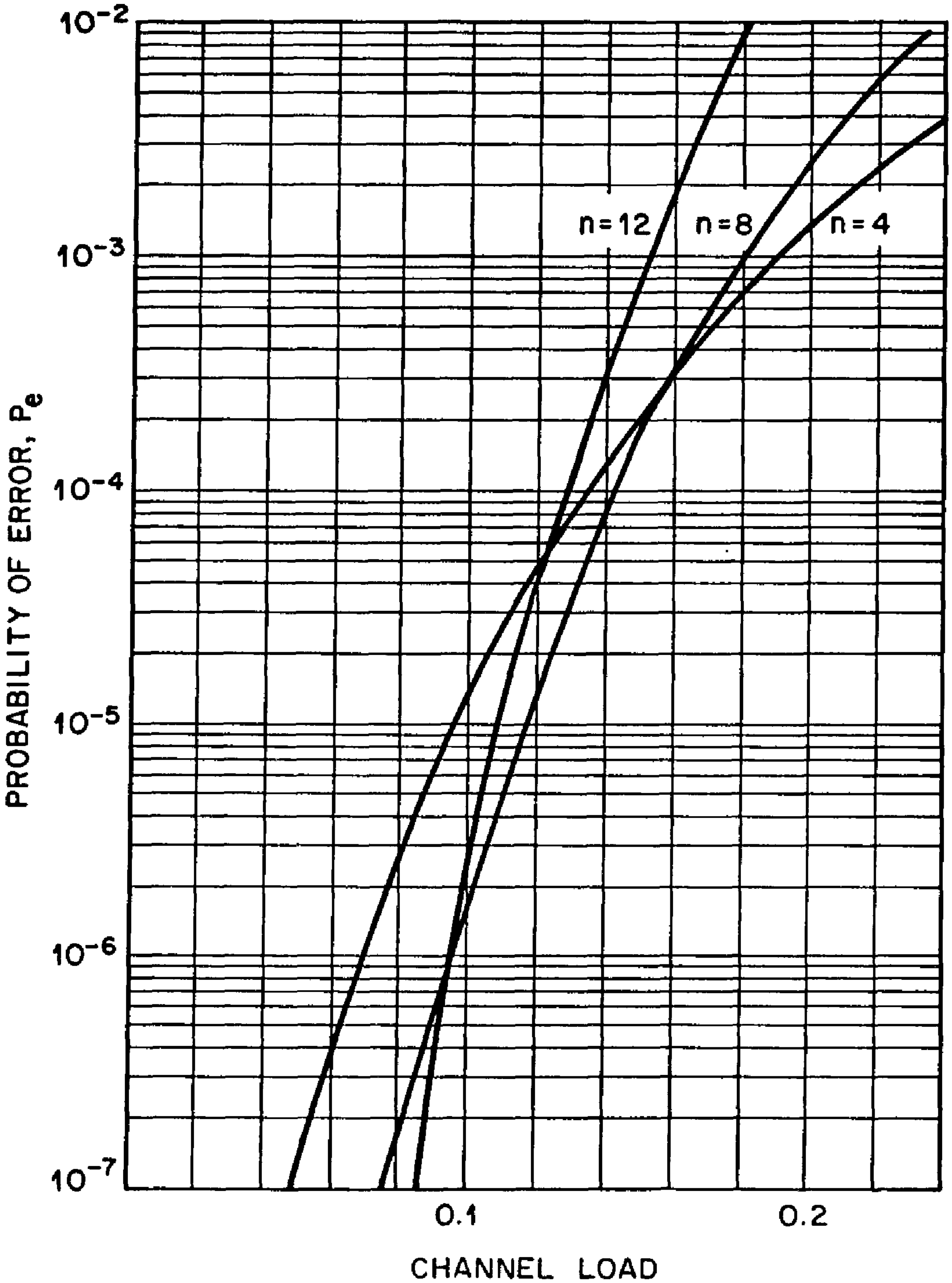

Fig.3.10. OOK/OR/TH Channel with APS: $P_e=f(C_1)$

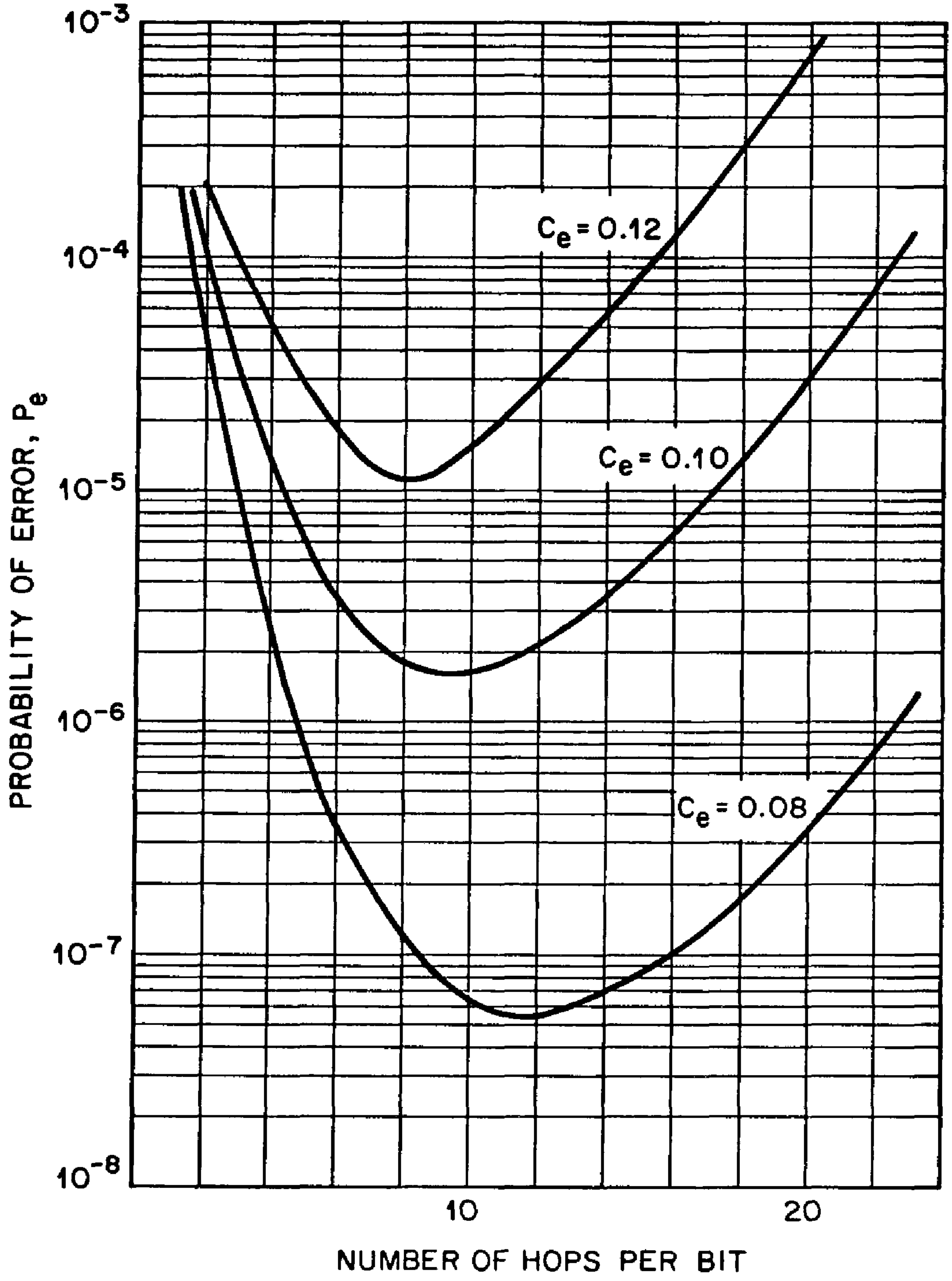

Fig.3.11. OOK/OR/TH Channel with APS: $P_e=f(n)$

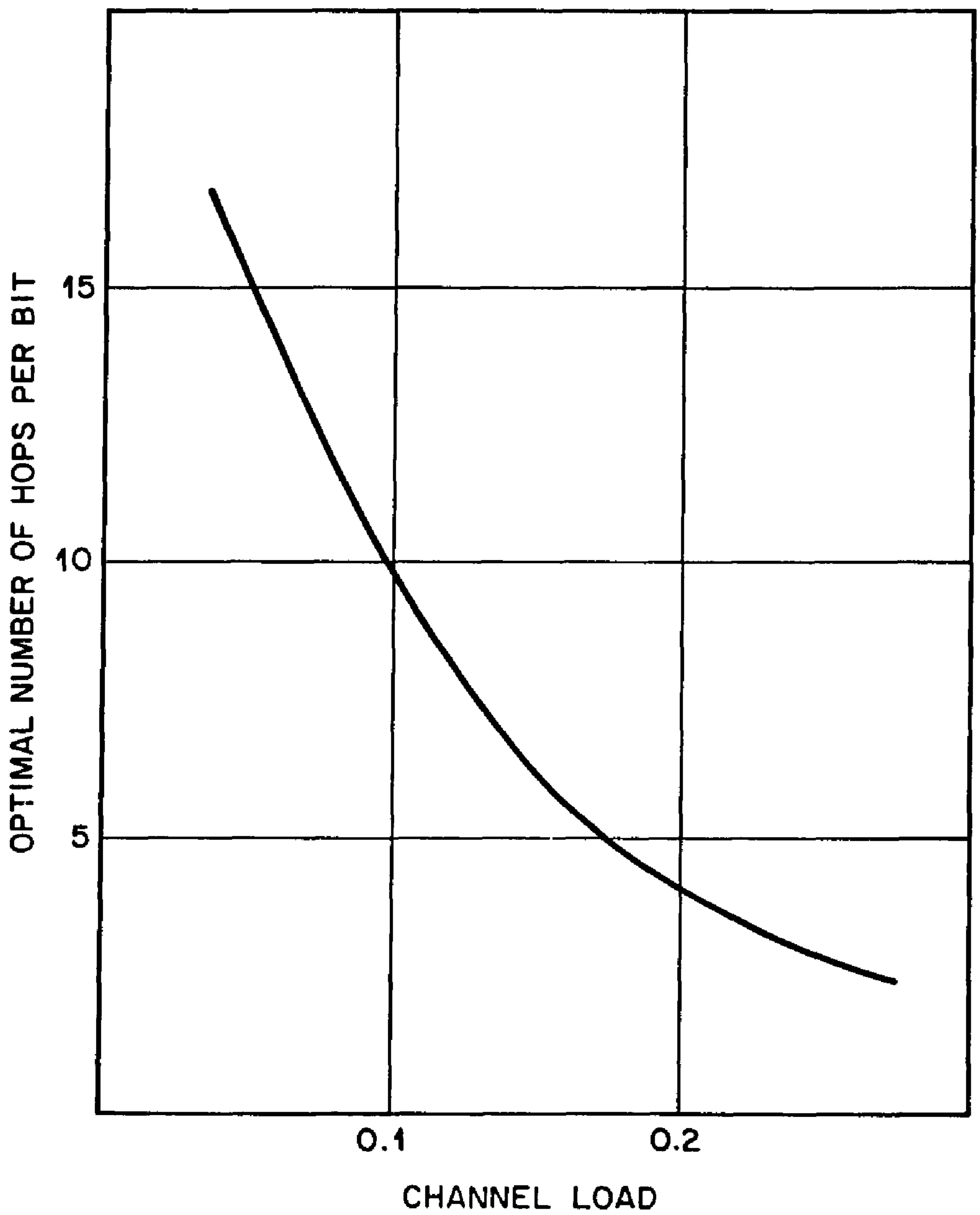

Fig.3.12. OOK/OR/TH Channel with APS: $n_{opt}=f(C_l)$

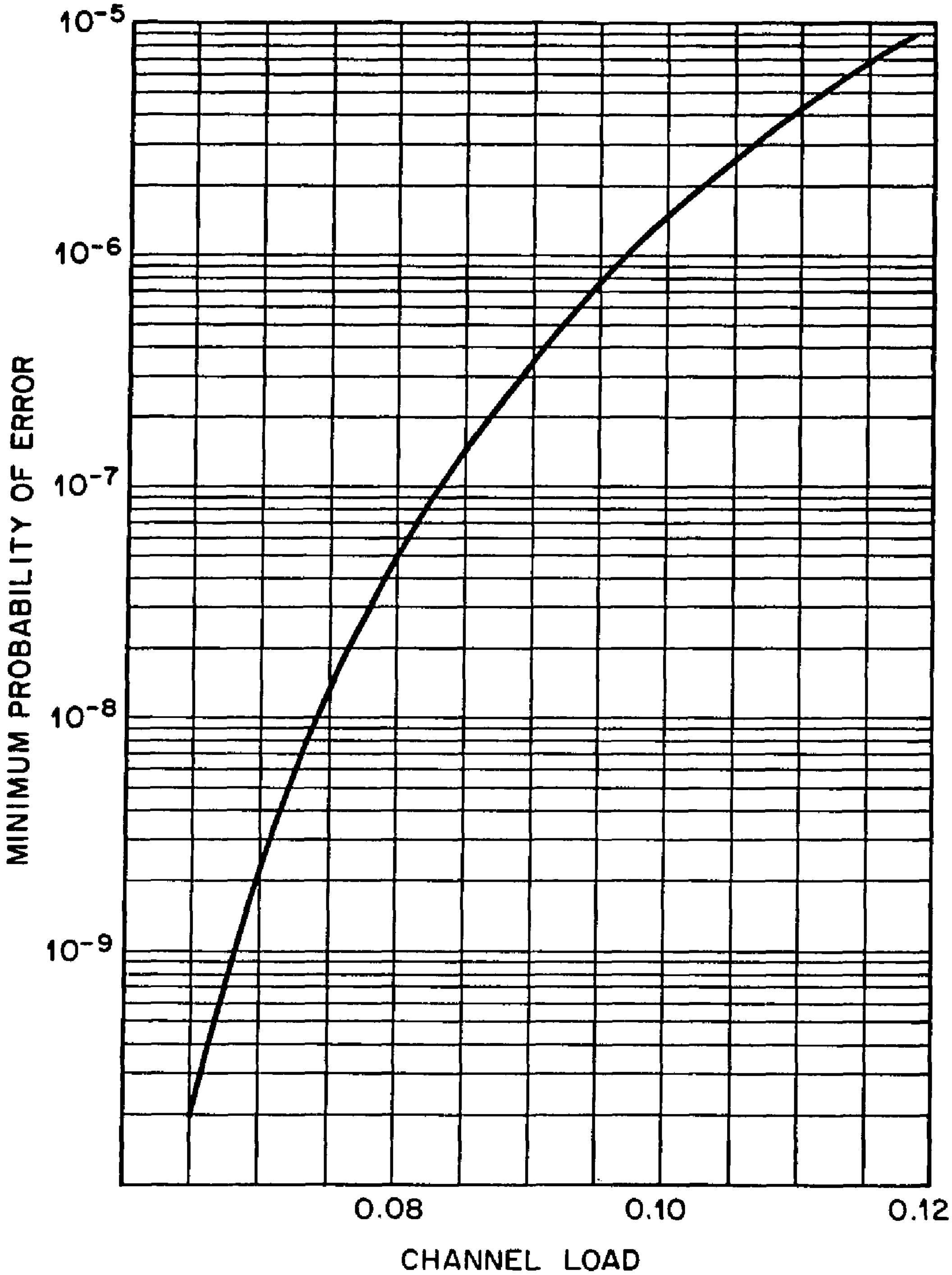

Fig.3.13. OOK/OR/TH System with APS: $P_{e_{min}}=f(C_l)$

3.4 OOK/OR/TH BURSTY CHANNEL PERFORMANCE

In bursty communications environment each source is characterized by the average duty cycle of the information flow. One example of this kind of environment is packet communications. Another example is communicating voice using speech detectors.

We will now analyze the OOK/OR/TH bursty channel performance that employs passive pause signaling.

Let $\overline{\eta}$ be the average duty cycle of all M information sources in the system. The signals from all users overlap in time. Thus at any instant of time there is some probability $\eta_N(M)$ to have N signals out of total M overlapping. This probability can be found as follows:

$$\eta_N(M) = \binom{M}{N} \overline{\eta}^N (1 - \overline{\eta})^{M-N} \tag{3.4.1}$$

We will call signal burst of order N a portion of the multiple user noise that consists of coinciding signals from N users. Then $\overline{\eta_N(M)}$ is the average duty cycle of the N-th order burst.

For the system with M active interfering bursty users the average probability of error becomes:

$$\overline{P_e} = \sum_{N=1}^{M} \binom{M}{N} P_e(N)\, \overline{\eta}^N (1 - \overline{\eta})^{M-N} \tag{3.4.2}$$

Where $P_e(N)$ can be found from (3.3.25).

Fig.3.14 illustrates the probability of error as a function of the number of interfering users for different duty cycles of the bursty information sources. It can be seen from the figure that duty cycle of 0.4, for example, allows the channel throughput to be increased to over 40 %.

Fig.3.15 illustrates the time distribution of the bit error rate. In other words, it shows the distribution of the duty cycle of different values of the probability of error for a case of 40 interfering bursty users in a system with $K_f = 127$. It can be observed that most of the time the probability of error is within 10^{-7} to 10^{-5} range, while only during 1 % of the time it is at 10^{-3} value.

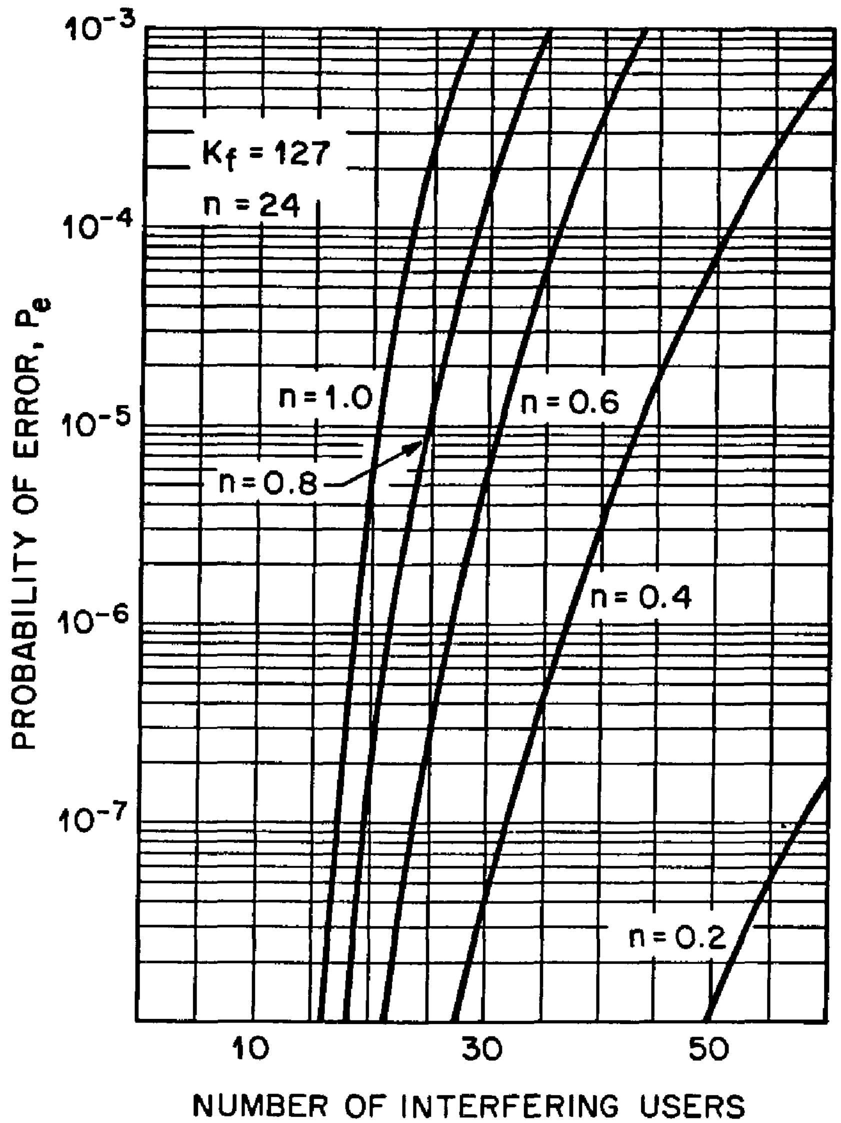

Fig.3.14. OOK/OR/TH Bursty Channel with PPS, P_e=f(N)

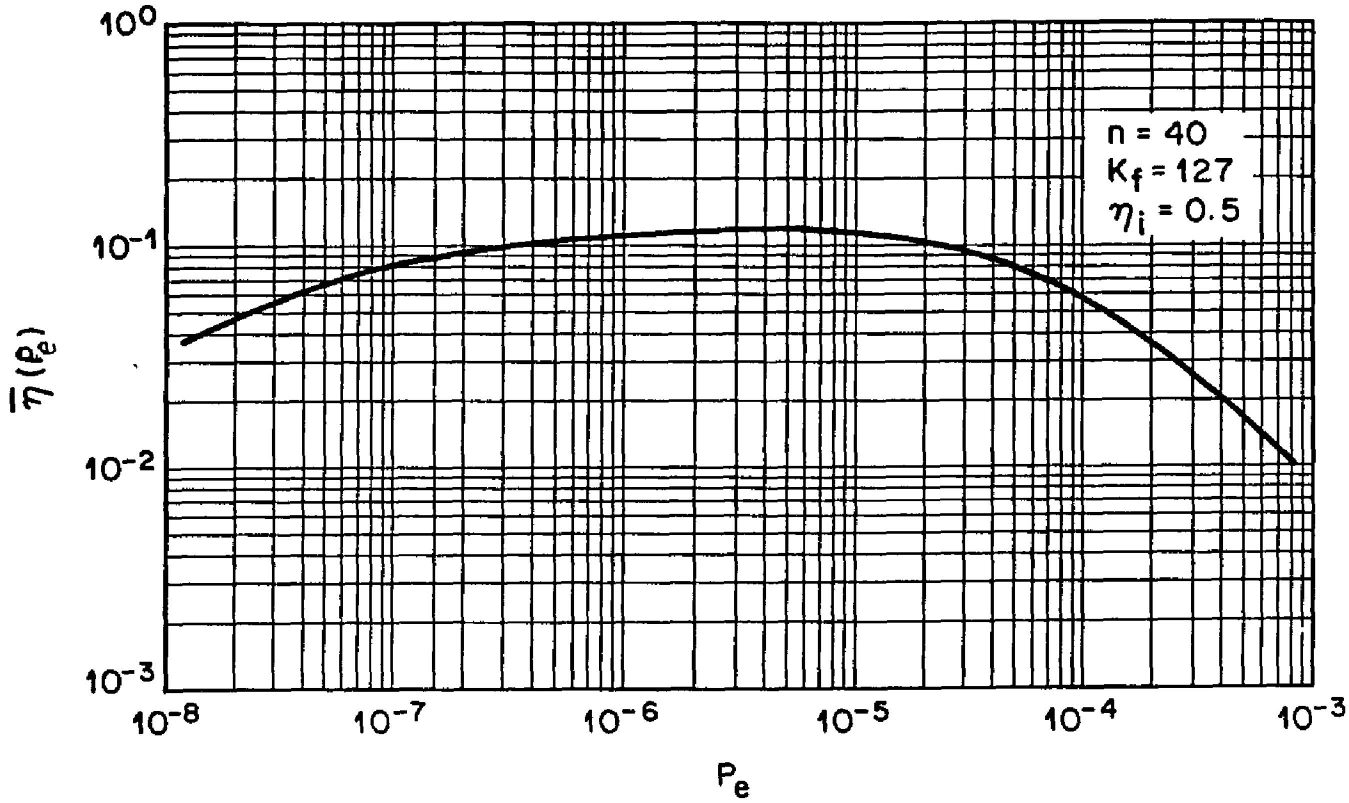

Fig.3.15. OOK/OR/TH Bursty Channel with PPS: BER Time Distribution.

3.5 CONCLUSIONS

We proposed an effective technique of Code Division Multiplexing of multiple user signals in the single Fiber Optic Channel. The main restrictions that the Fiber Optic medium imposes on the communication system design are limiting to positive signaling and the necessity to clip the channel signal in order to sustain dynamic range variations. As a result the system model is a digital OR Channel.

In spite of these limitations the signaling schemes we proposed offer sufficient throughput to be acceptable for Local Area Networking applications. The OOK/OR/TH system that employs passive pause signaling demonstrates better than 20 % channel throughput with probability of error less than 10^{-5} with no coding on the top of spread spectrum. Identical system with active pause signaling demonstrates (10-12) % throughput. In bursty communication environment when the duty cycle of bursts is no more than 0.4 the system with PPS demonstrates over 40 % throughput.

The high level of performance that has been determined for the Fiber Optic OOK/OR/TH Channel can be explained by the high bandwidth and relative stability offered by the Fiber Optic medium, low thermal component of the system noise and the precision of the Tapped Delay Line correlators that can be achieved by performing the signal processing in the optical domain. This properties of fiber optics justify the assumptions that were made for the analysis.

4. COLOR-HOPPED CDMA SYSTEM

4.1 INTRODUCTION

In analogy to a frequency hopped spread spectrum system we propose an optical channel signaling scheme that uses several optical sources. Every source emits light of different wavelength. The data modulates alternately these sources following some pseudo-random pattern.

We will call this process Color Hopping or Lambda Hopping and denote as λH .

We propose to use this scheme for multiple access. The block diagram of a λH system is shown in Fig.4.1.

A PN-Code generator with parallel output generates pseudo random binary words which are decoded in a 1/L lines decoder. The outputs of the decoder enable the data bit stream to pass to only one of the L optical sources to modulate the source intensity. The signals from all sources are coupled into one fiber using WDM (Wavelength Division Multiplexing) uni-directional couplers.

At the receiver end a WDM splitter is used to separate the signals of different wavelengthes. Each of these optical signals is then converted to electrical and the information baseband signal is recovered by assembling the composite signal from it's components via interleaving. This operation is done in the Interleaver. The simplest realization of this device is an m-input OR gate. In this case the model of the channel can be considered as OOK/OR/ λH.

We will distinguish between Fast and Slow Hopping and the boundary between these two schemes will be the hopping rate equal to the data transmission speed. Thus a slow hopped system will have one hop per data bit or less. A fast hopped system will have several hopes per data bit duration.

We can represent the signal of the i-th user in a λ - hopped channel model as:

$$S_i(t) = \sum_{k=-\infty}^{\infty} \sum_{j=1}^{m} d_k \ \psi_\lambda(t - jT_\lambda)\ \xi(t - jT_d) \qquad (4.1.1)$$

Where: $d_k \in \{0,1\}$ — unipolar data

λ — pseudo-randomly selected wavelength and $\psi_\lambda(t)$ — is the pulse shape function at the output of each photo-detector:

$$\psi(t) = \begin{cases} 1 & jT_\lambda \leq t < (j+1)T_\lambda \\ 0 & \text{elsewhere} \end{cases}$$

$\xi(t)$ — is the data pulse shape function:

$$\xi(t) = \begin{cases} 1 & kT_d \leq t < (k+1)T_d \\ 0 & \text{elsewhere} \end{cases}$$

The technique that we will consider is the one that uses fast hopping. In case of a fast hopped system the receiver is detecting patterns of different wavelengthes separately and then interleaves them to recover the data. This process is illustrated in Fig.4.2.

The signal at the output of the Interleaver in the absence of multiple user interference can be written as follows:

$$S_i(t) = \sum_{k=-\infty}^{\infty} \sum_{j=1}^{m} X_k \ \psi_\lambda(t - jT_\lambda) \qquad (4.1.2)$$

The pseudo random wavelength pattern and the data bit stream are synchronized so the beginning of the data bit corresponds to the beginning of the pattern, Fig.4.2.

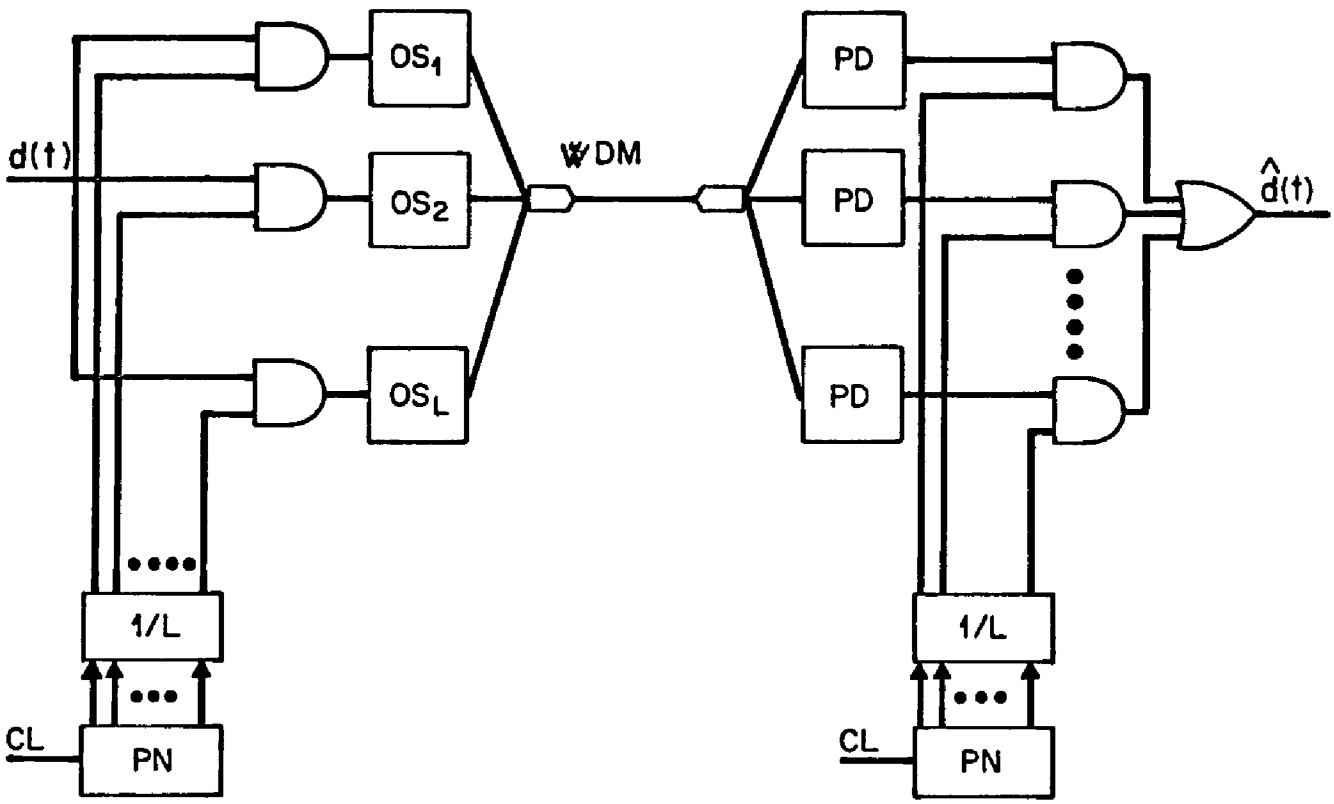

Fig.4.1. MI System

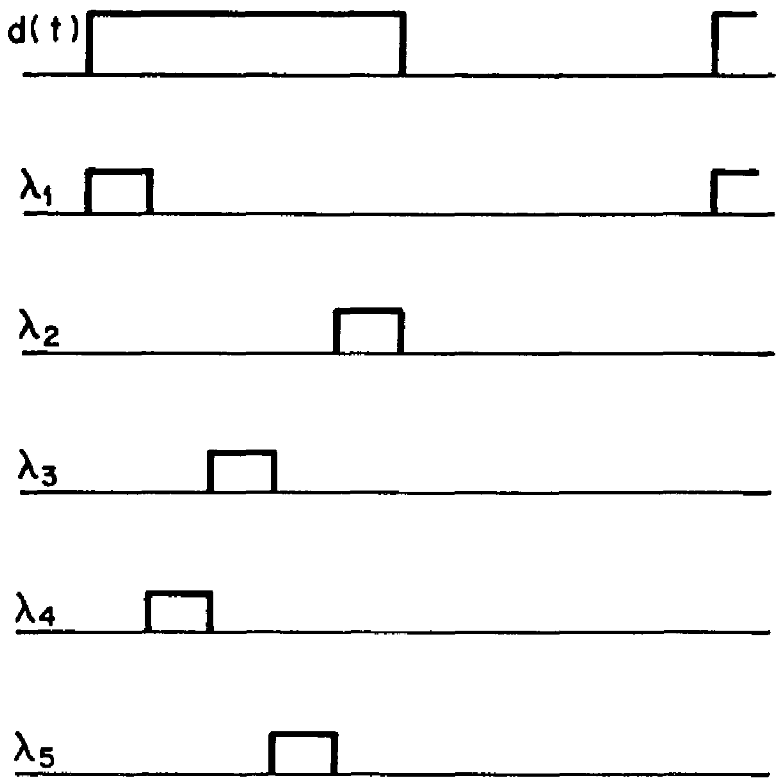

Fig.4.2. Fast λ Hopping

4.2 MULTIPLE USER OPERATION IN THE COLOR-HOPPED SYSTEM

Let us first consider a system that employs Passive Pause Signaling, (PPS), scheme. The data bit value of one is being communicated by a pseudo random pattern of pulses that appear at different wavelengthes, Fig.4.2.

Let τ_λ be the duration of the pulse at the wavelength λ .

Let L be the number of optical sources in the system.

We will determine the multiple user noise parameters using approach similar to the one used for Time-Hopped system.

If all users are assigned codes that make use of all of the available optical sources and have the same number of hops per bit n_λ at each wavelength then each user contributes to the multiple user noise ν_i pulses per second:

$$\nu_i = \frac{n_\lambda}{T_d} \, p(1) \qquad (4.2.1)$$

where:

L is the number of wavelengths,

p(1) is the probability of the data to take on the value of one.

Then the average number of pulses per wavelength in the system noise becomes:

$$\nu_\lambda = \frac{N n_\lambda}{T_d} \, p(1) \qquad (4.2.2)$$

We will assume Poisson distribution of the start times of these pulses and therefore the parameters of the multiple user noise can be found the same way we fund the statistics of the noise for the Time-Hopped system. We will assume that each code uses up all L wavelengths and has only one pulse at each wavelength:

$$n_\lambda = 1 \tag{4.2.3}$$

The maximum number of possible distinct codes is:

$$N_{max} = L\,! \tag{4.2.4}$$

If a Tapped Delay Line Correlator is employed the equivalent diagram of the receiver can be viewed as it is shown in Fig.3.3.

The optical signals at different wavelengths are being decoupled and routed to the corresponding Optical To Electrical, (O/E), converters where the optical signals are converted to electrical ones. Then the electrical pulses are delayed integer number of time intervals τ_λ and passed on to the AND gate. The output signal of the AND gate y(t) is strobed by the synchronization pulses z(t) and the resultant signal a(t) is then processed by the Integrate-and-Dump circuit. The decision about the transmitted symbol is made based on the comparison of the integrator output to a fixed threshold.

If we assume no jitter in the incoming signal and perfect synchronization between the transmitter and the receiver, then there will be no loss of the information when data value of one is transmitted. As in the Time-Hopped system the assumption of the jitterless signal does not imply that the proposed system will not function if there is jitter. On contrary, it is designed to sustain it. The presence of the threshold $V_T < V_{max}$, where V_{max} is the maximum possible output value of the integrator insures system's resistivity to the timing fluctuations. But since we neglect the pulse jitter effect on the detection process beside the selection of the threshold value, then we can say that the probability of incorrectly detecting the one pattern is zero, or:

$$p(1/1) = 1 \qquad (4.2.5)$$

The errors occur when a data value of zero is transmitted and multiple user noise signals at each wavelength align in a way when they produce coinciding outputs of all L delay lines.

This model leads to the Z-channel.

For each wavelength the average pulse rate of the system noise is then:

$$\overline{\mu_{x,\lambda}} = \nu_\lambda \, e^{-\nu_\lambda \tau_\lambda} \qquad (4.2.6)$$

And the average pulse width:

$$\overline{\tau_{x,\lambda}} = \frac{1 - e^{-\nu_\lambda \tau_\lambda}}{\nu_\lambda \, e^{-\nu_\lambda \tau_\lambda}} \qquad (4.2.7)$$

The probability density function for the durations of the multiple user noise pulses:

$$f_\lambda(\tau) = e^{-\nu_\lambda \tau_\lambda} \, \delta(\tau - \tau_\lambda) + \nu_\lambda e^{-\nu_\lambda \tau_\lambda} \, U(\tau - \tau_\lambda) \quad +$$

$$\sum_{k=1}^{\infty} (-1)^k \, \nu_\lambda^{\,k} \, e^{-\nu_\lambda (k+1)\tau_\lambda} \, \frac{[\tau - (k+1)\tau_\lambda]^k}{(k-1)!} \left\{1 + \frac{\nu_\lambda}{k} \, [\tau - (k+1)\tau_\lambda]\right\} U[\tau - (k+1)\tau_\lambda]$$

$$(4.2.8)$$

The complementary integral distribution of the pulse durations can be found as follows:

$$F_{c,x_\lambda}(\tau) = 1 + \sum_{k=1}^{\infty} (-1)^k \, \nu_\lambda^{k-1} \, e^{-\nu_\lambda k \tau_\lambda} \, \frac{(\tau - k\tau_\lambda)^{k-1}}{(k-1)!} \left[1 + \frac{\nu_\lambda}{k} \, (\tau - k\tau_\lambda)\right] U(\tau - \tau_\lambda) \tag{4.2.9}$$

From this formula we can observe that the probability for the multiple user noise pulses to be longer in duration than some value τ is smaller as τ increases.

4.3 PROBABILITY OF ERROR IN THE OOK/OR COLOR-HOPPED SYSTEM

We will determine now the probability of error for the OOK/OR/ λH system using the Poisson model of the system noise. The receiver for the system employs the TDL correlator identical to the one in Fig.3.3.

For the signal y(t) we have :

$$F_{c,y}(\tau) = \left(1 - \frac{1}{\overline{\tau_{x,\lambda}}}\int_0^{\tau} F_{c,x_\lambda}(\xi)d\xi\right)^{L-1} F_{c,x_\lambda}(\tau) \tag{4.3.1}$$

For the interval $0 \leq \tau \leq \tau_\lambda$ we have:

$$F_{c,y_\lambda}(\tau) = \left(1 - \frac{\tau}{\overline{\tau_{x,\lambda}}}\right)^{L-1} \tag{4.3.2}$$

Or substituting (8) and (9) into (13) we receive:

$$F_{c,y_\lambda}(\tau) = \left(1 - \frac{\mu_\lambda \tau e^{-\mu_\lambda \tau_\lambda}}{1 - e^{-\mu_\lambda \tau_\lambda}}\right)^{L-1} \tag{4.3.3}$$

Using the same reasoning as in chapter three we receive the average characteristics of the strobed signal a(t):

$$\overline{\mu_a} = \overline{\mu_y}\, \mu_z \left(\overline{\tau_y} + \tau_z\right) \tag{4.3.4}$$

$$\overline{\tau_a} = \frac{\overline{\tau_y}\tau_z}{\overline{\tau_y} + \tau_z} \tag{4.3.5}$$

And the complementary integral distribution:

$$F_{c,a}(\tau) = \frac{1}{\overline{\tau_a}+\tau_z} \left(1 - \frac{\tau}{\overline{\tau_{x,\lambda}}}\right)^{L-1} \left(\frac{\overline{\tau_{x,\lambda}} - \tau}{L} - \tau_z - \tau\right) \tag{4.3.6}$$

for $0 \leq \tau \leq \tau_\lambda$

The integration process with the consequent decision making by comparison of the integrator output with a fixed threshold will lead to false alarms due to the fact that some of the a(t) pulses will exceed in duration some value τ_T that is related to the threshold V_T in the following way:

$$\frac{\tau_T}{\tau_z} = \frac{V_T}{V_{max}} \tag{4.3.7}$$

The probability for the duration of the pulse to exceed $\tau_T < \tau_z$ can be written as follows:

$$P_r(\tau > \tau_T) = F_{c,a}(\tau_T) = \frac{1}{\overline{\tau_a}+\tau_z} \left(1 - \frac{\tau_T}{\overline{\tau_x}}\right)^{L-1} \left(\frac{\overline{\tau_{x,\lambda}} - \tau_T}{L} + \tau_z - \tau_T\right) \tag{4.3.8}$$

And the average rate of these pulses:

$$\overline{\mu_T} = \frac{\overline{\mu_a}}{\overline{\tau_y}+\tau_z} \left(1 - \frac{\tau_T}{\overline{\tau_{x,\lambda}}}\right)^{L-1} \left(\frac{\overline{\tau_{x,\lambda}} - \tau_T}{L} + \tau_z - \tau_T\right) \tag{4.3.9}$$

And the probability of error:

$$P_e = \overline{\mu_T} T_d p(0) \tag{4.3.10}$$

Or expressing the strobed signal rate $\overline{\mu_T}$ via the average rate of unstrobed pulses $\overline{\mu_y}$ we receive for the probability of error:

$$P_e = \frac{\overline{\mu_y}}{2}\left(1 - \frac{\tau_T}{\overline{\tau_{x,\lambda}}}\right)^{L-1}\left(\frac{\overline{\tau_{x,\lambda}}-\tau_T}{L} + \tau_z - \tau_T\right) \qquad (4.3.11)$$

Using (4.2.6), (4.2.7) and introducing the parameters K_z and K_T we have:

$$P_e = \frac{1}{2}\left[1 - e^{-\frac{N\tau_\lambda}{2T_d}}\left(1 + \frac{NK_TK_z\tau_\lambda}{2T_d}\right)\right]^{L-1} \quad x$$

$$\left[1 - e^{-\frac{N\tau_\lambda}{2T_d}}\left(1 + \frac{NK_TK_z\tau_\lambda}{2T_d} - \frac{LNK_z\tau_\lambda}{2T_d} + \frac{LNK_TK_z\tau_\lambda}{2T_d}\right)\right] \qquad (4.3.12)$$

Since we consider the case of only one pulse at each wavelength per code then:

$$\frac{T_d}{\tau_\lambda} = L \qquad (4.3.13)$$

Then substituting (4.3.13) into (4.3.12) we receive the probability of error for the λH system with PPS as a function of the number of interfering users and the number of wavelengthes employed:

$$P_e = \frac{1}{2}\left[1 - e^{-\frac{N}{2L}}\left(1 + \frac{K_TK_zN}{2L}\right)\right]^{L-1} \quad x$$

$$\left[1 - e^{\frac{N}{2L}}\left(1 + \frac{NK_TK_z}{2L} - \frac{NK_z}{2} + \frac{NK_TK_z}{2}\right)\right] \qquad (4.3.14)$$

Fig.4.3 illustrates this dependence. It can be observed from the figure that the number of users in the system is proportional to the number of wavelengthes available.

We will introduce the channel load parameter for the λH system and define it as:

$$C_l = \frac{N}{L^2} \tag{4.3.15}$$

Then the probability of error for the system as a function of the channel load can be written as:

$$P_e = \left[1 - e^{-\frac{LC_l}{2}}\left(1 + K_T K_z \frac{C_l}{2}\right)\right]^{L-1} \quad x$$

$$\left[1 - e^{-L\frac{C_l}{2}}\left(1 + LK_T K_z \frac{C_l}{2} - L^2 K_z \frac{C_l}{2} + L^2 K_z K_T \frac{C_l}{2}\right)\right] \tag{4.3.16}$$

Fig.4.4 illustrates the probability of error for the OOK/OR/ λH system as a function of the channel load. The curve for the optimal number of wavelengthes is depicted in Fig.4.5. Fig.4.6 illustrates the minimum achievable probability of error.

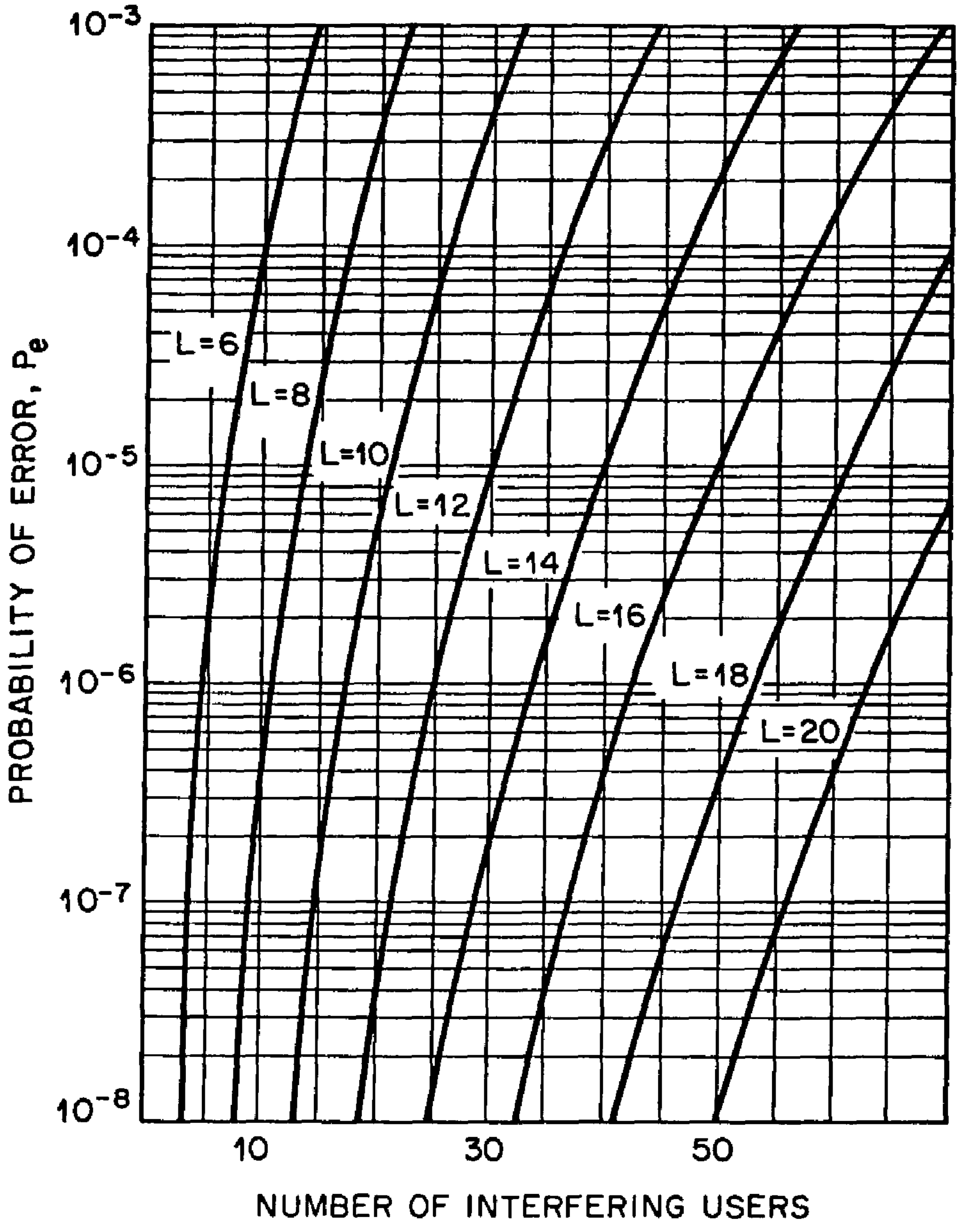

Fig.4.3. OOK/OR/ MI System with PPS, P_e=f(N)

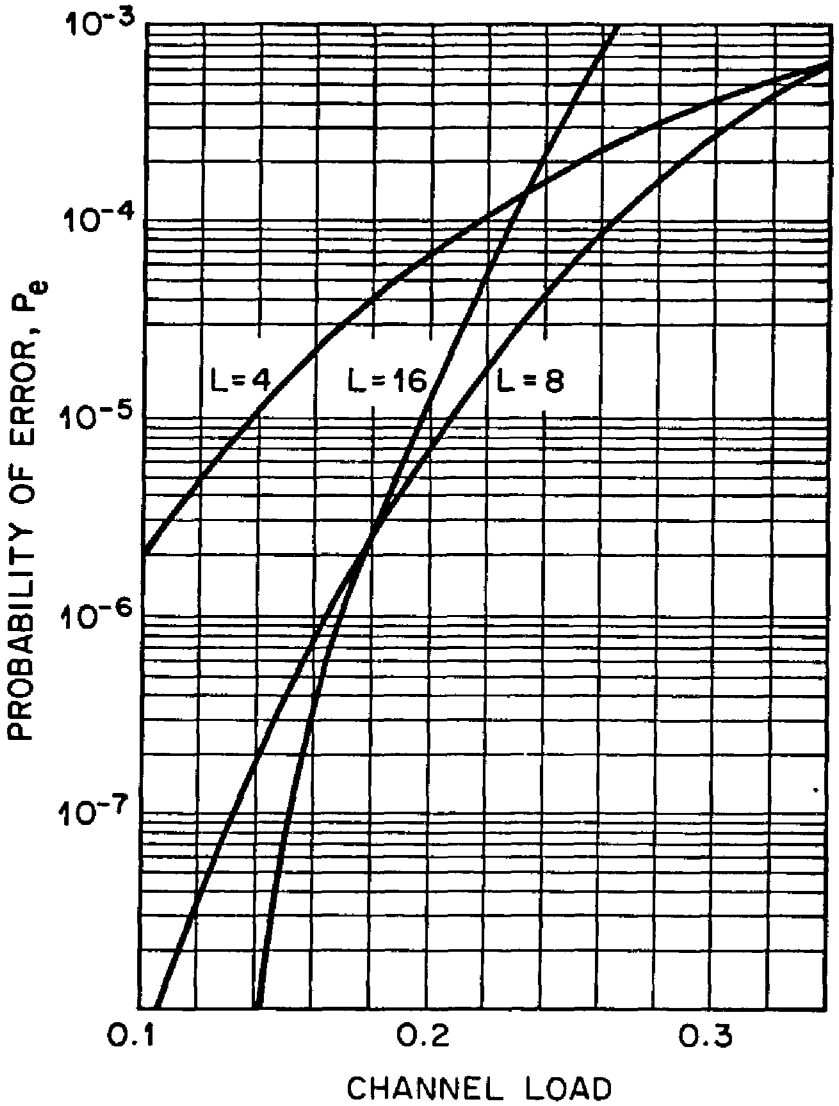

Fig.4.4. OOK/OR/ MI System with PPS, $P_e=f(C_l)$

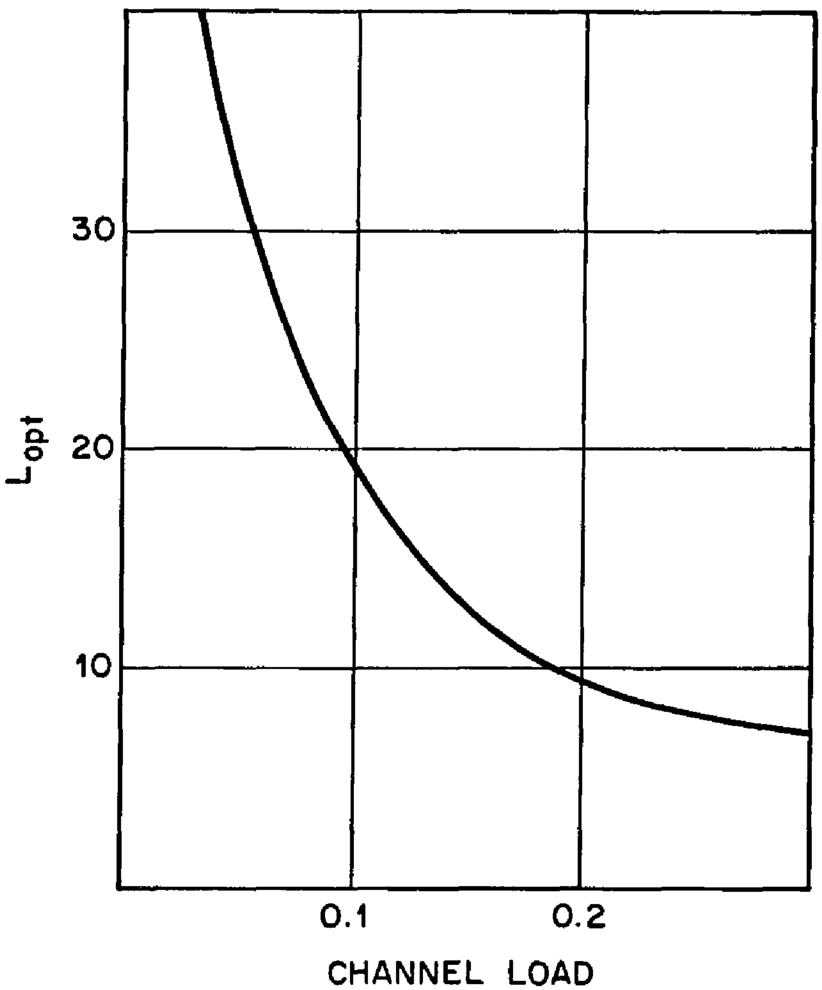

Fig.4.5. OOK/OR/ λH System with PPS, $L_{opt}=f(C_l)$

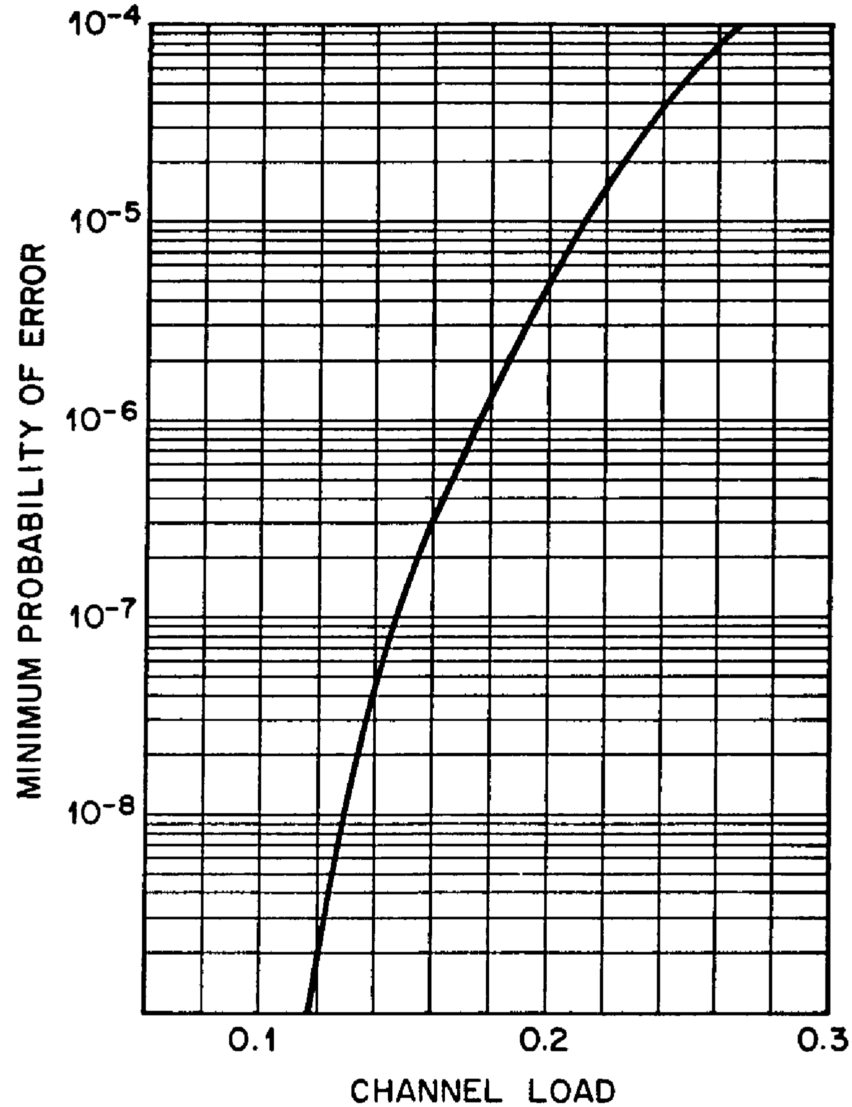

Fig.4.6. OOK/OR/ MI System with PPS, $P_{e_{min}}=f(C_l)$

Active Pause Signaling

Let's now consider an active pause signaling scheme where each user is assigned two distinct pseudo random wavelength patterns. Fig.4.7 shows the block diagram of a transmitter and a receiver for this system. The transmitter consists of two PN sequence generators which are identical to the one used in the Passive Pause Signaling scheme. One of the generators is enabled when data value of one is transmitted another is enabled when data value of zero is to be transmitted. The generators alternately control the optical sources thus generating one of the two possible $\lambda-$ patterns at a time. The equivalent diagram of the receiver includes two sets of the delay lines similar to the one in the receiver of the system with Passive Pause Signaling. The outputs of the delay lines are passed trough the AND gate, strobed and the resultant signal is routed to the Integrate-and-Dump circuitry. The output signals of the integrators, that exceed in value some fixed threshold V_T , appear at the inputs of the comparator. The decision about the transmitted data bit is made based on the prevailing signal.

If the pulse jitter can be neglected then there will be no losses of the transmitted information since the corresponding integrator's output will be at it's maximum:

$$V_1 = V_{1,max} \tag{4.3.17}$$

when the one-pattern was transmitted and:

$$V_0 = V_{0,max} \tag{4.3.18}$$

when the zero-pattern is transmitted.

The error will occur when maximum will be reached by the integrator output that corresponds to the pattern that was not transmitted. This can happen due to the multiple user noise. But even then only half of these situations will cause an error because of the symmetry of the thermal noise statistics.

The contribution of each user to the multiple user noise at each wavelength average per second is as follows:

$$\nu_j = \frac{1}{T_d} \tag{4.3.19}$$

And all users contribute ν_λ pulses to the system noise at each wavelength, where:

$$\nu_\lambda = \frac{N}{T_d} \tag{4.3.20}$$

Using the same approach as for the TH system, we can assume that the errors in the jitter-less system can occur only if both integrators are at their maximum output and the decision is being made based on the prevailing output. In other words it will be up to the gaussian component of noise. The Integrate-And-Dump circuit is an optimal filter for the white gaussian noise channel.

Then the probability of error becomes:

$$P_e = \overline{\mu_y} \left(1 - \frac{\tau_z}{\overline{\tau_{x,\lambda}}}\right)^{L-1} \left(\frac{\overline{\tau_{x,\lambda}} - \tau_z}{L}\right) \tag{4.3.21}$$

By substituting the expression for $\overline{\mu_y}$ and taking to consideration conditions (4.3.17) and (4.3.18) we receive:

$$P_e = \left[1 - e^{-\frac{N}{L}} \left(1 + \frac{NK_z}{L}\right)\right]^L \tag{4.3.22}$$

We will now introduce the channel load parameter for the OOK/OR/ λH system:

$$C_l = \frac{N}{L^2} \tag{4.3.23}$$

Then the probability of error becomes:

$$P_e = \left[1 - e^{-LC_l} \left(1 + LK_zC_l\right)\right]^L \tag{4.3.24}$$

Fig.4.7 illustrates the plots of the probability of error for the OOK/OR/ λH system with active pause signaling as a function of the number of interfering users. Fig.4.8 shows the plots of the probability of error versus channel load. Optimal number of wavelengths is given by Fig.4.9. And the minimum achievable probability of error as a function of the channel load is shown in Fig.4.10.

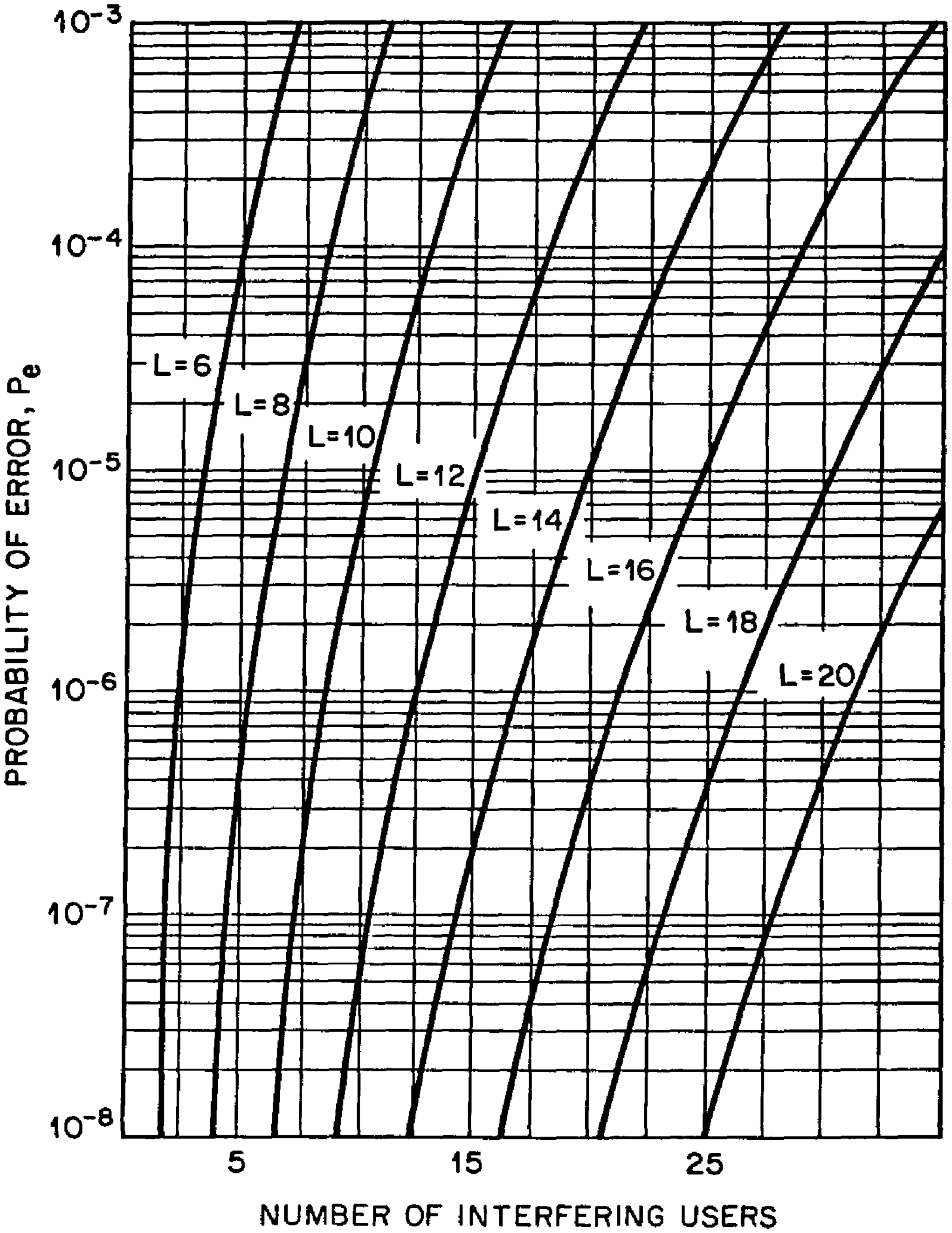

Fig.4.7. OOK/OR/ MI System with APS, P_e=f(N)

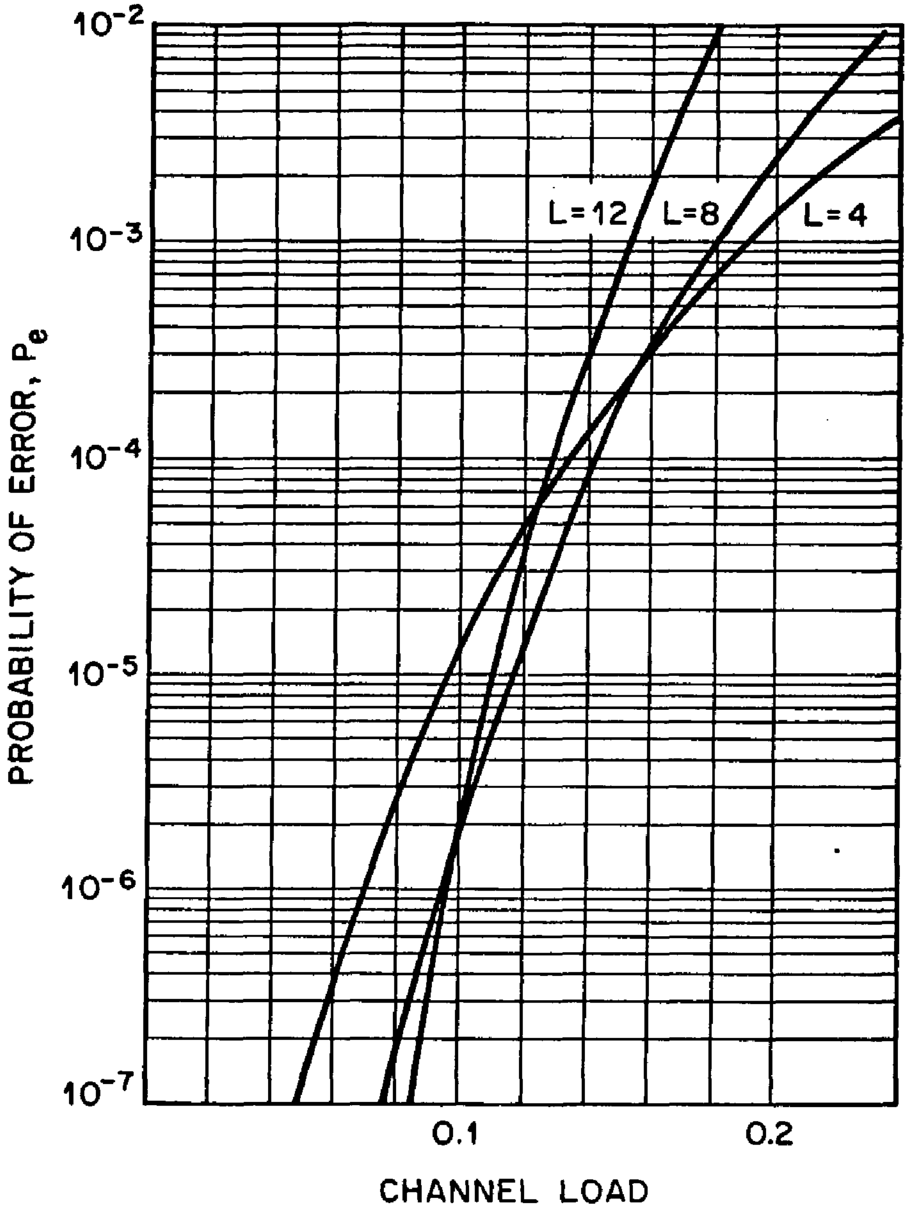

Fig.4.8. OOK/OR/ λH System with APS, $P_e=f(C_l)$

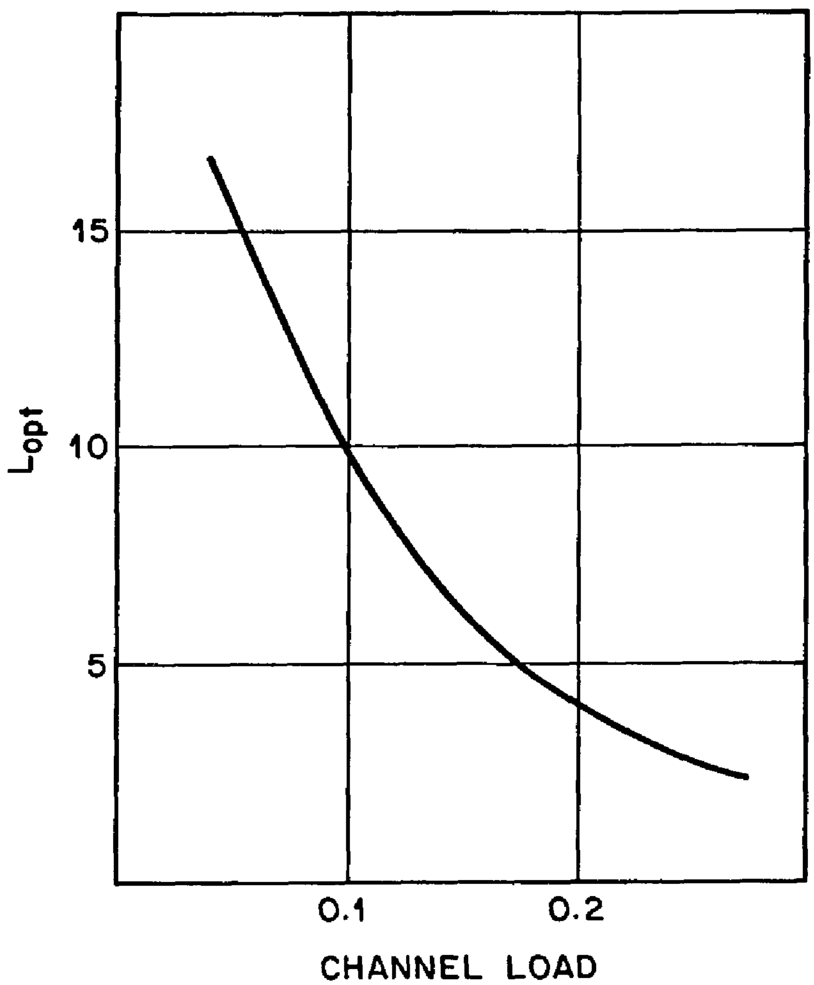

Fig.4.9. OOK/OR/ λH System with APS, $L_{opt}=f(C_l)$

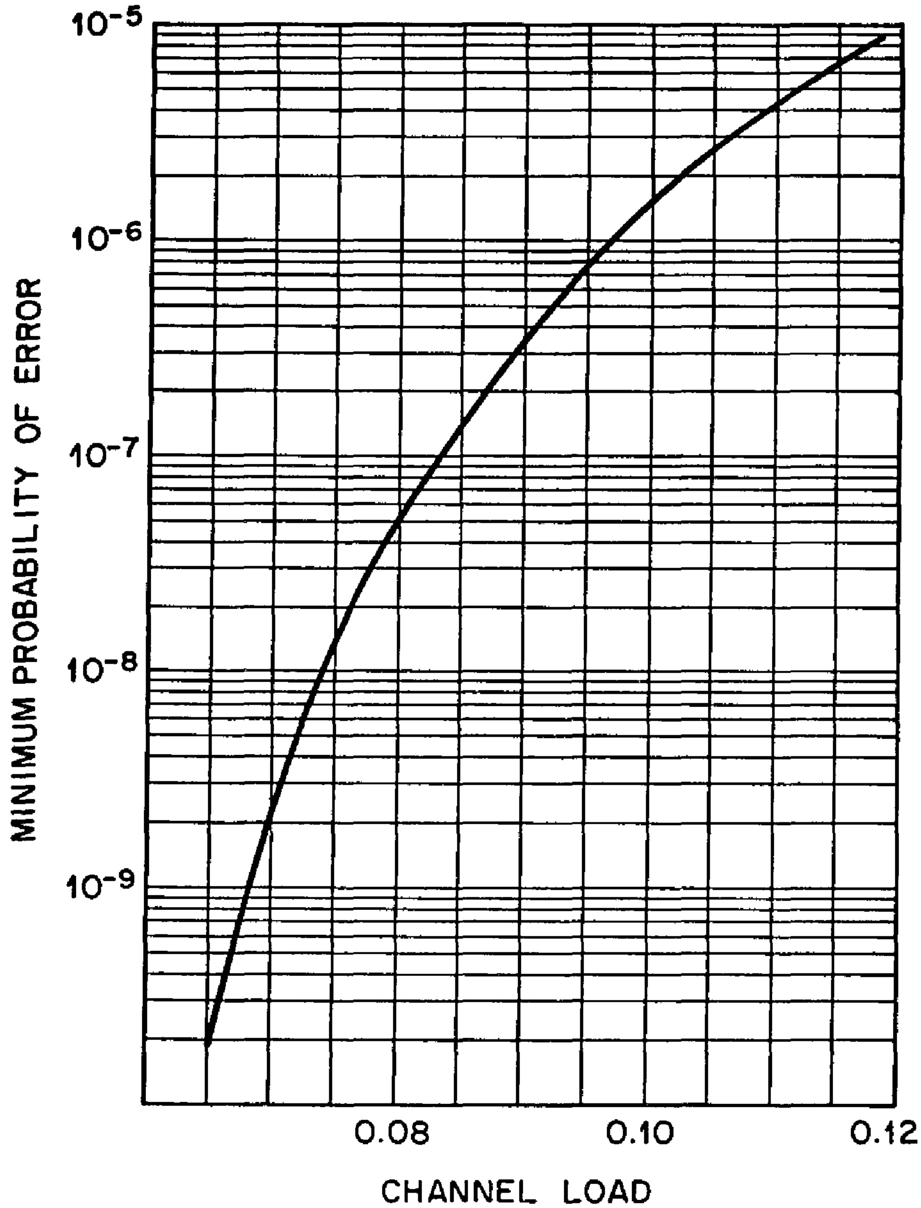

Fig.4.10. OOK/OR/ MI System with APS, $P_{e_{min}}=f(C_1)$

4.4 CONCLUSIONS

We introduced a new fiber optic Code Division Multiple Access scheme based on optical bandwidth spreading method. This system offers significant throughput and allows multiplexing multiple user signals into a single fiber optic medium.

Color Hopping should be used when optical bandwidth utilization is preferable to electronic, when spreading the electronic bandwidth is a problem. The data pulses in the Color-Hopped system stay unspread until they reach the E/O conversion stage.

We derived the expression for the probability of error that ties the bit error rate to the number of users and the number of available wavelengthes. For system designs with efficient bandwidth utilization we plotted the optimal number of the colors as a function of the channel load.

5. HYBRID MULTIPLE ACCESS COMMUNICATION

5.1 INTRODUCTION

In order to increase the Code Division Multiple Access channel throughput we propose a multiple access scheme that utilizes a combination of Color and Time Hopping. It allows the use of a two-dimensional addressing scheme which makes it possible to multiplex more users into a single fiber. Unlike the TH and λH systems the hybrid scheme allows to use the non-optimal PRIS codes and yet create optimal two-dimensional hopping patterns at each wavelength. The mechanism of this kind of code generation however is not yet researched and is beyond the scope of this research.

Different combinations of the Time and Color hopping techniques are possible. One can construct a system that will employ fast Time Hopping and slow λ Hopping and visa-versa. We will limit our analysis to the system with fast Time and fast Color Hopping.

Another set of combinations have to be pointed out. It is possible to implement a system that will have Time-Synchronous, or Chip-Synchronous, hopping patterns while maintaining asynchronism in the wavelength hopping pattern. The opposite is also possible. All combinations might find their applications. In this research we limit our analysis to completely asynchronous case.

The block-diagram of a hybrid T−λH multiple access system is shown in Fig.5.1.

A PN-Sequence generator which is used in this system incorporates a shift-register that has a parallel as well as a serial output. The parallel binary pseudo-random code words are being routed to a 1/L lines decoder whose outputs are used to select the optical source. The PN-generator's serial output is modulo-two added to the data bit stream and the resulting signal is routed to all optical sources.

The address assignment in this multiple access system is realized according to a two-dimensional (Time Interval-Wavelength) matrix. The 2-D pattern matrix consists of integer numbers $I_1, I_2, \cdots, I_n$ of chip-slots which signify the distances of the pulses from the beginning of the code. The subscripts show the pulse number in the pattern. The columns of the matrix correspond to the wavelength values $\lambda_1, \lambda_2, \cdots, \lambda_L$:

$$A = \begin{pmatrix} I_1 & . & I_3 & . & . \\ . & I_2 & . & . & . \\ . & . & . & . & . \\ I_4 & . & . & . & . \\ . & . & . & . & I_n \end{pmatrix}$$

where n is the number of pulses in the pattern.

Of course this number can be different for one- and zero-patterns.

Another way to represent the patterns is by using a binary matrix and having the rows correspond to the pulse distances from the beginning of the pattern and the columns correspond to the number of the optical source, i.e., to the wavelength.

In general the spreading code generator and the wavelength controlling generator can be realized as separate devices but they have to be chip-synchronous to prevent λ – hops to occur within one pulse in the pattern.

In the matrix representation the column shows the time sequences that correspond to one wavelength.

This system can accommodate significantly larger population of users communicating over a single fiber. The OOK/OR system that employs hybrid signaling which is a combination of Time Hopping and λ Hopping we will denote as OOK/OR/T λ H system.

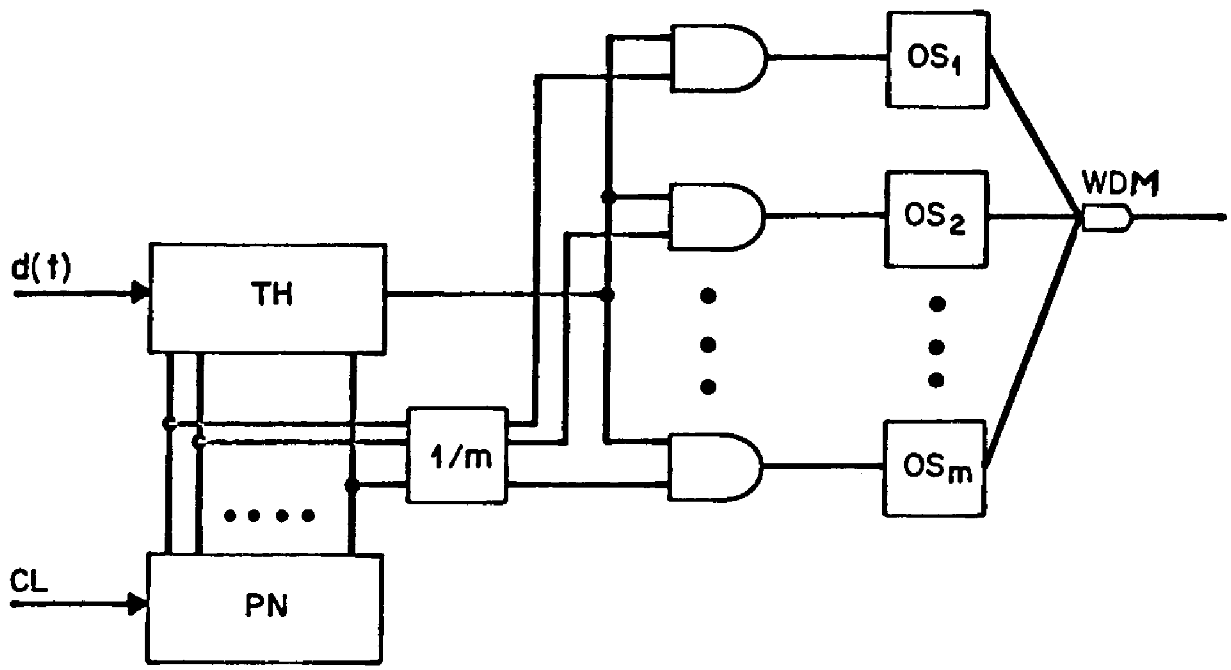

Fig.5.1. TλH System

5.2 MULTIPLE USER NOISE IN OOK/OR HYBRID SYSTEM

The phenomena of the multiple user noise in this system is some-what identical to the one in the TH system. The difference is that multiple wavelengths will reduce the interference among users since the contributions by the users to the system noise is smaller per wavelength in this system versus TH system assuming the same number of hops per bit in the PRIS code. Therefore employment of Wavelength Division Multiplexing allows to "pack" more users into a single fiber. Let n_λ be the number of time hops per bit at some wavelength λ . And let L be the number of wavelengths used in each code. Without loss of generality we can assume that the system uses identical codes in terms of number of pulses in the pattern. Each code uses up all L optical wavelengths available and the number of time hops per bit at each wavelength is the same for each user.

If the passive pause signaling is employed then each user contributeds to the multiple user noise on the average per unit of time $\nu_{\lambda,i}$ pulses at each wavelength, where:

$$\nu_{\lambda,i} = \frac{n_\lambda}{T_d}\, p(1) \tag{5.2.1}$$

And N users will contribute ν_λ pulses:

$$\nu_\lambda = \frac{Nn_\lambda}{T_d}\, p(1) \tag{5.2.2}$$

We use the Poisson model and the approach similar to the one used for the TH system. The average rate of multiple user pulses at each wavelength can be written as:

$$\overline{\mu_{x,\lambda}} = \nu_\lambda \, e^{-\nu_\lambda \tau_c} \tag{5.2.3}$$

And the average duration of the multiple user noise pulses:

$$\overline{\tau_{x,\lambda}} = \frac{1-e^{-\nu_\lambda \tau_c}}{\nu_\lambda e^{-\nu_\lambda \tau_c}} \tag{5.2.4}$$

The probability density function of the pulse durations is then:

$$f_x(\tau) = e^{-\nu_\lambda \tau_c}\delta(\tau-\tau_c) + \nu_\lambda e^{-\nu_\lambda \tau_c}U(\tau-\tau_c) + \sum_{k=1}^{\infty}(-1)^k \nu_\lambda{}^k e^{-\nu_\lambda (k+1)\tau_c} \quad x$$

$$\frac{\left[\tau - (k+1)\tau_c\right]^k}{(k-1)!} \left\{1 + \frac{\nu_\lambda}{k}\left[\tau - (k+!)\tau_c\right]\right\} U\left[\tau-(k+1)\tau_c\right] \tag{5.2.5}$$

It can be observed that there is a finite probability of pulse durations equal exactly to τ_c.

5.3 PROBABILITY OF ERROR IN THE HYBRID SYSTEM

Passive Pause Signaling

We will analyze the system that employs a receiver consisting of WDM splitter and otherwise identical to the one depicted in Fig.3.3. The number of delay lines in the TDL correlator is equal to Ln_λ .

To find the characteristics of the output signal from the TDL correlator, (Fig.3.3), we will assume all pulse trains $x_j(t)$ independent and statistically identical. The correlator effectively consists of Ln_λ delay lines. Then the average rate of the y(t) pulses can be found as:

$$\overline{\mu_y} = L\, n_\lambda\, \nu_\lambda\, e^{-\nu_\lambda \tau_c} \left(1 - e^{-\nu_\lambda \tau_c}\right)^{Ln_\lambda - 1} \tag{5.3.1}$$

The average duration of the y(t) pulses:

$$\overline{\tau_y} = \frac{\overline{\tau_{x,\lambda}}}{Ln_\lambda} \tag{5.3.2}$$

If we use the same reasoning that we used for the Time-Hopped system we arrive at the expression for the probability of error for the hybrid channel:

$$P_e = \overline{\mu_y} \left(1 - \frac{\tau_T}{\overline{\tau_{x,\lambda}}}\right)^{Ln_\lambda - 1} \left(\frac{\overline{\tau_{x,\lambda}} - \tau_T}{Ln_\lambda} + \tau_z - \tau_T\right) p(0) \tag{5.3.3}$$

Or using (5.3.1) we receive:

$$P_e = Ln_\lambda \nu_\lambda p(0)\, e^{-\nu_\lambda \tau_c} \left(1 - e^{-\nu_\lambda \tau_c}\right)^{Ln_\lambda - 1} \left(1 - \frac{\tau_T}{\overline{\tau_{x,\lambda}}}\right)^{Ln_\lambda - 1} \left(\frac{\overline{\tau_{x,\lambda}} - \tau_T}{Ln_\lambda} + \tau_z - \tau_T\right)$$

(5.3.4)

We will now introduce parameters K_z and K_T :

$$K_z = \frac{\tau_z}{\tau_c} \tag{5.3.5}$$

$$K_T = \frac{V_T}{V_{max}} = \frac{\tau_T}{\tau_z} \tag{5.3.6}$$

The channel load for a hybrid system is a ratio of the number of interfering users to the total possible number of users in a TDMA system that employs Wavelength Division Multiplexing:

$$C_l = \frac{N}{LK_{f,\lambda}} \tag{5.3.7}$$

Where $K_{f,\lambda}$ is the electronic Bandwidth Expansion Coefficient at each wavelength:

$$K_{f,\lambda} = \frac{T_d}{\tau_c} \tag{5.3.8}$$

Then the average duration of the multiple user noise pulses at each wavelength becomes:

$$\overline{\tau_{x,\lambda}} = \frac{1 - e^{-\frac{n_\lambda N}{2K_{f,\lambda}}}}{\frac{Nn_\lambda}{2\tau_c K_{f,\lambda}} e^{\frac{n_\lambda N}{2K_{f,\lambda}}}} \tag{5.3.9}$$

And the probability of error assuming symmetric and infinite data sources then becomes:

$$P_e = \frac{1}{2}\left[1 - e^{\frac{-n_\lambda N}{2K_{f,\lambda}}}\left(1 + \frac{n_\lambda K_T K_z N}{2} K_{f,\lambda}\right)\right]^{Ln_\lambda - 1} \quad x$$

$$\left[1 - e^{\frac{Ln_\lambda C_l}{2}}\left(1 + \frac{n_\lambda K_T K_z N}{2K_{f,\lambda}} - \frac{Ln_\lambda{}^2 K_z N}{2K_{f,\lambda}} + \frac{Ln_\lambda{}^2 K_T K_z N}{2K_{f,\lambda}}\right)\right] \tag{5.3.10}$$

Or introducing the channel load parameter:

$$P_e = \left[1 - e^{-Ln_\lambda \frac{C_l}{2}}\left(1 + Ln_\lambda K_T K_z \frac{C_l}{2}\right)\right]^{Ln_\lambda - 1} \quad x$$

$$\left[1 - e^{-Ln_\lambda \frac{C_l}{2}}\left(1 + Ln_\lambda K_T K_z \frac{C_l}{2} - L^2 n_\lambda{}^2 K_z \frac{C_l}{2} + L^2 n_\lambda{}^2 K_T K_z \frac{C_l}{2}\right)\right] \tag{5.3.11}$$

Fig.5.6 shows the curves of the probability of error as a function of the number of interfering users. If we introduce a parameter D which we will call Code Dimension and define it as a product of the number of wavelengthes and of the number of hops per bit in the code at each wavelength:

$$D = L \;\; n_\lambda \tag{5.3.12}$$

Then the probability of error becomes:

$$P_e = \left[1 - e^{-\frac{DC_l}{2}}\left(1 + DK_TK_z\frac{C_l}{2}\right)\right]^{D-1} \quad x$$

$$\left[1 - e^{-\frac{DC_l}{2}}\left(1 + DK_TK_z\frac{C_l}{2} - D^2K_z\frac{C_l}{2} + D^2K_TK_z\frac{C_l}{2}\right)\right] \qquad (5.3.13)$$

From (5.3.13) it is clear that the number of wavelengthes and the number of hops per bit at each wavelength present in the formula symmetrically, thus have identical effect on the system performance. This finding is very important because it gives the system designer the freedom of trading off electronic bandwidth for optical and visa-versa. Also the system growth can be on the expense of adding new wavelengthes and not having to further expand the electronic bandwidth at each wavelength.

Fig.5.2 illustrates the probability of error given by (5.3.13) as a function of the channel load for different values of code dimension D. It can be observed from the figure that there exists an optimal value of D for a given channel load. This dependence is shown in Fig.5.3. Since the number of wavelengthes and the number of hops per bit have the same contribution to the performance then their optimal value for a given channel load can be found as follows:

$$n_{opt} = \frac{D_{opt}}{L} \qquad (5.3.14)$$

$$L_{opt} = \frac{D_{opt}}{n_\lambda} \qquad (5.3.15)$$

Fig.5.5 illustrates the minimum achievable probability of error versus channel load for optimal code dimension at each value of the channel load.

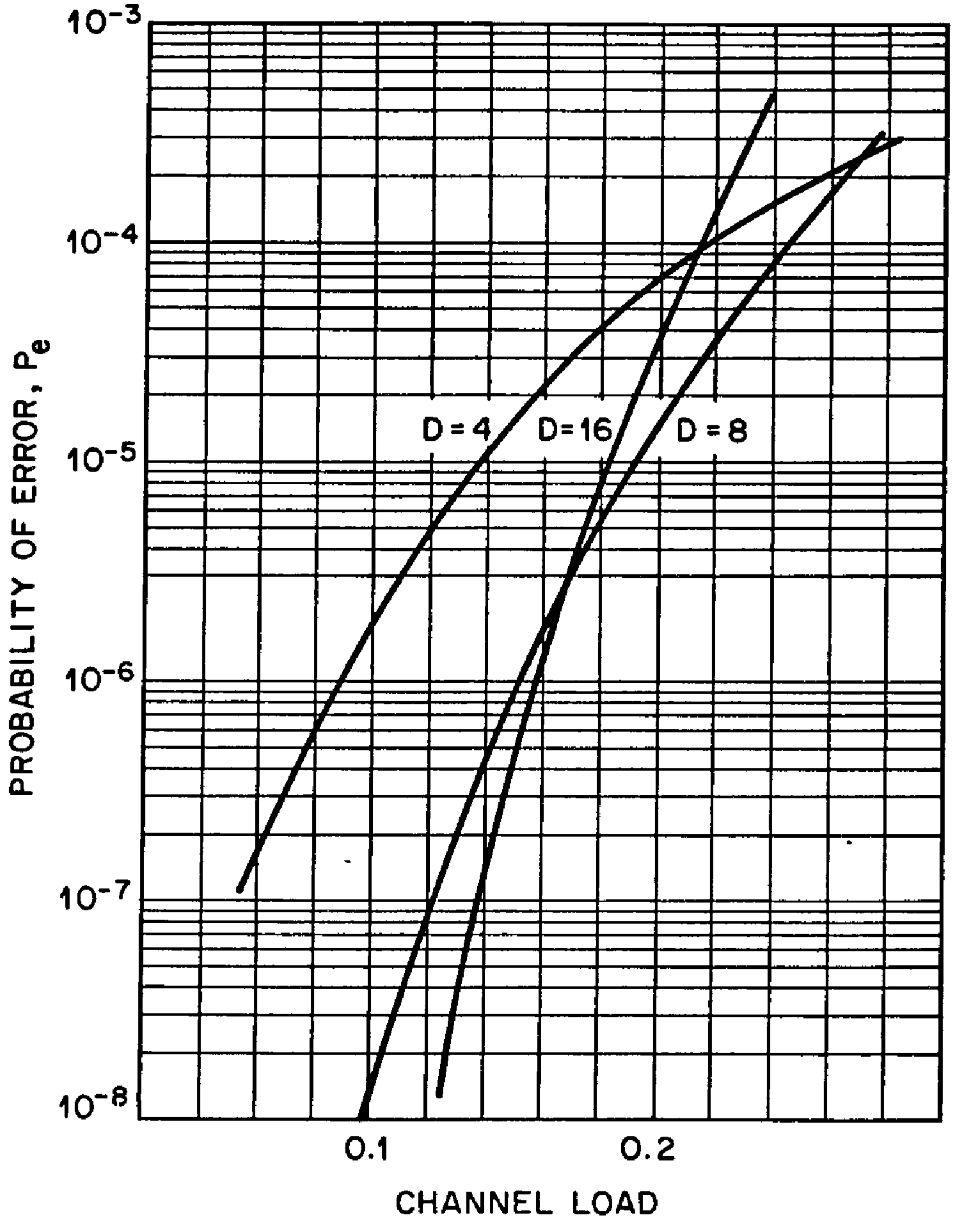

Fig.5.2. OOK/OR/T λ H System with PPS, $P_e = f(C_l)$

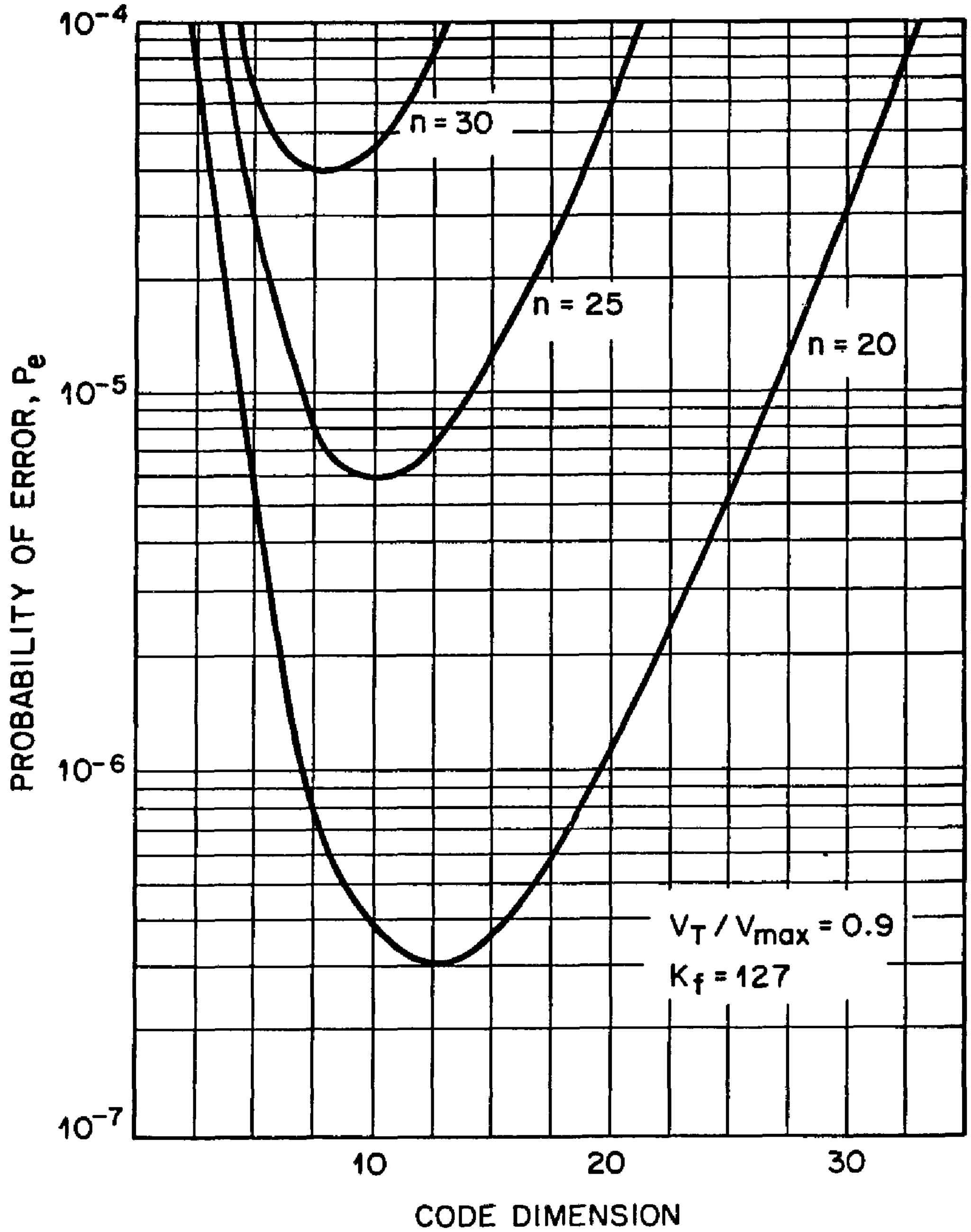

Fig.5.3. OOK/OR/TMH System with PPS, P_e=f(D)

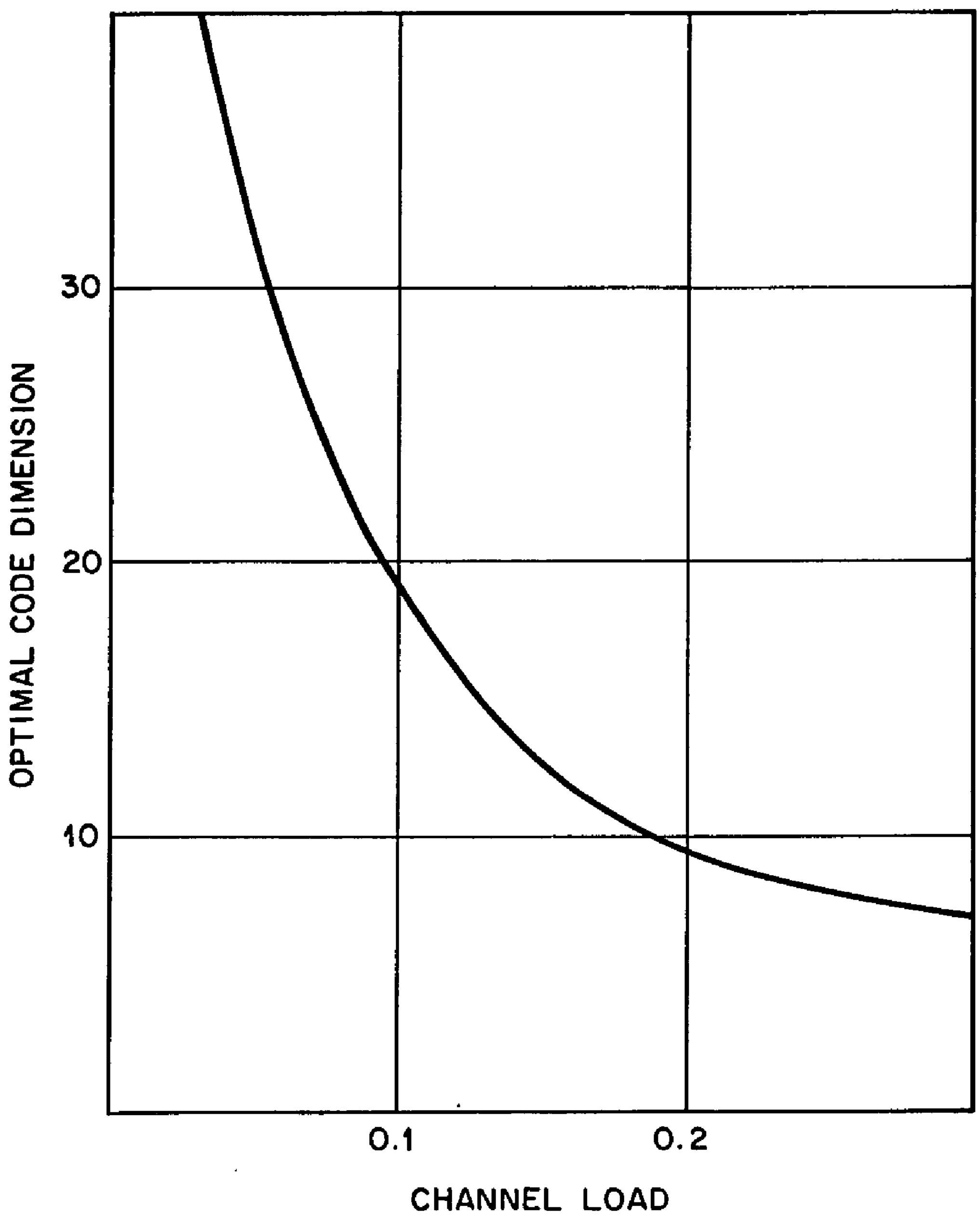

Fig.5.4 OOK/OR/T λ H System with PPS: $D_{opt}=f(C_l)$

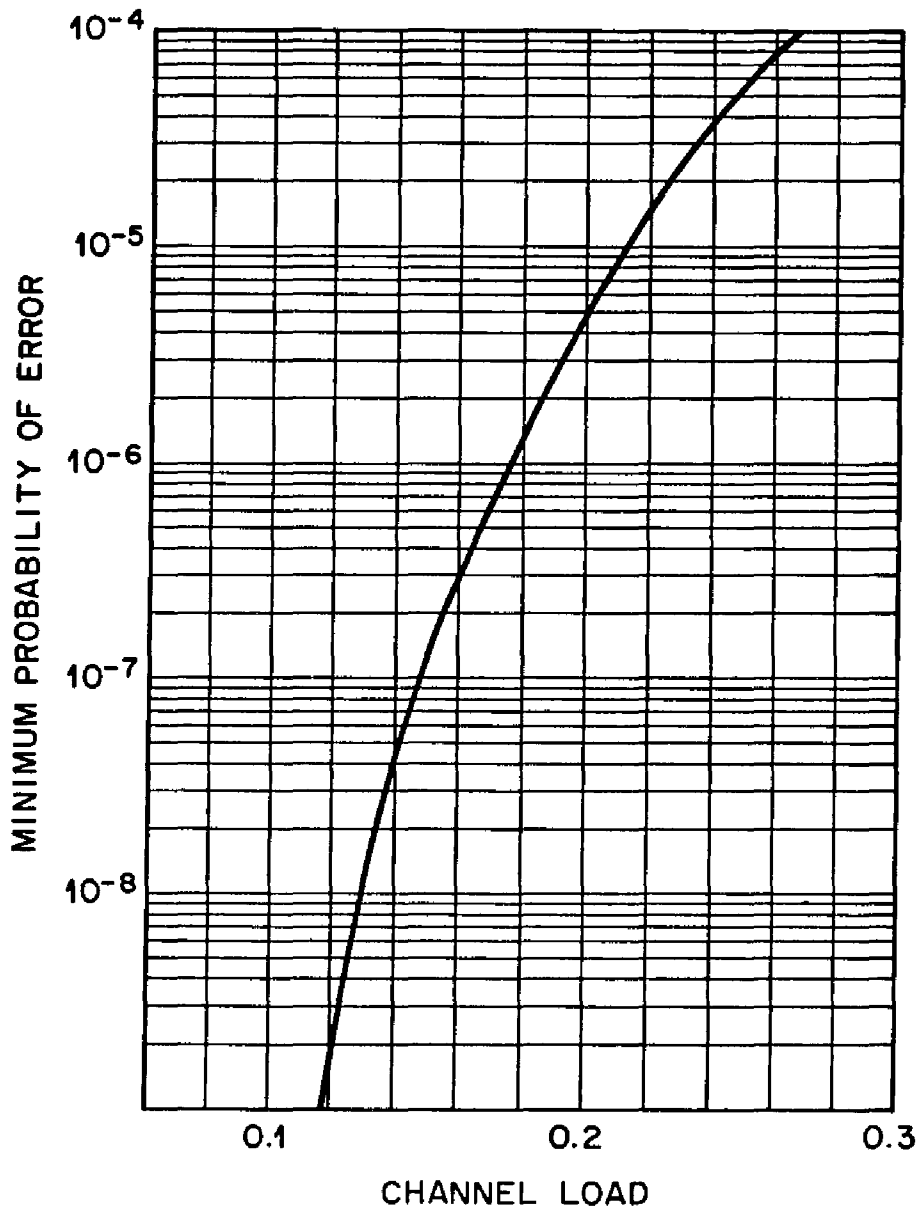

Fig.5.5 OOK/OR/T \ H System with PPS: $P_{e_{min}}=f(G_1)$

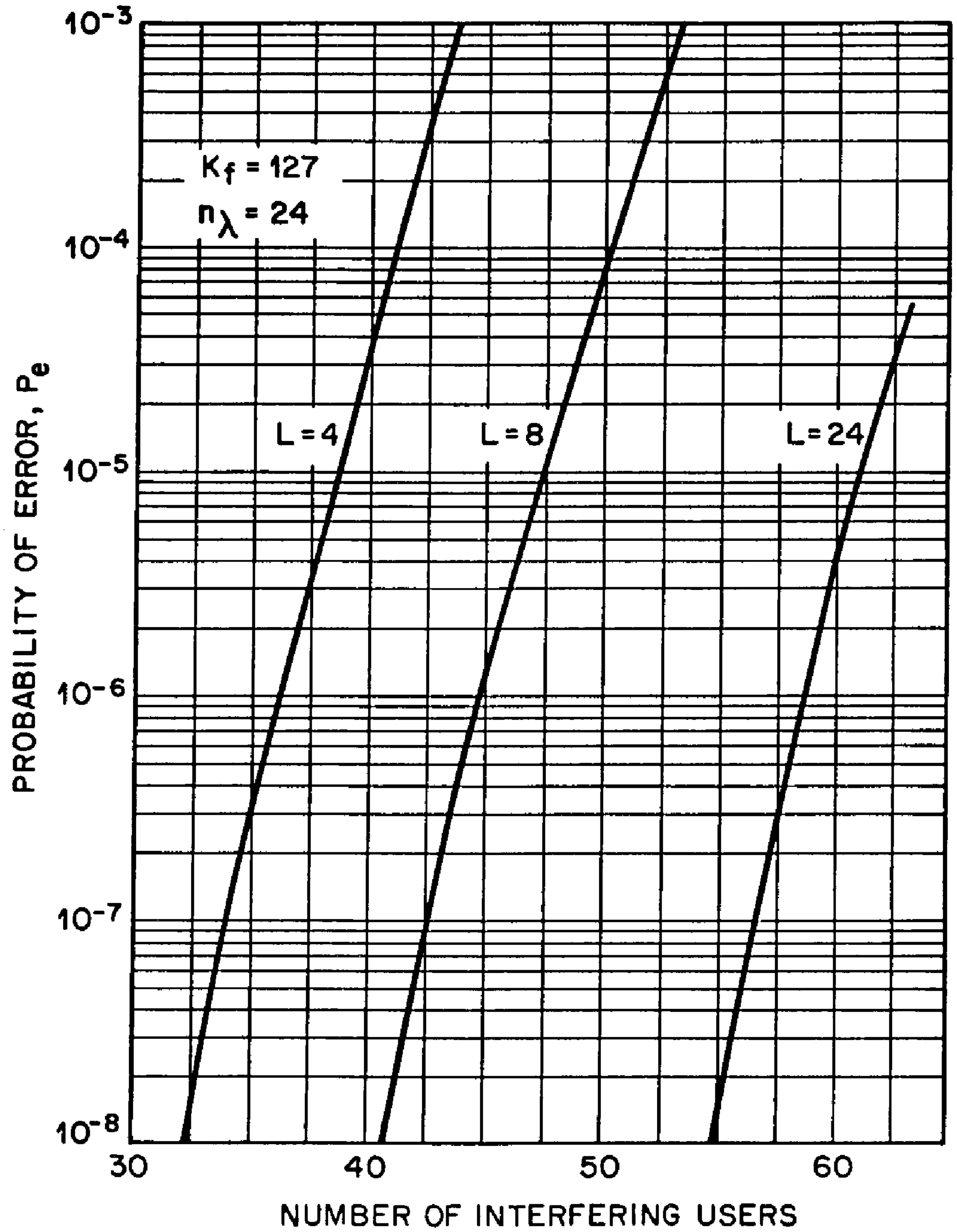

Fig.5.6. OOK/OR/T λ II System with PPS, P_e=f(N)

Active Pause Signaling

For the analysis of a hybrid signaling schemes we can also use the Poisson model. The parameter of the distribution at each wavelength can be written as:

$$\mu_\lambda = N \frac{n_{0,\lambda} p(0) + n_{1,\lambda} p(1)}{T_d} \tag{5.3.16}$$

Where: $n_{1,\lambda}$ and $n_{0,\lambda}$ are numbers of hops per bit in the one- and zero-patterns correspondently.

The average rate and the average duration of the multiple user noise pulses can be found from (5.2.3) and (5.2.4). Let's consider a case with identical codes for one- and zero-patterns in terms of the number of hops per bit:

$$n_{1,\lambda} = n_{0,\lambda} = n_\lambda \tag{5.3.17}$$

Then using the same reasoning as in chapter three we receive for the probability of error:

$$P_e = \overline{\mu_y} \left(1 - \frac{\tau_z}{\overline{\tau_{x,\lambda}}}\right)^{Ln_\lambda - 1} \left(\frac{\overline{\tau_{x,\lambda}} - \tau_z}{n}\right) \tag{5.3.18}$$

Assuming symmetric data sources the probability of error becomes:

$$P_e = \left[1 - e^{-\frac{Ln_\lambda N}{K_f}} \left(1 + \frac{Ln_\lambda N K_z}{K_f}\right)\right]^{Ln_\lambda} \tag{5.3.19}$$

Introducing the channel load parameter we receive:

$$P_e = \left[1 - e^{-Ln_\lambda C_l}\left(1 + Ln_\lambda K_z C_l\right)\right]^{Ln_\lambda} \tag{5.3.20}$$

And using (5.3.12) we arrive at the final expression for the probability of error for a hybrid TλH system that employs Active Pause Signaling:

$$P_e = \left[1 - e^{-DC_l}\left(1 + DK_z C_l\right)\right]^{D} \tag{5.3.21}$$

The plots of the probability of error as a function of channel load for different values of the code dimension are illustrated in Fig.5.7. There is obviously an optimum in the value of D for a given channel load. The dependency of the D_{opt} from the channel load is shown in Fig.5.8. It can be seen from the figure that as the channel load increases the optimal value of the code dimension goes down. It can be explained by the necessity to reduce each user's contribution to the system noise. The curve for the minimum achievable probability of error can be found in Fig.5.9.

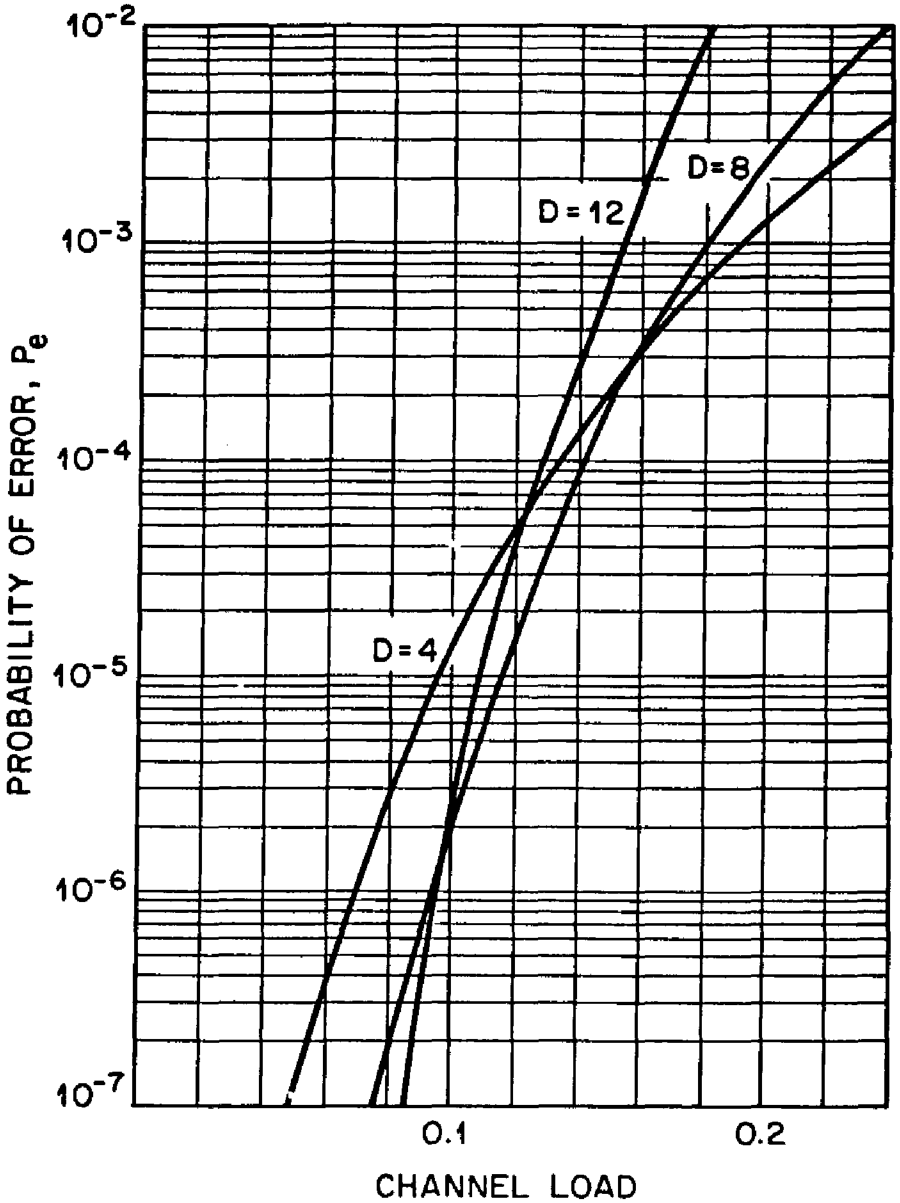

Fig.5.7 OOK/OR/TAH System with APS, $P_e=f(C_l)$

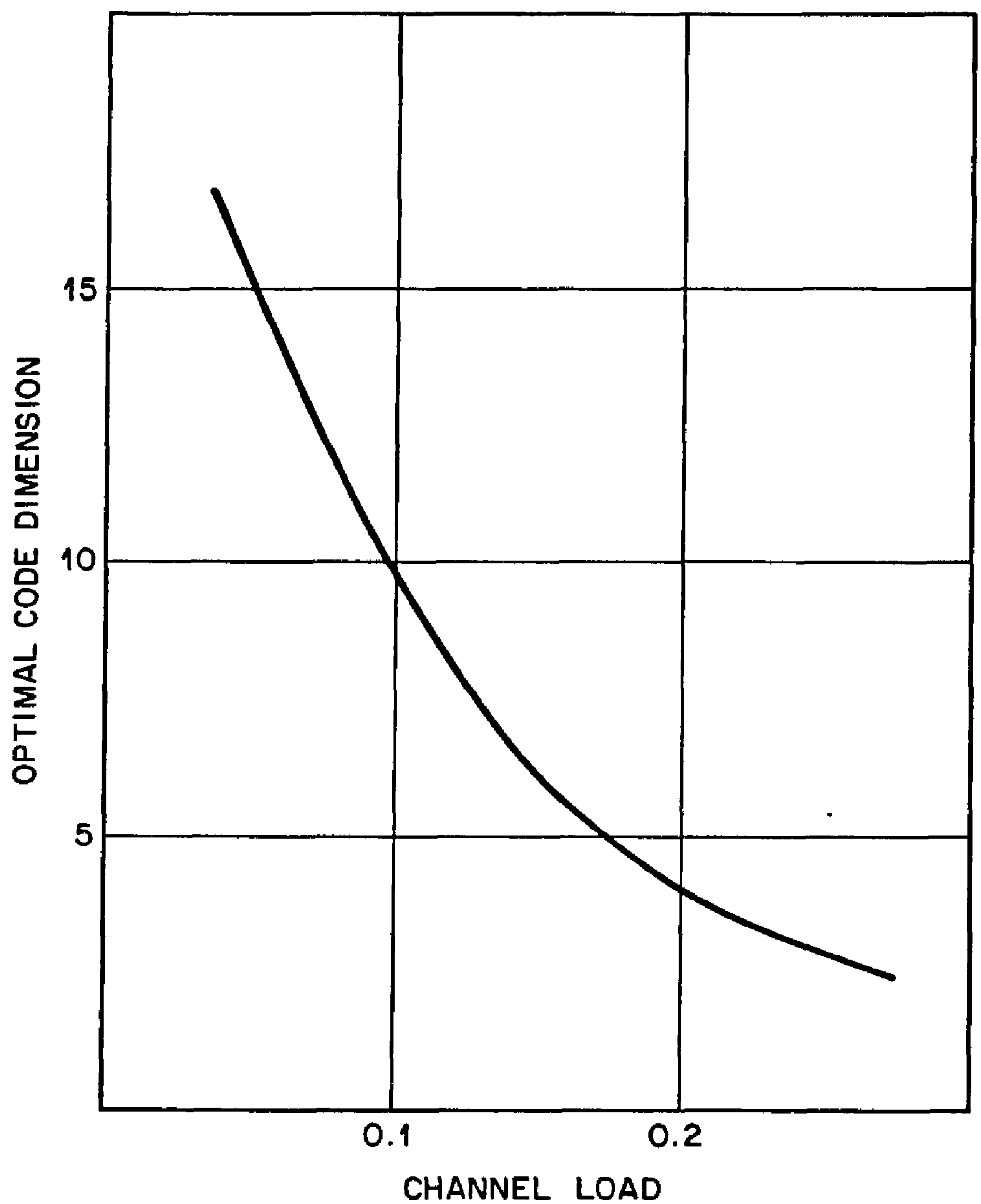

Fig.5.8. OOK/OR/ TMI System with APS, $D_{opt}=f(C_l)$

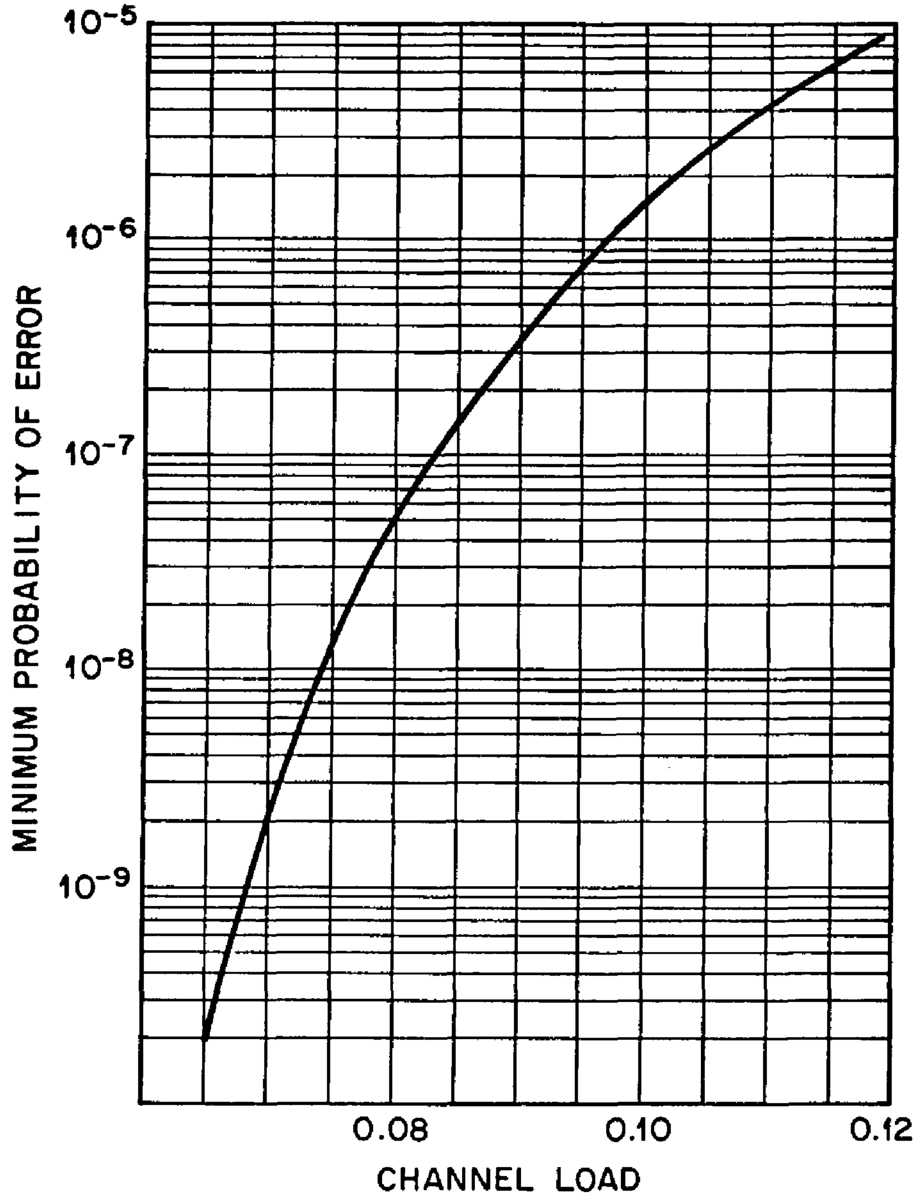

Fig.5.9. OOK/OR/TMH System with APS, $P_{e_{min}}=f(C_l)$

5.4 CONCLUSIONS

We analyzed the hybrid CDMA multiple access channel that employs a combination of Time and Color Hopping. This signaling scheme implies two-dimensional spreading of the signal spectrum. One is electronic the second is optical. The electronic spectrum spreading is characterized by the Bandwidth Expansion Coefficient $K_{f,\lambda}$ while the spreading in optical domain is characterized by the number of available wavelengthes L. It becomes clear from the analysis that introducing the second dimension into the spreading process allows to increase the number of users that can simultaneously communicate over a single fiber optic channel.

We introduced a code parameter D that characterizes the size of the codes used in the system. One can observe the similarity between the probability of error expressions for the $T\lambda H$, TH and λH systems where D plays the role of n and L correspondently. This similarity shows the generality of the parameter D that we introduced for the hybrid system. In other words the TH and λH systems can be considered particular cases of the hybrid system.

6. SYNCHRONIZATION ASPECTS OF CDMA SYSTEMS

6.1 INTRODUCTION

In previous chapters we conducted Code Division Multiple Access systems performance analysis for different signaling schemes assuming perfect synchronization between the transmitter's and the receiver's codes. What it means in terms of our system configurations and the system models used is that the synchronization signal $z(t)$ is absolutely errorless and therefore did not cause any false detections. In the mean time the problem of deriving the sync pulses from the incoming signal in presence of multiple user noise is rather complicated. In this chapter we propose and analyze a synchronization scheme for an OOK/OR/TH system. This scheme is applicable to the λH and the TλH systems as well with minor modifications.

The idea which is behind the proposed synchronization mechanism takes advantage of the statistical properties of the multiple user noise. By introducing a memory into the process of signal tracking on the data level the system uses the fact that the longer is the data bit error burst the less probable it is. In other words if K bits are consequently detected and they are spaced in time with the correct interval T_d and K is such that the probability of K consequent false detections is negligibly small then synchronization can be declared with a thrusting probability which is a function of the value of K. The realization of this principle depends very much on the signaling scheme which is employed by the system.

6.2 SYNCHRONIZATION IN THE OOK/OR/TH SYSTEMS WITH PPS

When Passive Pause signaling is employed we propose periodic insertion of sync words or usage of data scrambling techniques to insure a desired density of the binary one runs on the data level. The diagram illustrating the proposed synchronization algorithm is shown in Fig.6.1. The target signal mixed with the multiple user noise appears at the input of the TDL correlator. Decoded addresses will produce pulses at the correlator output. Pulses which are shorter than τ_c are filtered out in the Pulse Width Selector, (PWS). Some of these pulses will be false due to the system noise.

We propose to precede every data burst by a preamble which is a run of data values of one. The size of the preamble will determine the system performance.

Let K be the number of pulses in the preamble, or it's size. Then at the instant when the K-th bit of the preamble is received and decoded the SYNC signal sets the Flip-Flop, (F/F), thus declaring the synchronism and enabling the generation of the strobing signal z(t). The circulation counter (CC) is reset to zero. the SYNC pulse starts circulating in the delay line and number of it's passes via the delay line is being counted by the circulation counter. If q passes took place and the counter was not reset by the SYNC signal false synchronism is declared, F/F is reset and no z(t) pulses are produced. As soon as new sync pulse appears the cycle starts from the beginning. Every new SYNC pulse takes the previous pulse out of circulation by opening the circulation gate, (CG).

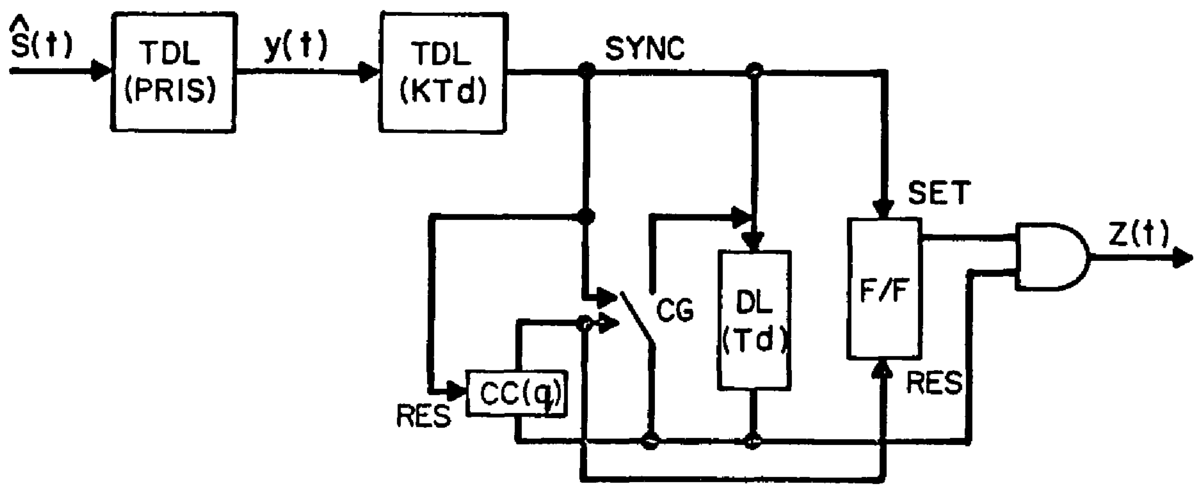

Fig.6.1. OOK/OR/TH System with PPS: Synchronization Scheme

6.3 SYNCHRONIZATION SCHEME FOR OOK/OR/TH SYSTEMS WITH APS

In the system that employs Active Pause Signaling, (APS), there is no need to insert synchronizations words for periodic retiming of the strobing signal. The system can use the timing derived from K previous data intervals to strobe the (K+1)-st.

The block-diagram of the synchronisation scheme for the system with APS is shown in Fig.6.2.

The unstrobed signals y(t) (see Fig.3.3) from the TDL correlators are ORed and routed to the TDL correlator that is matched to K intervals equal to the data period T_d . A Pulse Width Filter, (PWF), may be used to remove pulses which are much shorter or longer than τ_c .

We propose to call this technique Predictive Tracking Because it uses the timing information from the previous signals to predict the timing of the current data bit. Realization of Predictive Tracking is possible only in very stable communications media and signal processing environments. Single mode fiber and all-optical Tapped Delay Line Correlators possess this property.

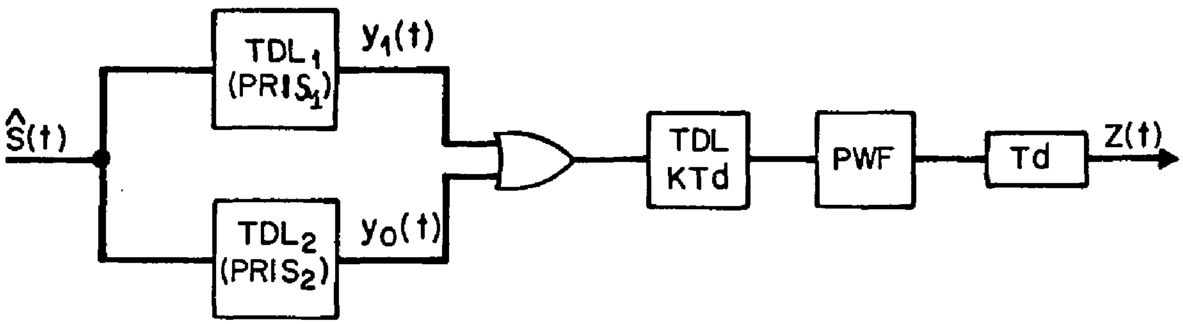

Fig.6.2. OOK/OR/TH System with APS: Synchronization Scheme

6.4 PROBABILITY OF FALSE ACQUISITION IN OOK/OR/TH SYSTEMS

6.4.1 False Acquisition in OOK/OR/TH System With PPS

False acquisition can occur when there is no target signal in the channel and multiple user noise produces false preambles. The system can reside in the idle state infinite time so it is very important to find the average rate of the false calls that will be received by the receiver as a function of the channel traffic.

In chapter three we determined the complementary distribution of the signal y(t) at the output of the TDL correlator prior to strobing. This distribution gives us the probability of the output pulse from the correlator to be longer than some value of τ :

$$F_{c,y} = \left(1 - \frac{\tau}{\tau_x}\right)^{n-1} \qquad (6.4.1)$$

The synchronization circuit can be viewed as another TDL correlator matched to the run of data values of one spaced in time with intervals equal to the period of the data signal, T_d . We will call it Sync Correlator. Then we can find the complementary distribution of the false pulses at the output of the Sync Correlator as:

$$F_{c,s}(\tau) = \left[1 - \frac{1}{\tau_x} \int_0^{\tau} F_{c,y}(\xi) d\xi\right]^{K-1} F_{c,y}(\tau) \qquad (6.4.2)$$

Substituting (6.4.1) into (6.4.2) we receive:

$$F_{c,s} = \left\{1 - \frac{1}{n}\left[1 - \left(1 - \frac{\tau}{\tau_x}\right)^{n}\right]\right\}^{K-1} \left(1 - \frac{\tau}{\tau_x}\right)^{n-1} \qquad (6.4.3)$$

The system qualifies only the pulses that are longer than τ_c . The probability for these pulses is then:

$$F_{c,s}(\tau_c) = \left\{1 - \frac{1}{n}\left[1 - \left(1 - \frac{\tau_c}{\overline{\tau_x}}\right)^n\right]\right\}^{K-1} \left(1 - \frac{\tau_c}{\overline{\tau_x}}\right)^{n-1} \qquad (6.4.4)$$

Substituting the expression for $\overline{\tau_x}$ from (1.5.26) we receive:

$$F_{c,s}(\tau_c) = \left\{1 - \frac{1}{n}\left[1 - \left(1 - \frac{\tau_c \nu e^{-\nu\tau_c}}{1 - e^{-\nu\tau_c}}\right)^n\right]\right\}^{K-1} \left(1 - \frac{\tau_c \nu e^{-\nu\tau_c}}{1 - e^{-\nu\tau_c}}\right)^{n-1} \qquad (6.4.5)$$

For the PPS scheme we can substitute the expression for ν in a TH system:

$$F_{c,s}(\tau_c) = \left\{1 - \frac{1}{n}\left[1 - \left(1 - \frac{\tau_c \frac{Nn}{2T_d} e^{-\frac{Nn}{2T_d}\tau_c}}{1 - e^{-\frac{Nn}{2T_d}\tau_c}}\right)^n\right]\right\}^{K-1} \left(1 - \frac{\tau_c \frac{Nn}{2T_d} e^{-\frac{Nn}{2T_d}\tau_c}}{1 - e^{-\frac{Nn}{2T_d}\tau_c}}\right)^{n-1} \qquad (6.4.6)$$

Or introducing channel load parameter we receive:

$$F_{c,s}(\tau_c) = \left\{1 - \frac{1}{n}\left[1 - \left(1 - \frac{\frac{nC_l}{2} e^{-n\frac{C_l}{2}}}{1 - e^{-n\frac{C_l}{2}}}\right)^n\right]\right\}^{K-1} \left(1 - n\frac{C_l}{2}\frac{e^{-n\frac{C_l}{2}}}{1 - e^{-n\frac{C_l}{2}}}\right)^{n-1}$$

(6.4.7)

The average rate of the false pulses before pulse-width selection can be found using (3.3.6):

$$\overline{\mu_s} = K\,\overline{\mu_y}(\overline{\mu_y}\;\overline{\tau_y})^{K-1} \tag{6.4.8}$$

And the average duration of these pulses will be:

$$\overline{\tau_s} = \frac{\overline{\tau_y}}{K} = \frac{\overline{\tau_x}}{Kn} \tag{6.4.9}$$

The average rate of the qualified false pulses then can be found as follows:

$$\overline{\mu_{FA}} = \overline{\mu_s}\,F_{c,s}(\tau_c) \tag{6.4.10}$$

After substituting (6.4.7), (6.4.8) and using (6.4.9) we receive for the average rate of the false acquisition pulses:

$$\overline{\mu_{FA}} = \frac{Kn^2C_l}{2\tau_c}\,e^{-\frac{nC_l}{2}}\left(1-e^{-\frac{nC_l}{2}}\right)^{n(K+1)-2}\left\{1-\frac{1}{n}\left[1-\left(1-\frac{\frac{nC_l}{2}e^{-\frac{nC_l}{2}}}{1-e^{-\frac{nC_l}{2}}}\right)^{n}\right]\right\}^{K-1} \tag{6.4.11}$$

The probability of at least one false acquisition in the idle state of the receiver per period of time equal to qT_d can be found as follows:

$$P_{FA}(qT_d) = 1 - e^{-\overline{\mu_{FA}}qT_d} \tag{6.4.12}$$

Substituting (6.4.11) into (6.4.12) and taking to consideration that:

$$\tau_c = \frac{T_d}{K_f}$$

we receive for the probability of false acquisition over the period of q data bit intervals:

$$P_{FA}(qT_d) = 1 -$$

$$\mathrm{EXP}\left(- K_f q \frac{Kn^2 C_l}{2} e^{-\frac{nC_l}{2}} \left(1 - e^{-\frac{nC_l}{2}}\right)^{n(K+1)-2} \left\{ 1 - \frac{1}{n} \left[1 - \left(1 - \frac{\frac{nC_l}{2} e^{-\frac{nC_l}{2}}}{1 - e^{-\frac{nC_l}{2}}} \right)^{n} \right] \right\}^{K-1} \right) \qquad (6.4.13)$$

Fig.6.3 illustrates the Probability of false acquisition as a function of channel load for different sizes of the preamble.

We will now determine the average time during which the system will reside in false sync once it acquires it. The model that we will use is as follows. Once the false sync is acquired the minimum time that it will take for the system to realize it is:

$$\tau_{FS_{min}} = q\,T_d \qquad (6.4.14)$$

After q data bit intervals if no sync word is received the synchronization will be dropped. If during these q intervals a new false sync word is detected then the system will remain in false synchronism etc. We will model the arrival times of false sync words as Poisson process with the parameter $\overline{\mu_{FA}}$. Then the average time that the system will remain in false sync can be found as follows:

$$\overline{\tau_{FS}} = \frac{1 - e^{-\overline{\mu_{FA}} q T_d}}{\overline{\mu_{FA}} e^{-\overline{\mu_{FA}} q T_d}} \qquad (6.4.15)$$

Substituting (6.4.11) into (6.4.15) we can receive the expression for the average time in false synchronism. Due to the large size of the formula we do not give the final expression. Fig.6.4 illustrates the plots of the average false sync time as a function of the channel load and different sizes of the sync word. Fig.6.5 shows the same dependence for different values of q.

If the system is correctly synchronized it can loose sync should multiple user noise cause K consequent false detections of ones. Since the mechanism for this is the same as for false acquisition then the probability of loosing sync is equal to the probability of false acquisition:

$$P_{LS} = P_{FA}$$

It can happen at any time during the interval between two enforced sync words with equal probability. Once loosing sync the system will reside in this state till next sync word, or till the end of the current burst, or till K consequent data bits will appear, what ever comes first.

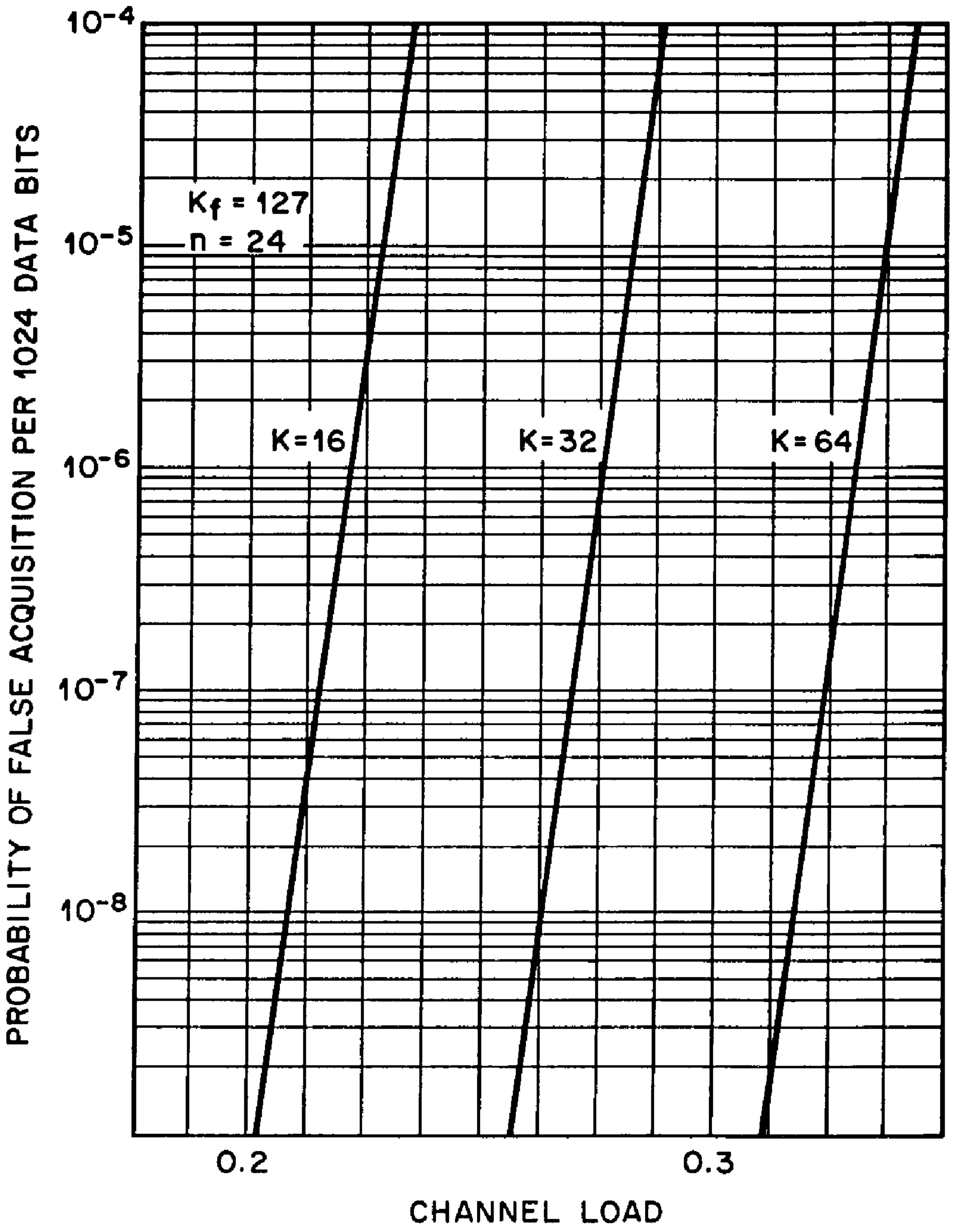

Fig.6.3. OOK/OR/TH System with PPS: Probability of False Acquisition

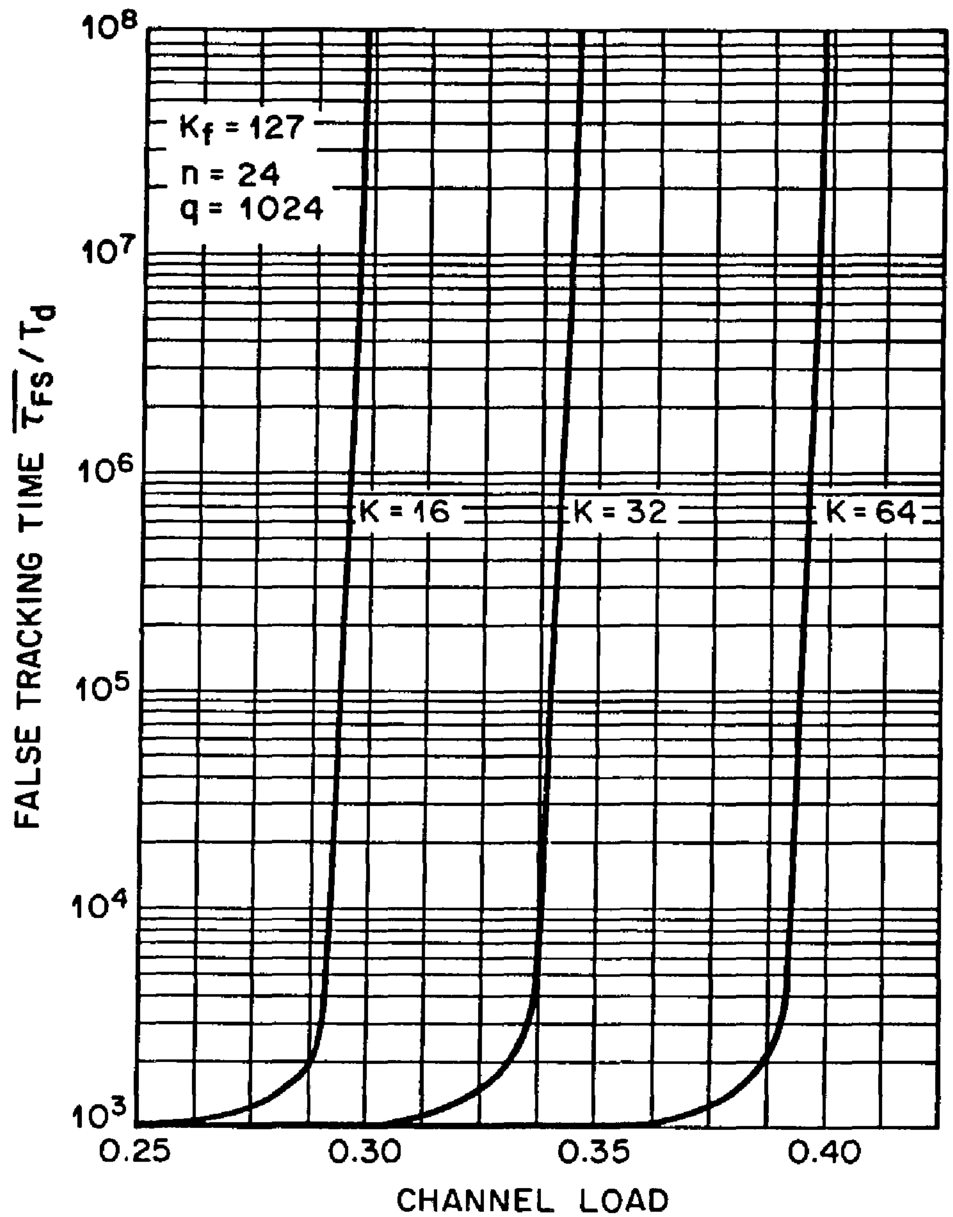

Fig.6.4. OOK/OR/TH System with PPS: False Sync Time vs C_l and K

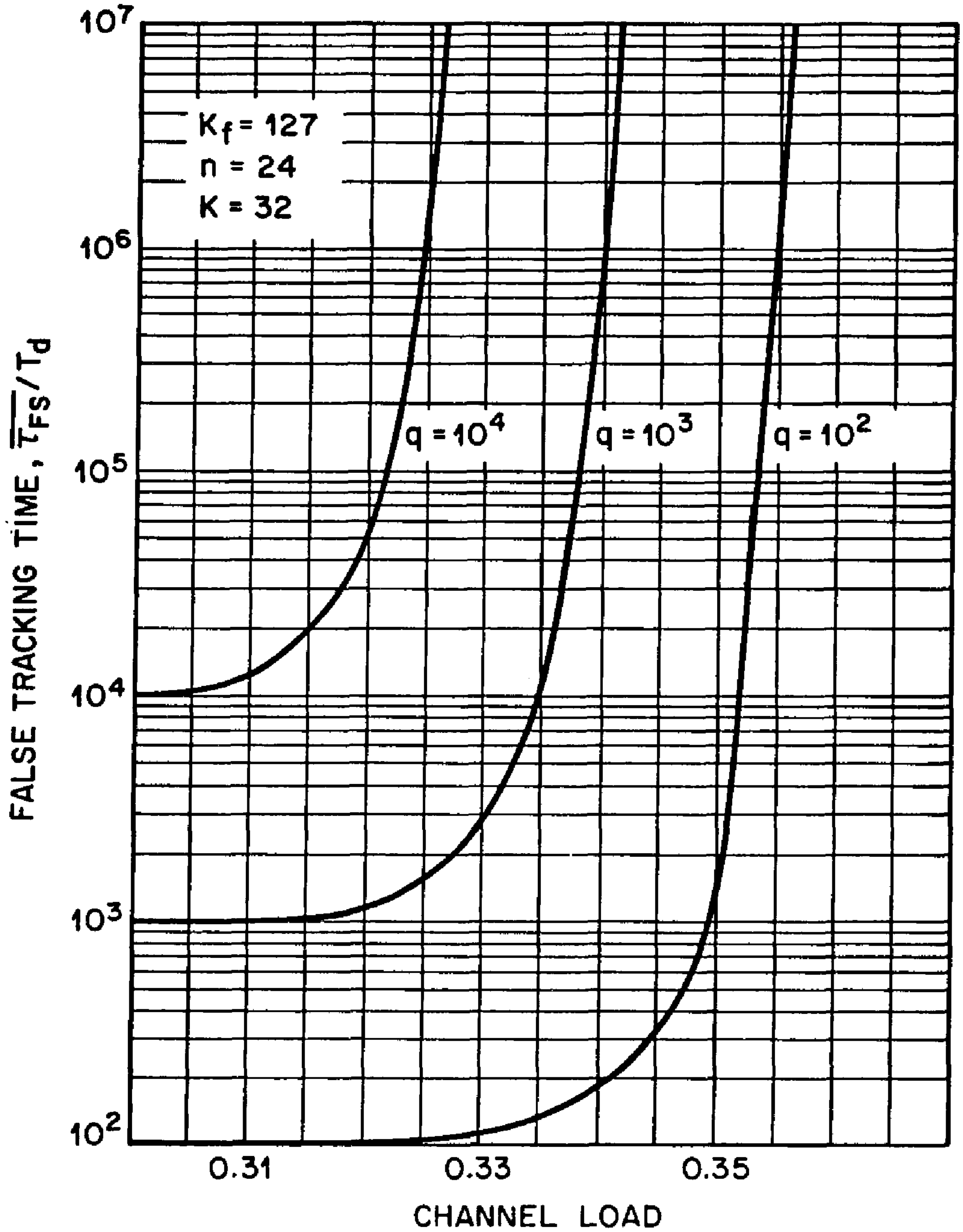

Fig.6.5. OOK/OR/TH System with PPS: False Sync Time vs C_l and q

6.4.2 False Acquisition in OOK/OR/TH System With APS

For the system with Active Pause Signaling a preamble is also required but there is a difference in the reason for it. The system is capable of acquiring synchronism without the preamble as well, however K-1 of the first data bits in the burst will be lost. In the absence of target signal the probability of false SYNC pulses to be longer than τ_c can be found using (6.4.5) by substituting into it the expression for parameter ν for the TH system:

$$F_{c,s}(\tau_c) = \left\{1 - \frac{1}{n}\left[1 - \left(1 - \frac{\tau_c \frac{Nn}{T_d} e^{-\frac{Nn}{T_d}\tau_c}}{1 - e^{-\frac{Nn}{T_d}\tau_c}}\right)^{n}\right]\right\}^{K-1} \left(1 - \frac{\tau_c \frac{Nn}{T_d} e^{-\frac{Nn}{T_d}\tau_c}}{1 - e^{-\frac{Nn}{T_d}\tau_c}}\right)^{n-1} \qquad (6.4.16)$$

Or introducing the channel load parameter we receive:

$$F_{c,s}(\tau_c) = \left\{1 - \frac{1}{n}\left[1 - \left(1 - \frac{nC_l e^{-nC_l}}{1 - e^{-nC_l}}\right)^{n}\right]\right\}^{K-1} \left(1 - nC_L \frac{e^{-nC_l}}{1 - e^{-nC_l}}\right)^{n-1}$$

(6.4.17)

Using (6.4.8), (6.4.10) and (6.4.15) we receive the average rate of the false acquisition pulses for the OOK/OR/TH System that employs Active Pause Signaling:

$$\overline{\mu_{FA}} = \frac{Kn^2C_l}{\tau_c}\, e^{-nC_l} \left(1 - e^{-nC_l}\right)^{n(K+1)-2} \left\{1 - \frac{1}{n}\left[1 - \left(1 - \frac{nC_l e^{-nC_l}}{1 - e^{-nC_l}}\right)^{n}\right]\right\}^{K-1} \tag{6.4.18}$$

And the probability of at least one false acquisition over the period of time qT_d using (6.4.12) and (6.4.16):

$$P_{FA}(qT_d) = 1 -$$

$$\mathrm{EXP}\left[- K_f q K n^2 C_l e^{-nC_l} \left(1 - e^{-nC_l}\right)^{n(K+1)-2} \left\{1 - \frac{1}{n}\left[1 - \left(1 - \frac{nC_l e^{-nC_l}}{1 - e^{-nC_l}}\right)^{n}\right]\right\}^{K-1}\right] \tag{6.4.19}$$

Fig.6.7 illustrates the probability of false acquisition for the system with APS as a function of the channel load. It can be observed that the probability of false acquisition is higher for this signaling scheme than for the system that employs PPS. It can be explained by higher level of the system noise which is due to the multiple user interference.

Once false synchronism is acquired the system can expect a newly detected pulse every T_d interval. Should it miss at least one pulse the burst will be considered terminated and the synchronism will be dropped.

The false sync words are arriving at a rate $\overline{\mu_{FA}}$. We will consider these arrival times constituting Poisson process. Then the average time that the system will reside in false synchronism added to the false acquisition time can be found as follows:

$$\overline{\tau_{FS}} = \frac{1 - e^{-\overline{\mu_{FA}} K T_d}}{\overline{\mu_{FA}}\, e^{-\overline{\mu_{FA}} K T_d}} \tag{6.4.20}$$

Fig.6.8 illustrates the plots of the false sync time as a function of the channel load.

If the system acquired correct synchronization it can loose it due to the same mechanism that causes false acquisition in the idle state. But it will acquire the correct sync immediately within one T_d interval and will generate two sync pulses. This dual sync state should be resolved in higher layers of the communication protocol. It is also possible to have triple, quadruple etc. sync.

The average time that the system will reside in the state with at least one false sync is given by (6.4.20). A mechanism can be built into the system to prevent multiple syncs from confusing the detection process and lock the system into one sync only. Not necessarily it will be the correct one. However this mechanism will prevent the system from loosing the correct synchronism once it is acquired.

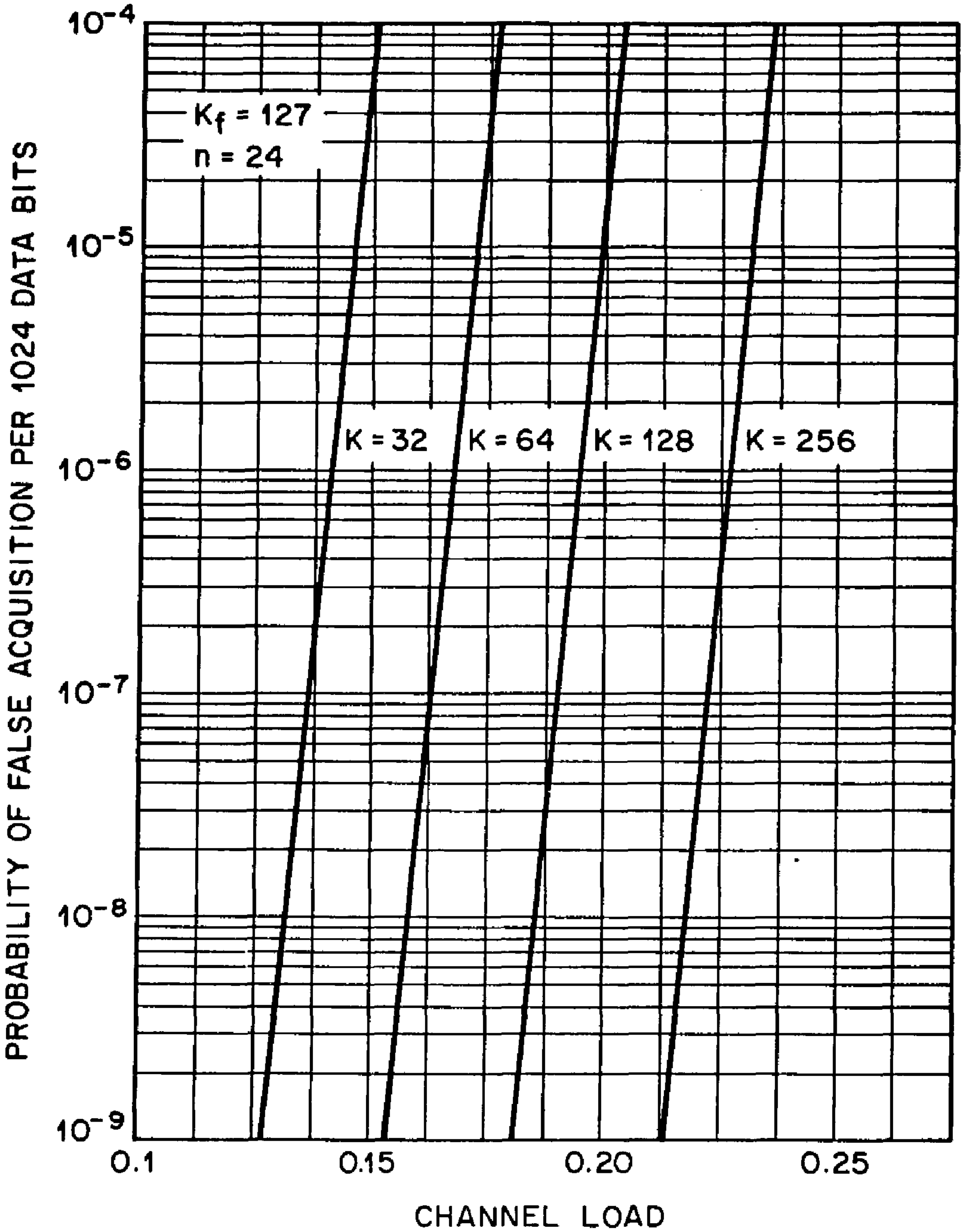

Fig.6.7. OOK/OR/TH System with APS: Probability of False Acquisition

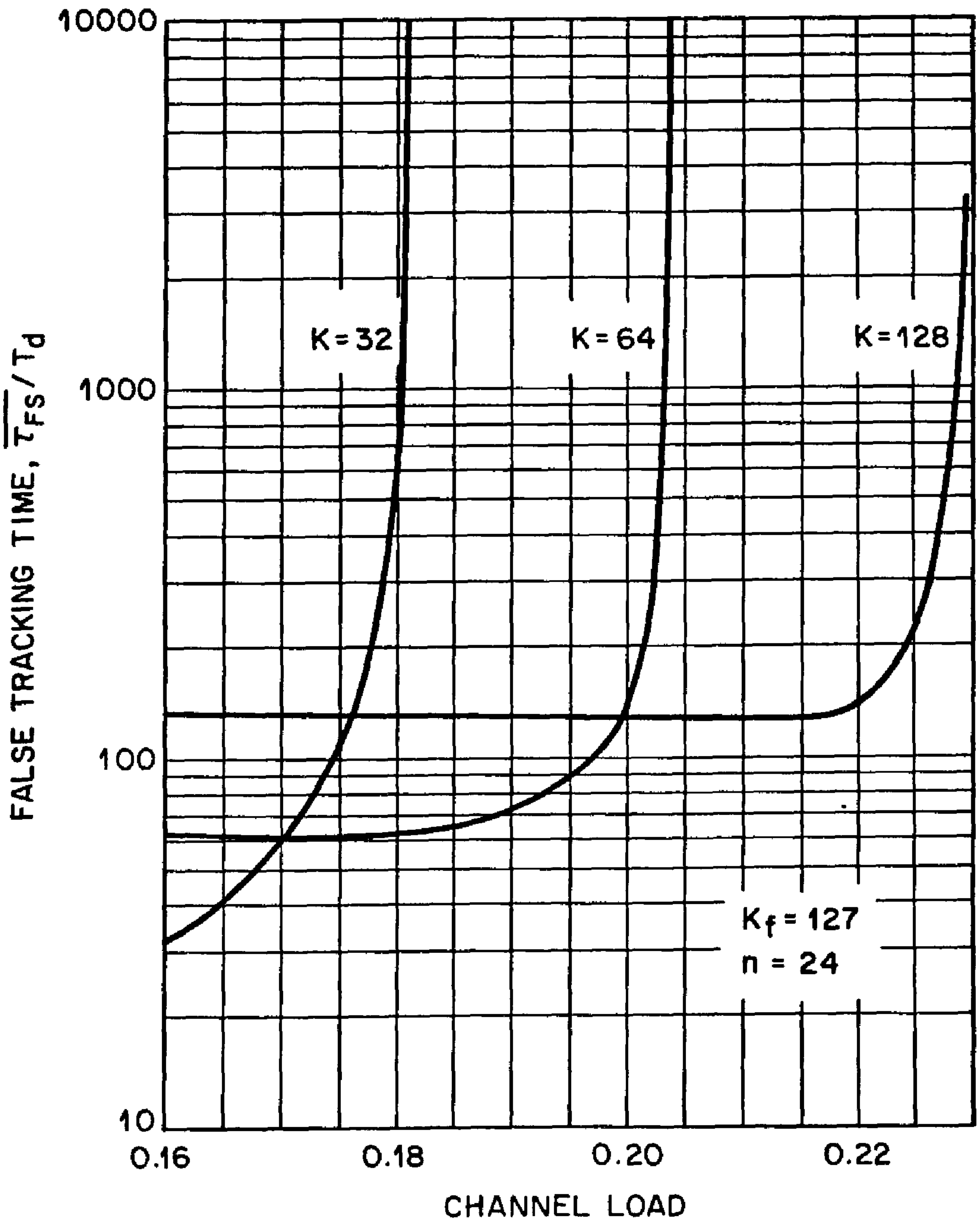

Fig.6.8. OOK/OR/TH System with APS: False Sync Time vs Channel Load

6.5 CONCLUSIONS

We proposed synchronization schemes for Time-Hopped systems that are applicable to other types of CDMA signaling with minor modifications. We analyzed the performance of the proposed schemes by determining the probability of false acquisition, probability of loosing synchronization as well as average time intervals that the system will spend in false synchronism. It has to be noticed that the analysis that was performed took to consideration only pseudo random carrier information and properties for code synchronization. In real systems the reliability of the synchronization schemes can be greatly improved by adding some overhead. In other words if the preamble, for example, carries information decodable by the receiver then false sync can be detected and dropped immediately. Using specially constructed sync words for acquisition and tracking modes can also improve the performance of the system. When the system resides in idle state long synchronization preambles should be used to awake it. It will reduce the probability of false calls. Then the size of the sync word can be reduced. After the End Of Session is declared the system will expect the longer preamble again.

The next step is to use an adaptable synchronization scheme that has a set of sync words in it's library and uses them according to some algorithm that takes to consideration the channel traffic.

7. A NOVEL METHOD OF THE OOK/ADDER/DS CHANNEL SIGNAL DEMULTIPLEXING

7.1 WIDE-BAND RECEIVER FOR OOK/ADDER/DS SYSTEMS

Fiber Optic Adder Channel has rather limited applications in view of the necessity to control the dynamic range of the signal to prevent overdriving the Optical to Electrical transducers. However sometimes when the number of users is small the system designer might take advantage of the fact that the components for direct sequence systems are well developed and are easily available.

In this chapter we propose a novel method of demultiplexing of the OOK/ADDER/DS signal.

In the Adder Channel the optical signals from all sources are being added resulting in a multi-level signal effected by the non-linearity of the channel. There is attenuation present and pulse delays as well as noise contributed by the optical sources, thermal noise and quantum noise in the detection process [2].

In Local Area Networks applications the traveling distances of the light are relatively short and the available bandwidth is therefore high, also the gaussian component of noise is relatively small. These properties allow to use high frequency components of the received signal spectrum in the detection process.

Based on the the above assumptions we propose the receiver structure, depicted in Fig.7.1.

A linear optical detector is used for optical detection. The multi-level electrical signal is being passed through the differentiator, compared to a fixed threshold and then correlated with the derivative of the PN-code replica. The detection process is illustrated in Fig.7.2. The derivative of the received multi-level signal consists of the target impulse train with pseudo-random intervals between the impulses and the impulse trains resulted from other users.

There is some uncertainty in the relative positions of the PN-code transitions due to clock jitter and channel delay fluctuations. This is the reason for the finite window size which is selected to compensate for the pulse delays.

Let N be the number of active users on the system. Assume for now that each of the users is continuously transmitting data modulated by a spreading sequence L chips long and having n_+ and n_- transitions respectively. The number of chips with no transitions is:

$$n_0 = L - n_+ - n_-$$

The spreading sequence of the i-th channel can be written in the following way:

$$c_i\,(t) = \sum_{j=1}^{L} C_{ij}\,\psi\,(t-jT_c\,) \qquad (7.1.1)$$

T_c — is the duration of the chip,

$\psi(t)$ — is the chip shape function,

$C_{ij} \;\epsilon\; \left\{0,1\right\}$

We assume rectangular chips, so

$$\psi(t) = \begin{cases} 1 & jT_c \leq t < (j+1)T_c \\ 0 & \text{elsewhere} \end{cases} \tag{7.1.2}$$

The spread signal for the i-th user is:

$$S_i\,(t) = \sum_{k=-\infty}^{\infty} [d_{i,k} \quad \oplus \quad c_i\,(t-kLT_c\,)] \tag{7.1.3}$$

Where:

d - is k-th data of the i-th user,

$$d_{i,k} \;\epsilon\; \left\{ 0,1 \right\}$$

S (t) modulates the intensity of the optical source. In the fiber optic medium the signals are being added thus producing a multi-level optical signal which is detected by a linear detector:

$$x(t) = \sum_{i=1}^{N} S_i\,(t) \tag{7.1.4}$$

We assume no other noise except the one resulting from the multiple user interference.

After differentiation the signal becomes:

$$D(t) = \sum_{i=1}^{N} \sum_{k=-\infty}^{\infty} Z_{i,j} \sum_{j=1}^{L} a_{ij}\, \delta(t-jT_c\,) \tag{7.1.5}$$

Where:

$Z_{i,k}$ is a bipolar data sequence derived from $d_{i,k}$ by the following transformation:

$$Z_{i,k} = (-1)^{d_{i,k}+1} \tag{7.1.6}$$

and

$$\sum_{j=1}^{L} a_{ij}\, \delta(t-jT_c) = \frac{d}{dt}\bar{c}_i\,(t) \tag{7.1.7}$$

This is a ternary sequence:

$$a_{ij} \in \left\{-1,0,+1\right\}$$

The signal (7.1.5) is being correlated with the reference signal:

$$W_i\,(t) = \sum_{j=1}^{L} a_{ij}\, \xi(t-jT_c) \tag{7.1.8}$$

Where:

$$\xi(t) = \begin{cases} 1 & jT_c \leq t < jT_c + \Delta \\ 0 & \text{elsewhere} \end{cases} \tag{7.1.9}$$

The detection process performed by the receiver consists of correlation of the derived this way ternary impulse train with the reference windowing sequence:

$$D_{i,k} = \sum_{j=1}^{L} \int_{jT_c}^{jT_c+\Delta} D(t)\, a_{ij}\, dt \tag{7.1.10}$$

$D_{i,k}$ is random. It's value depends on the number of interfering users and the shot noise resulted from the threshold crossovers by the thermal noise component.

For the purpose of this analysis we neglect this noise component.

Under the assumption of only multiple user interference $D_{i,k}$ is determined by the number of the interfering code transitions occurred during the window duration Δ .

The expected value of $D_{i,k}$ is the value when no other users are interfering:

$$E(D_{i,k} / d_{i,k}) = \sum_{j=1}^{L} Z_{i,k} \; a_{ij} \; \tau_c \tag{7.1.11}$$

Where τ_c is the duration of the pulse after shaping.

Then the expected value of $D_{i,k}$ is data dependent:

$$\begin{aligned} E(D_{i,k} / d_{i,k} = 0) &= -(n_+ + n_-)\, \tau_c \\ E(D_{i,k} / d_{i,k} = 1) &= +(n_+ + n_-)\, \tau_c \end{aligned} \tag{7.1.12}$$

Where: n_+ and n_- are numbers of positive and negative transitions in the spreading sequence correspondingly.

We assume that the value of Δ is selected sufficient to compensate for the impulse jitter and also assume perfect tracking.

These assumptions imply that the target transitions of the i-th PN-code uccur during the window interval with the probability equal to one.

The impulse signals contributed by the interfering users are considered to have Poisson distribution of the arrival times at the output of the differentiator.

Every user contributes on the average $(n_+ + n_-)$ impulses per data bit duration, or on the average $\frac{(n_+ + n_-)}{2}$ positive impulses and $\frac{(n_+ + n_-)}{2}$ negative ones. Then the average frequency of the positive and the negative impulse trains is:

$$\nu = \nu_+ = \nu_- = N \frac{n_+ + n_-}{2T_d} \qquad (7.1.13)$$

Let us examine the random value of $(D_{i,k} / d_{i,k} = 0)$ and $(D_{i,k} / d_{i,k} = 1)$

Let

$$Y_{i,k} = (D_{i,k} / d_{i,k} = 0) + 1 = (D_{i,k} / d_{i,k} = 1) - 1 \qquad (7.1.14)$$

Here $Y_{i,k}$ is the error signal which is the result of the multiple user interference.

$Y_{i,k}$ is a function of the number of active users and the ratio $\frac{\Delta}{T_c}$.

In the ideal system where the inter-transition intervals are deterministic and therefore Δ can be made infinitely small the ternary Pseudo- Random impulse trains are orthogonal and the probability of error becomes equal to zero (assuming that the tracking is perfect).

Realistically, Δ is finite and the PN-Code transitions are represented not by the Delta-functions but rather by the impulse responses of the receiver front end F(t).

Then the signal (7.1.5) becomes:

$$D(t) = \sum_{i=1}^{N} \sum_{k=-\infty}^{\infty} Z_{i,k} \sum_{j=1}^{L} a_{ij} F(t-T_c) \qquad (7.1.15)$$

Where:

$$F(t) = \begin{cases} 1 & 0 \le t \le \tau_0 \\ 0 & \text{elsewhere} \end{cases} \qquad (7.1.16)$$

The noise consists of positive and negative components:

$$\begin{aligned} I_+(t) &= \sum_{i=-\infty}^{\infty} F(t-t_i) \\ I_-(t) &= -\sum_{i=\infty}^{\infty} F(t-t_i) \end{aligned} \qquad (7.1.17)$$

Where the arrivals times t_i have Poisson distribution. We will use signal decomposition technique to analyze the system performance. The multiple user noise, Fig.7.2 , can be represented by it's positive and negative components.

In order to be able to compare this system to the ones analyzed in the previous chapters we use an approximation of the mathematical model for the multiple user noise by a model that is similar to the one used for the TH system.

This approximation will require decomposition of the system noise into positive and negative components as it is given by (7.1.17). The positive component of the multiple user noise is a result of the OR operation on the impulse responses from the post-differentiation filter to positive impulses from the differentiator. These impulses correspond to the positive transitions in the user codes and have Poisson statistics. The negative component of the noise is derived the same way from the impulses corresponding to the negative transitions in the users' codes. These two noise components can be considered independent from each other. The signal can be represented the same way by it's positive and negative components. It can be seen that this system can employ detectors identical to the ones used in the TH system with Active Pause Signaling. However problems can occur at the beginning and at the end of the PN codes due to preceding and succeeding data bit values that might alter the code's first and last transitions. What this fact implies is that the TDL correlator has to be matched to the PN code transitions excluding the first and the last. Fig.7.3. illustrates this statement for a fifteen chips long PN code. As it can be seen from the figure only seven transitions will be used by the detector.

The receiver block diagram is depicted in Fig.7.4. The TDL correlators that are incorporated by the receiver are matched to the positive and negative component of the signal. The positive component of the multiple user noise is comprised by the secondary process $x_+(t)$. The average contribution of each user per second to this part of noise is equal to ν_i pulses per second, where:

$$\nu_i = \frac{n_+ + n_-}{2T_d} \tag{7.1.18}$$

Then for N interfering users we have:

$$\nu = N \, \frac{n_+ + n_-}{2T_d} \tag{7.1.19}$$

If to assume symmetric data sources then both components of noise are statistically identical. The average duration of the positive and negative multiple noise pulses can be found using (1.5.24) and (1.5.23):

$$\overline{\tau_x} = \overline{\tau_{x_+}} = \overline{\tau_{x_-}} = \frac{1 - e^{-\nu\tau_0}}{\nu e^{-\nu\tau_0}} \tag{7.1.20}$$

And the average rate:

$$\overline{\mu_x} = \overline{\mu_{x_+}} = \overline{\mu_{x_-}} = \nu e^{-\nu\tau_0} \tag{7.1.21}$$

The probability density function for the noise pulse durations can be found for the positive and negative components using (1.5.21).

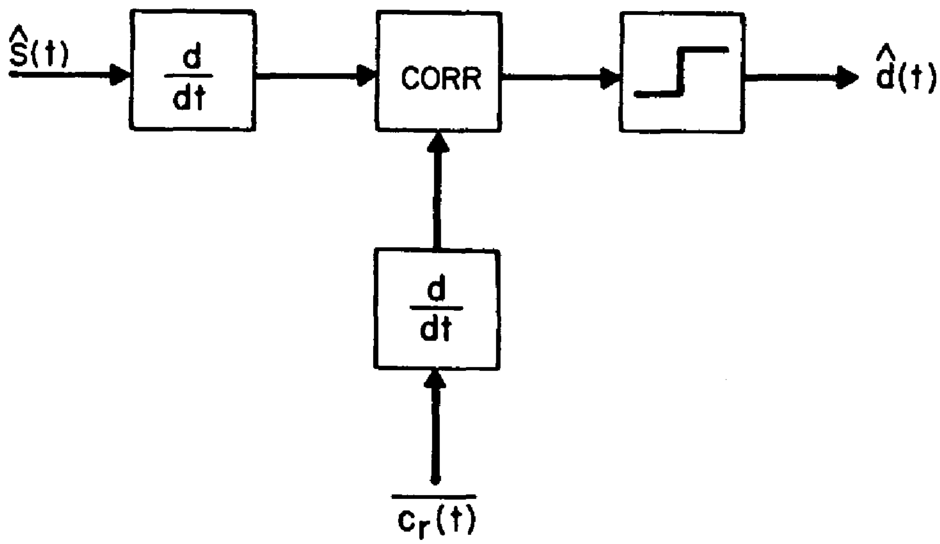

Fig.7.1. OOK/ADDER/DS System Receiver Structure

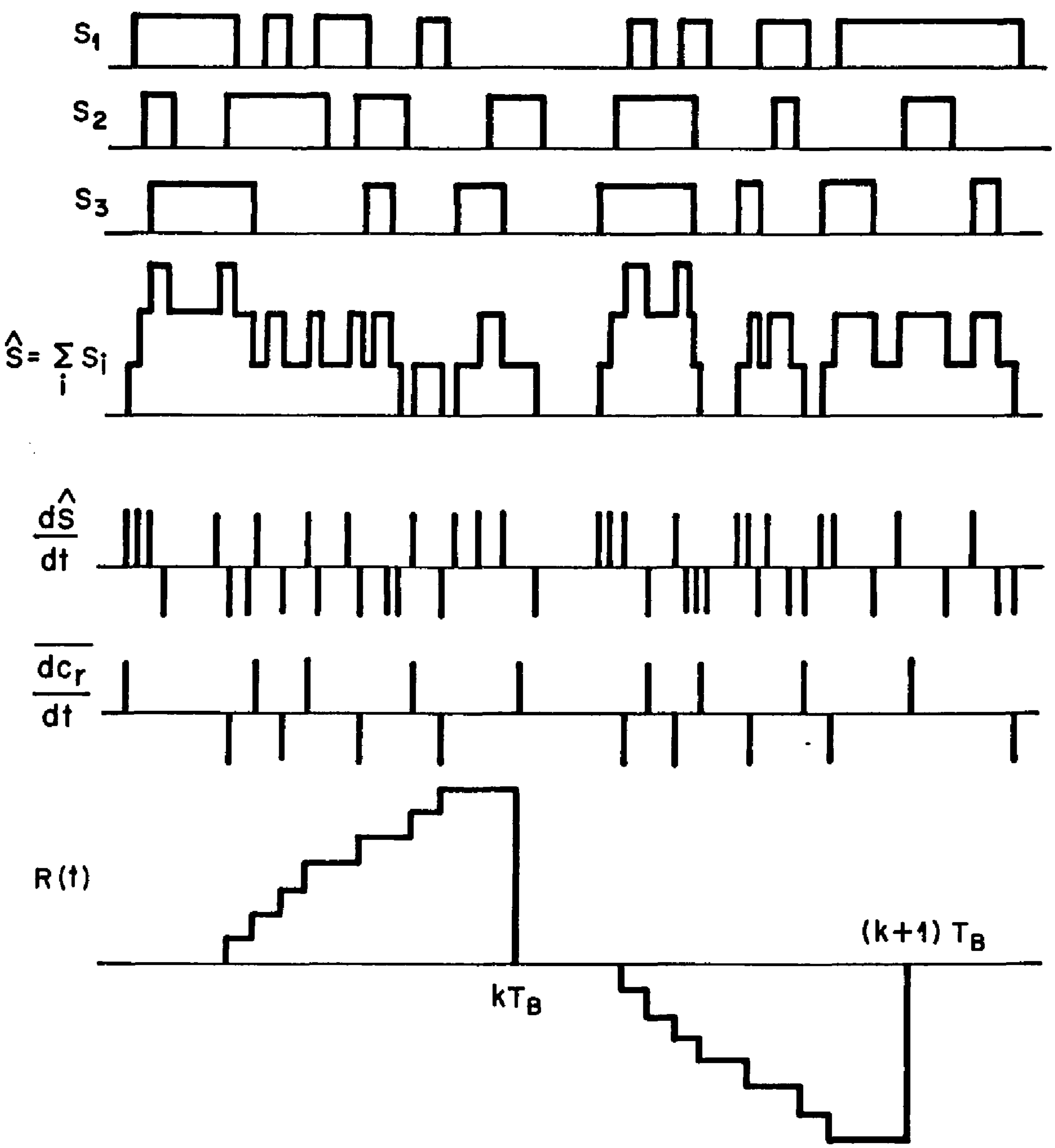

Fig.7.2. OOK/ADDER/DS Signal Demultiplexing

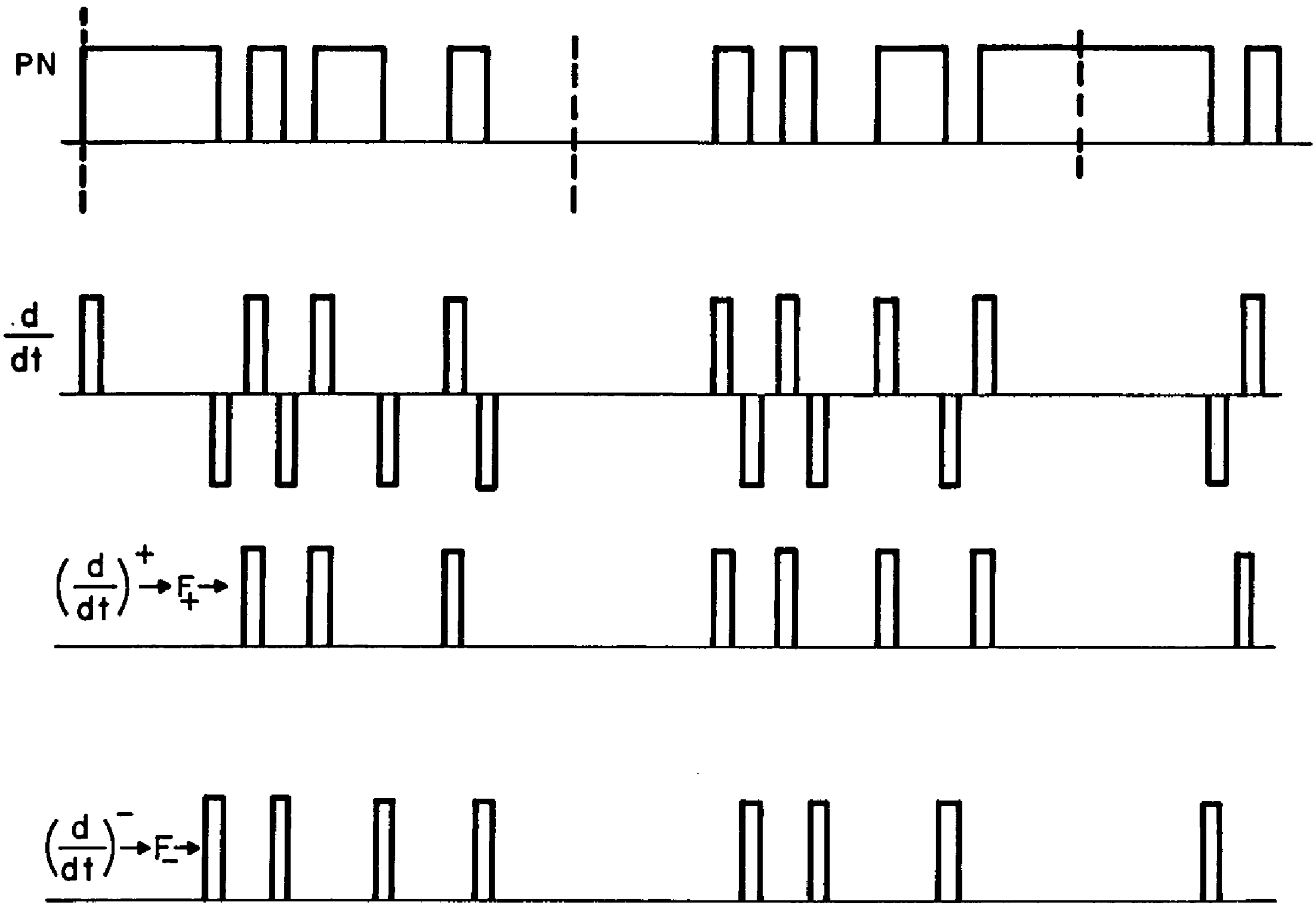

Fig.7.3. PN-Sequence to PRIS Conversion in The Receiver

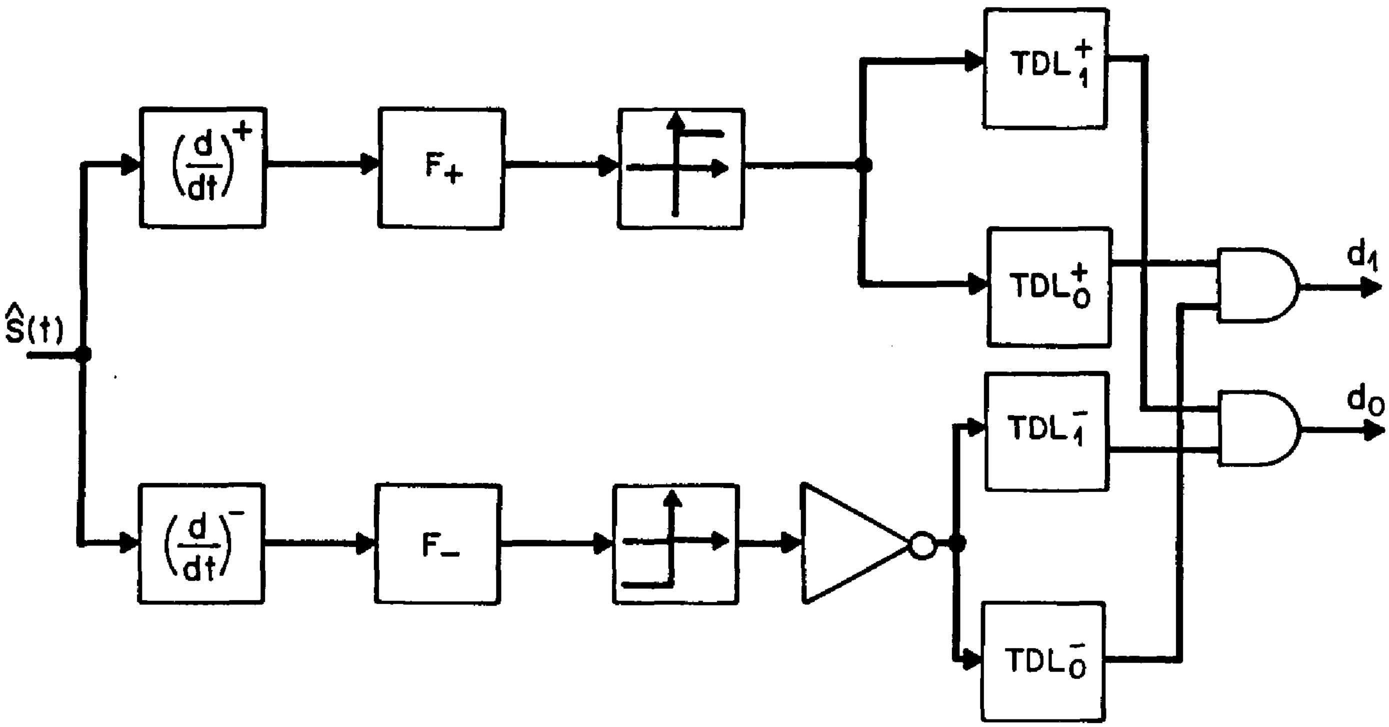

Fig.7.4 TDL Correlator Receiver for OOK/ADDER/DS System

7.2 SYSTEM PERFORMANCE ANALYSIS

The errors can occur due to the possibility of noise signal alignment favorable to false detections by the matched filters.

Now we will determine the probability of false detections caused by the multiple user noise components at the inputs of each of the two TDL correlator detectors. The detector structure is identical to the one used in the OOK/OR/TH system with strobing signal z(t) recovered using the method described in chapter six for the system with Active Pause Signaling. The threshold signal we will assume to be set at it's maximum that will correspond to imposing a requirement on the output pulses to be at their maximum duration τ_0 . Then the probability of false detection can be found using (3.3.46):

$$P_{fd} = \left[1 - e^{-\frac{n_+ + n_-}{2K_f K_p}N}\left(1 + \frac{n_+ + n_-}{2K_f K_p}N\right)\right]^{n_+ + n_-} \qquad (7.2.1)$$

Where :

$$K_p = \frac{T_d}{T_c} \qquad (7.2.2)$$

This parameter is the processing gain of the DS system.

K_f is the receiver bandwidth expansion coefficient and is defined as :

$$K_f = \frac{T_c}{\tau_0} \qquad (7.2.3)$$

The Direct Sequence Channel load we define as:

$$C_l = \frac{N}{K_p} \tag{7.2.4}$$

Then the probability of false detection in terms of the channel load can be written as follows:

$$P_{fd} = \left[1 - e^{-\frac{n_+ + n_-}{2K_f}C_l}\left(1 + \frac{n_+ + n_-}{2K_f}C_l\right)\right]^{n_+ + n_-} \tag{7.2.5}$$

Fig.7.5 illustrates the probability of error as a function of the channel load and the receiver bandwidth expansion coefficient. As it can be observed the more bandwidth is expended the better is system's performance. Fig.7.6 illustrates the probability of error for different values of processing gain K_p . There is obviously an optimal processing gain that yields the minimum probability of error. The mechanism for that is identical to the one in the TH system.

Fig.7.7 shows the optimal processing gain as a function of the channel load. And again, as in the TH system, the tendency is to reduce the number of pulses in the code as the channel load goes up.

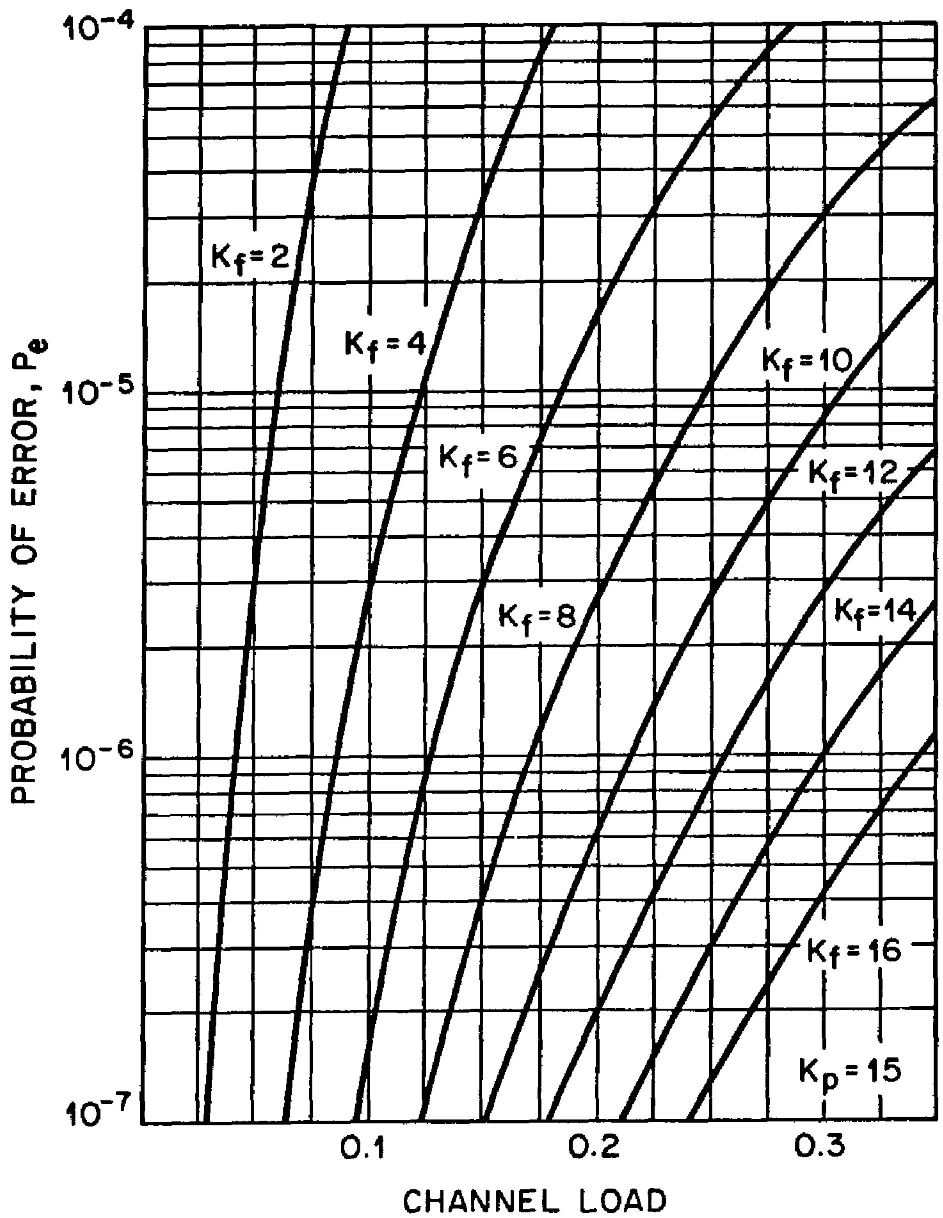

Fig.7.5. OOK/ADDER/DS System. $P_e = f(C_l, K_f)$

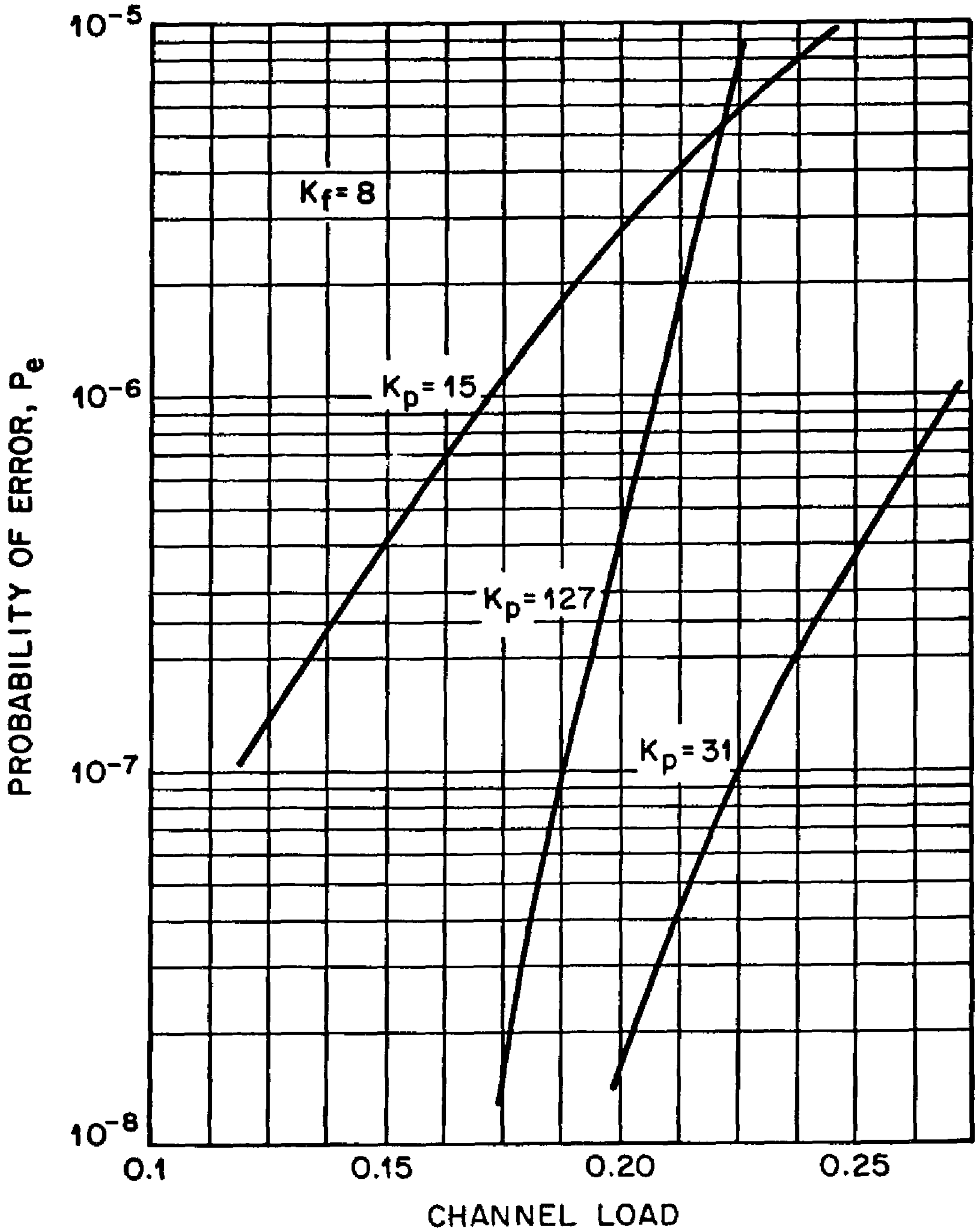

Fig.7.6. OOK/ADDER/DS System, $P_e = f(C_l, K_p)$

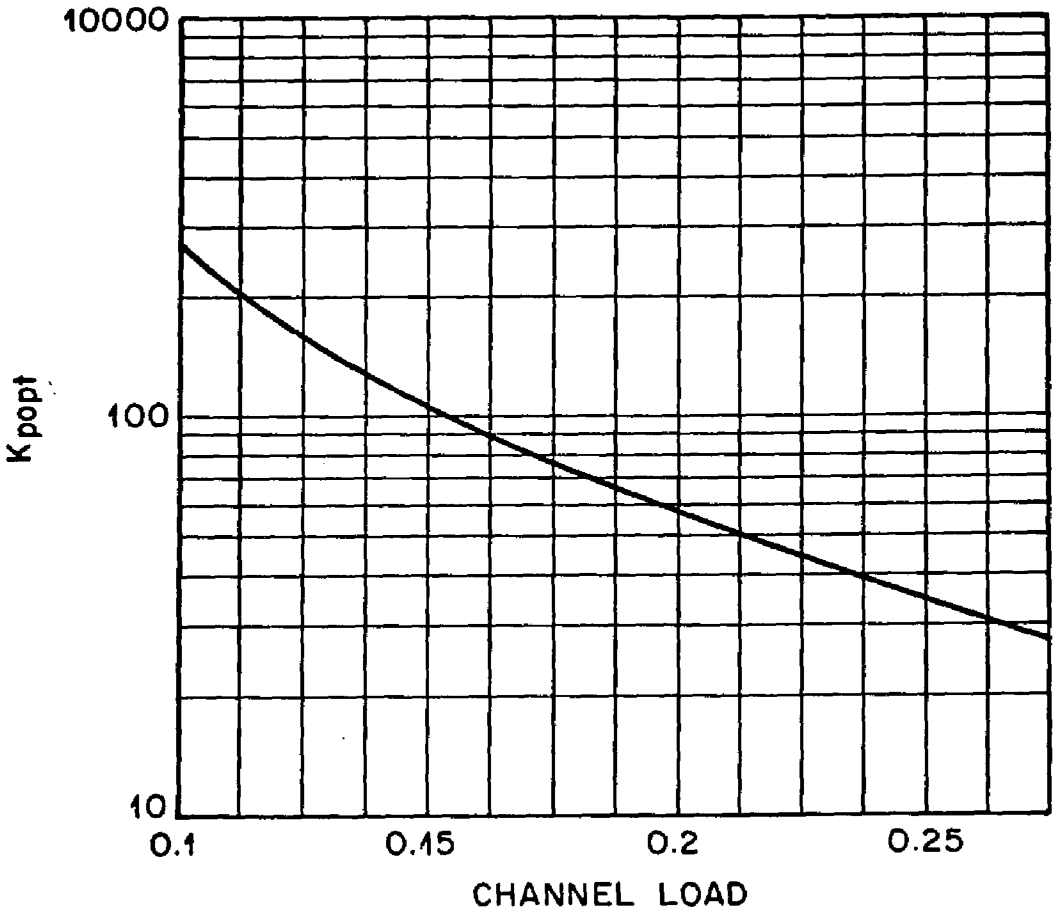

Fig.7.7. OOK/ADDER/DS System, Optimal Processing Gain

7.8 CONCLUSIONS

We proposed a novel method of the OOK/ADDER/DS signal demultiplexing based on additional signal bandwidth expansion in the receiver. The proposed technique allows to improve the channel throughput. However it requires high dynamic range of the optical composite signal and therefore can be used only when the number of users is small and the thermal component of noise in the receiver is negligible.

8. APPLICATIONS

8.1 INTRODUCTION

There are numerous applications of the signaling techniques that were proposed and analyzed in previous chapters. In two subsequent sections we will illustrate two typical examples of Fiber Optic spread spectrum signaling applications. First example describes an asynchronous non-orthogonal multiplexing technique. The second example describes a new type of a Fiber Optic Local Area Network that is based on Code Division Multiple Accessing of a single Fiber Optic medium.

8.2 ASYNCHRONOUS RATE-INVARIANT MULTIPLEXING

Time Division and Frequency Division multiplexing techniques are based on the orthogonal signaling and therefore allow each of the signals to occupy preassigned time or frequency slot. These techniques guarantee absence of interference among channels but when some of the channels are idle others can't take advantage of the available time or bandwidth. There are multiplexors that attempt to realize dynamic bandwidth allocation by reassigning the subchannels among signals when some of them are idle. This technique is rather complex and requires gradual rate adjustments for some media (like Voice, per example) and very often requires a set of compression techniques to handle gradual rate changes.

To avoid problems connected with reprofiling the channel we propose to use non-orthogonal Code Division Multiplexing technique that allows construction of an Asynchronous Rate-Invariant Multiplexor, (ARIM), for multi-media communications. The architectural block-diagram of the proposed multiplexor is shown in Fig.8.1.

Digitized signals are modulated by a pseudo random carriers that differ in rate and code sizes. Then the Time-Hopped electrical signals are converted to optical ones and coupled into the single mode fiber using uni-directional couplers. Some of the operations that we allocated to the electrical domain will be performed in optical form in not too distant future.

Demultiplexing is performed by a set of TDL Correlators matched to the corresponding PRIS codes. If the data rates fit some standard hierarchy the common electrical or optical clock can be used. Otherwise every medium can have it's own clock absolutely independent from other media.

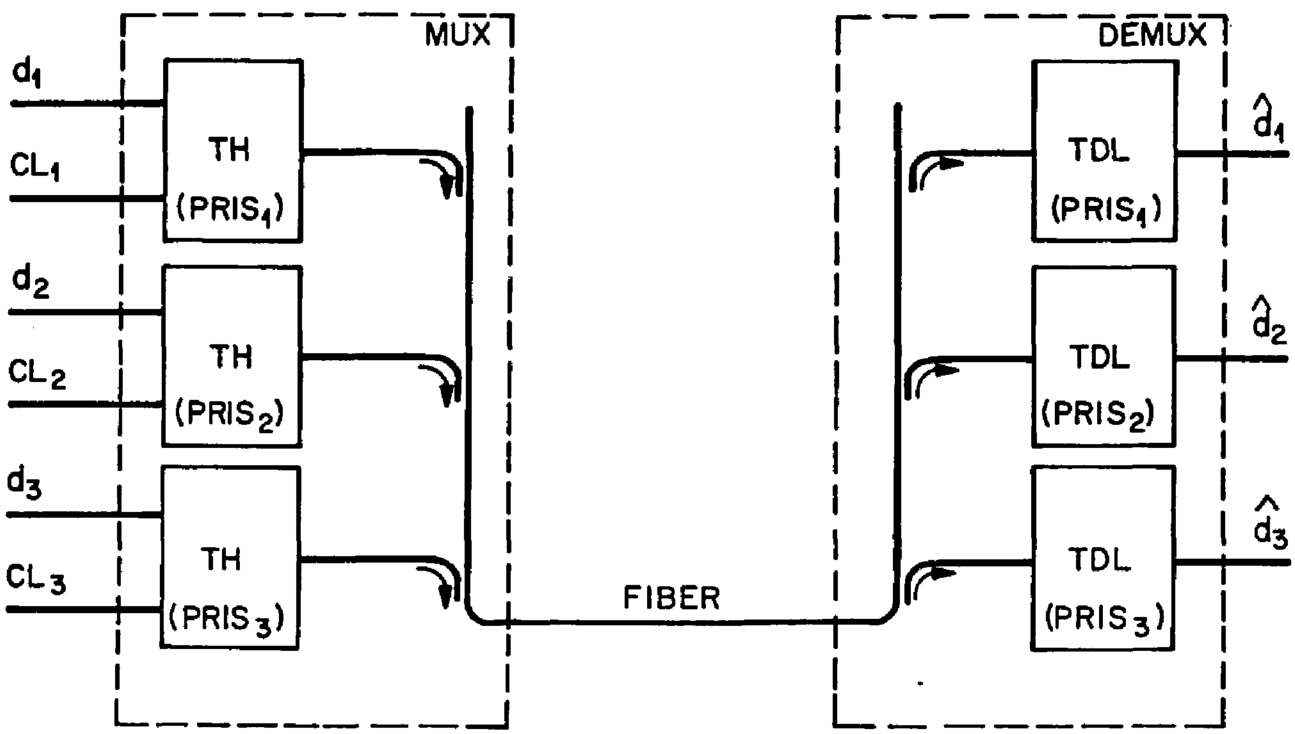

Fig.8.1. Rate-Invariant Multiplexing

8.3 CORENET

We propose a new type of a local integrated services digital network using Code Division Multiple Access protocol. The network should be capable of carrying packetized video, voice graphics and data signals and have point-to-point as well as broadcasting capability. This will allow to conduct secure full motion and audio-graphics teleconferencing in local area network environment, distribution of maps and mixed mode (text/graphics) communication.

The name of the proposed network, "CORENET", (Code Reservation Network), reflects the Spread Spectrum Code Reservation scheme which will be used in the network for code and bandwidth allocation.

CORENET is a fiber-based LAN using 1.3 micron optical sources and single mode fiber. Each node has a passive tap and no optical signal regeneration is required.

We consider a population of bursty users and no overhead required to handle the network layer of the communication protocol.

One of the possible network topologies is an open ring, Fig.8.2, with a central station that uses a control channel reserved for network management.

The central station keeps in it's data base the encryption keys assigned to the nodes. It uses the keys to communicate to each node. The nodes use encrypted signals on the control channel to request a virtual circuit connection with another node, to report End of Session and number of errors detected during the session (average per second), and to receive all necessary information to establish the virtual communication link with another station.

Another possible network topology is a star.

CDMA network has certain degree of immunity to collisions. However the stability of the network must be insured by monitoring the traffic conditions and limiting the inter-user interference via code assignments that trade off the bit error rate for smaller contribution of the user to the system noise. The channel measurements can be performed by the central station but can also be a function of the "intelligence" built into each node.

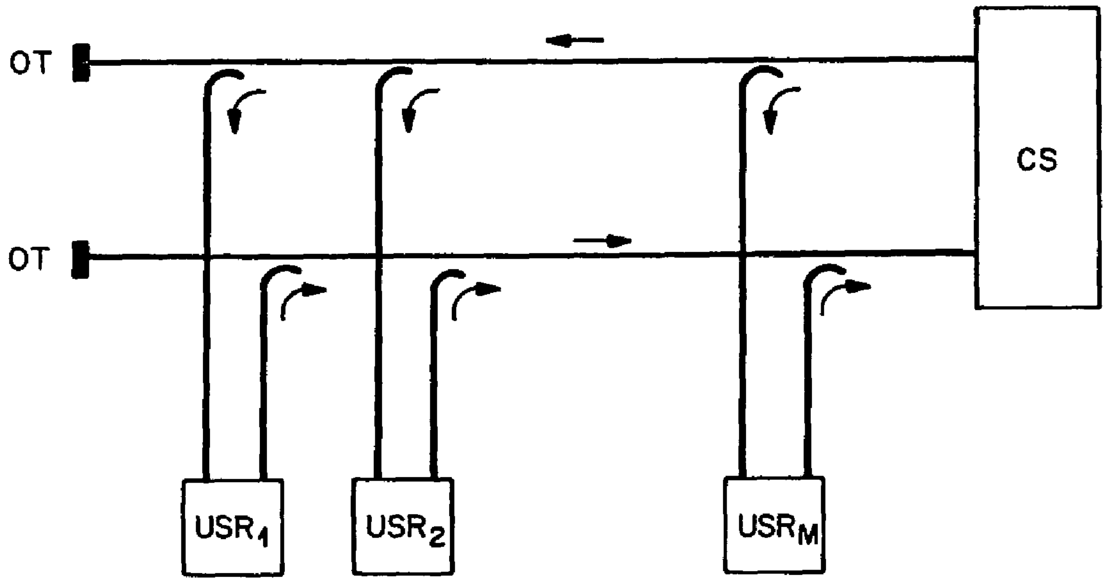

Fig.8.2. CORENET Topology

8.4 CONCLUSIONS

We proposed an architecture of a Rate-Invariant Multiplexor that utilizes non-orthogonal signaling techniques for multiplexing of the communications media signals. The applications of this multiplexor can be single-user/multi-media, multi-user/single medium and combinations thereof.

We proposed a Fiber Optic Local Area Network that is usable for real time communications. This network will be especially effective for multi-media communications when information sources employ different data rates and have different statistics of the information flow.

9. FUTURE AREAS OF RESEARCH

Codes For CDMA Systems

There is a need to create sets of Pseudo Random Intervals Sequences with auto- and crosscorrelation properties suitable for CDMA applications. These code sets should have controlled crosscorrelation functions that can be traded off for the number of codes in the set. It will allow Code Division Multiplexing of multiple users and in the same time will allow control of the network performance.

Components For CDMA Systems

The components needed for CDMA fiber optic systems are the TDL correlators with multiple taps and all-optical code generators. For Color-Hopped systems there is a necessity to create tunable lasers.

There is a necessity to create optical logical components in order to make possible all signal processing to be performed in the optical domain.

Networking Problem

To continue research directed to the realization of the Fiber Optic Local Area Network based on Code Division Multiple Access one has to define the link layer of the network protocol. It is quite possible that for data applications when collision detection is needed there will be a need to analyze coding on the top of spread spectrum signaling as a possible candidate for the collision detection mechanism. Detailed access discipline has to be defined for the network as well as contention resolution (if any) and data retransmission strategies. Only then the analysis of the network performance can be realized that will answer the question regarding network throughput and packet delays. When comparing the CDMA network to the ones that employ contention resolution techniques a composite criterion has to be defined to characterize the network throughput taking to consideration multi-media, including real time, communications. Because that what this research is all about.

10. REFERENCES

[1] Raymond L. Pickholtz, Donald L. Schilling and Laurence B. Milstein "Theory of Spread-Spectrum Communications - A Tutorial", IEEE Trans. on Comm., Vol. Com-30, No. 5, May 1982.

[2] Stewart D. Personick, "Optical Fiber Transmission Systems", Plenum Press, New York, 1981.

[3] C.T. Spracklen and C. Smythe "Communication Protocols for a Spread Spectrum Local Area Network" Proceedings, FOC/LAN - 84.

[4] J.R. Lee, S.M. Ryu, C.K. Un and W.D. Cho "A Local area Network Based on the Code Division Multiple Access Method", GLOBCOM-84.

[5] P.A. Davies, A.A. Shaar, "Asynchronous Multiplexing for an Optical-Fibre Local-Area Network", Electronic Letters, Vol.19, No. 10, 1983.

[6] S. Tamura, S. Nakano and K. Okazaki "Optical Code-Multiplex Transmission by Gold Sequencies", Journal of Lightwave Technology, Vol. LT-3, No. 1, February 1985.

[7] G. Tartara, "On the Capacity of Asynchronous Code-Division Multiplexing Systems", Proceedings of the IEEE, August 1968.

[8] Miller, K. S., Scwartz, R. S., "On The Interference of Pulse Trains", J. Appl. Phys., Vol. 24, No. 8, 1953.

[9] Dennis A. Shedd and Dilip V. Sarwate, "Construction of Sequences with Good Correlation Properties", IEEE Trans. on IT, Vol. IT-25, No. 1, January 1979.

[10] IEEE Proc. on Comm., Special Issue on Optical Computing, Vol. 72, No. 7, July 1984.

[11] E. N. Gilbert and H. O. Pollak, "Amplitude Distribution of Shot Noise", BSTJ, March 1960.

[12] Kenji Yamada, Kazuhiro Daikoku and Hidenori Usui "Performance of Portable Radio Telephone Using Spread Spectrum", IEEE Trans. on Comm., Vol. Com-32 No.7, July 1984.

[13] Ahmed K. Elhakeem, H.M. Hafez and Samy A. Mahmoud "Spread Spectrum Access to Mixed Voice-Data Local Area Networks" Journal on Selected Areas in Comm. Vol. sac-1, No. 6, December 1983.

[14] A. A. Shaar and P.A. Davies, "Prime Sequences: Quasi- Optimal Sequences for OR Channel Code Division Multiplexing", Electronic Letters, Vol. 19, No. 21, October 1983.

[15] Sorin Davidovici, Laurence B. Milstein and Donald L. Schilling "A New Rapid Acquisition Technique for Direct Sequence Spread-Spectrum Communications" IEEE Trans. on Comm., vol. COM-32, no. 11, Nov. 1984

[16] Domenico Laforgia, Angelo Luvison and Valerio Zingarelli "Bit error Rate Evaluation for Spread-Spectrum Multiple Access Systems", IEEE Trans. on Comm., vol. Com-32, No. 6, June 1984.

[17] Farhad Hemmati and Donald L. Schilling "Upper Bounds on the Partial Correlation of PN Sequences" IEEE Trans. on Comm., Vol. Com-31, No. 7, July 1983.

[18] Dennis J. Maddock, Aetna Telecommunications Consultants, "Military Applications of Fiber Optics", Tutorial, presented at FOC/LAN-84.

[19] T. Nishida, H. Miyahara and K. Takashima "Group Random access Scheme in Spread Spectrum Multiple Access System", GLOBCOM-84.

[20] Elvino S. Sousa and John A. Silvester "A Spreading Code Protocol for a Distributed Spread Spectrum Packet Radio Network", GLOBCOM-84.

[22] A. D. Gelman, N. I. Kozlenko, "Acquisition in RADA Systems Using Synchronization Preambles", Transactions of Voronezh Polytechnical Institute, 1972.

[23] Jeffrey E. Wieselthier, Antony Ephremides "A Distributed Reservation scheme for Spread Spectrum Multiple Access Channels" GLOBCOM-83.

[24] P.A. Davies and A.A. Shaar "Asynchronous Multiplexing on the Optical Fibre OR Channel", Qolloquium on Practical Applications of Channel Coding Techniques, London, England, 1983.

[25] T. M. Cover, R. J. McEliece, E. C. Posner, "Asynchronous multiple-access channel capacity", IEEE Trans. Inform. Theory, Vol. IT-26, Nov. 1980.

[26] Norman Abramson, "Development of the ALOHANET", IEEE Trans. Inform. Theory, Vol. IT-31, March 1985.

[27] Robert G. Gallager, "A Perspective on Multiaccess Channels", IEEE Trans. Inform. Theory, Vol. IT-31, March 1985.

[28] John Gowar, "Optical Communication Systems", Prentice/Hall, 1984.

[29] D. V. Sarwate and M.B. Pursley, "Crosscorrelation Properties of Pseudorandom and Related Sequences", Proc. IEEE, Vol. 68, 1980.

[30] R. Gold, "Optimal Binary Sequences for Spread Spectrum Multiplexing", IEEE Trans. Inform. Theory, Vol. IT-13, 1967.

[31] Roland G. Wilson, "Orthogonal Multilevel Pseudorandom Sequences and Impulse Sequences Derived from Them", IEEE Trans. Inf. Theory, Vol. IT-27, No. 3, May 1981.

[32] Tom Hoholdt and Jorn Justesen, "Ternary Sequences with Perfect Periodic Autocorrelation", IEEE Trans. Inf. Theory, Vol. IT-29, No. 4, July 1983.

[33] A. J. Viterbi, "When Not to Spread Spectrum - a Sequel", IEEE Communications Magazine, Vol.23, No. 4, April 1985.

[34] M. K. Simon, J. K. Omura, R. A. Scholtz, B. K. Levitt, "Spread Spectrum Communications", Vol. 1,2,3, Computer Science Press, 1985.

[35] D. J. Torrieri, "Principles of Military Communication Systems", Artech, 1982.

[36] Herbert Taub and Donnald L. Schilling, "Principles of Communication Systems", McGraw-Hill, 1971.

[37] John M. Wozencraft and Irwin Mark Jacobs, "Principles of Communication Engineering", John Wiley & Sons, 1965.

[38] "Transmission Systems for Communications", Fifth Edition, Bell Laboratories, 1982.

[39] A.J. Viterbi, J.K. Omura, "Principles of Digital Communication and Coding", McGraw-Hill, 1979.

[40] R.G. Gallager, "Information Theory and Reliable Communication", John Wiley & Sons, 1968.

[411 N. I. Kozlenko, A. D. Gelman, "Noise Immunity of the Voice PPM-PWM-PAM Channel", (Russian), Voprosy Radioelectroniky, Section "Radiocommunications", 1971.

[42] Mischa Schwartz, "Computer-Communication Network Design and Analysis, Prentice-Hall, 1977.

[43] M. B. Pursley and H.F. Roefs, "Numerical Evaluation of correlation Parameters for Optimal Phases of Binary Shift-Register Sequences", IEEE Trans. on Communications., Vol. COM-27, pp. 1597-1604, 1979.

[44] K. Yao, "Error Probability of Asynchronous Spread Spectrum Multiple Access Communications Systems", IEEE Trans. on Communications., Vol. COM-25, pp. 803-809, 1977.

[45] T. Hellegeth, "Some Results About the Cross-Correlation Function Between Two Muximal Linear Sequences", Discrete Math., Vol.16, pp. 209-232,1976.

[46] D. A. Huffman, The generation of Impulse-Equivalent pulse Trains", IRE Trans. Inform. Theory, Vol. IT-8, pp. 510-516, 1962.

[47] A. M. Boehmer, "Binary Pulse Compression Codes", IEEE Trans. on Inform. Theory, Vol. IT-13, pp.156-167, 1967.

[48] P.A.N. Briggs and K.R. Godfrey, "New Class of Pseudo Random Ternary Sequences", Electronic Letters., Vol. 4, pp. 438-439, 1968.

[49] M. B. Pursley, "Evaluating Performance of Codes for Spread Spectrum Communications", Circuit and System Theory, pp.765-774, 1974.

[50] C. H. Dawson, H. Sklar, "False Addresses in a Random Access System Employing Discrete Time-Frequency Addressing", IEEE International Convention Records, 1964.

[51] R. A. Dillard, "Detectability of Spread Spectrum Signals", IEEE Trans. on Aerospace and Electronic Systems, Vol. AES-15, No. 4, July 1979.

[52] W. Stallings, "Digital Signalling Techniques", IEEE Communications Magazine, Vol. 22, No. 12, December 1984.

[53] D. H. Rice, G. E. Keiser, "Application of Fiber Optics to Tactical Communication Systems", IEEE Communications Magazine, Vol. 23, No. 5, May 1985.

[54] Giancarlo Prati, "Joint Pulse Spreading Estimation and Decoding in Stretched Pulse PPM Optical Channels", IEEE Transactions on Communications, Vol. COM-33, No. 8, August 1985.

[55] T. J. Healy, "Coding and Decoding for Code Division Multiple User Communication System", IEEE Transactions on Communications, Vol. COM-33, No. 4, April 1985.

[56] C. N. Georghiades, "Joint Baud and Frame Synchronization in Direct Detection Optical Communications", IEEE Transactions on Communications, Vol. COM-33, No. 4, April 1985.

[57] Paul F. Sass, "Why is the Army Interested in Spread Spectrum?", IEEE Communications Magazine, Vol. 21, No.4, July 1983.

[58] J. Lesh, "Capacity Limit of the Noiseless, Energy-Efficient Optical PPM Channel", IEEE Transactions on Communications, Vol. COM-31, No. 4, April 1983.

[59] F. Davidson, "Direct-Detection Optical Communication with Color Coded Pulse Position Modulation Signaling", IEEE Transactions on Communications, Vol. COM-33, No. 3, March 1985.

[60] N. I. Kozlenko, A. D. Gelman, "Autocorrelation Function and Power Spectral Density of the Signal at the Output of the PPM-PWM-PAM Channel", (Russian), Voprosy Radioelectroniky, Section "Radiocommunications", 1970.

[61] Shih-Chun Chang and Jack K. Wolf, "On the T-User M-Frequency Noiseless Multiple-Access Channel with and Without Intensity Information", IEEE Transactions on Information Theory, Vol. IT-27, No. 1, January 1981.

[62] S. W. Golomb, "On the Classification of Balanced Binary Sequences of Period $2^n - 1$", Transactions on Information Theory, Vol. IT-26, No. 6,

November 1980.

[63] A. A. Shaar and P. A. Davies, "A Survey of One-Coincidence Sequences for Frequency-Hopped Spread-Spectrum Systems", IEE Proceedings, Vol. 131, No. 7, December 1984.

[64] R. C. Sommer, "Asynchronously Multiplexed Binary Channel Capacity", IEEE Proceedings, Vol. 54, January 1966.